

A NEW T-SHAPED GRAPHITE FURNACE FOR ATOMIC ABSORPTION SPECTROMETRY

Vom Fachbereich Chemie (IAC)

der Universität Duisburg-Essen

Zur Erlangung des akademischen Grades eines

Dr. rer. nat

genehmigte Dissertation

von

Abdelsalam Ali Asweisi

aus Benghazi / Libyen

Referent: Prof. Dr. Heinz-Martin Kuss

Korreferent: Priv. Doz. Dr. Ursula Telgheder

Datum der Einreichung 02.11.2007

Datum der mündlichen prüfung 07.02.2008

AKNOWLEDGEMENTS

During the work on this thesis, I have been lucky to work in a research group that has helped me a lot and made this really very pleasant, I would like to thank them all, but particularly my thesis director *Prof. Dr. Heinz-Martin Kuss*, who has been constantly by my side, teaching, advising, discussing, supporting and easing the moments of indecision, thank you Prof. Kuss for guiding me in the first steps of my research project.

I must not forget my first colleagues, Dr. Bülend Bayraktar, who showed me to the basics of graphite furnace technique and Dr. Yevgen Berkhoyer, who helped me to start out in research and introduced me to the method of two-step atomizer.

I would like to thank Mr. Theo Lukaszyk for paying more attention during the manufacturing of the graphite furnaces and the rest of all parts which were needed during my research period and Mr. Jürgen Kupperschmied the leader of the University fine mechanic workshop.

I express my sincere gratitude to Dr. Uwe Oppermann from Shimadzu company-Germany for providing us the atomic absorption spectrometer (AA6800).

Schunk kohlenstofftechnik Gmbh, thanks for providing graphite materials and pyrocoating processes.

I especially want to thank Priv. Doz. Dr. Ursula Telgheder for here significant suggestions and final corrections of my thesis and to do the second reference.

I would like to acknowledge Dr. Holger Krohn, Dr. Bernd Wermeckes, Mr. Gerd Fischer, Mr. Werner Kaiser, Mrs. Roswitha Schragmann, Mrs. Claudia Ullrich for their assistance during my research period.

My friends Rajab El-kailany, Nabil Bader, Kahled Elsherif, Dr. Roman Rodreguez, Stefan Meisen, Sami Abdelsalam and Qian Yuan are warmly acknowledged.

I would like to acknowledge Mr. Mohamed Altous for helping me in drawing graphs using three dimensional software program.

I want also thank Prof. Trosten Schmidt, Prof. Karl Molt, Prof. Alfred Golloch, Dr. Myint Sein for the friendly atmosphere during my work in this department. All co-workers in instrumental analysis institute are also acknowledged.

Finally, my warm thanks to my wife for taking care of me and our kids and her patience during my study period.

TABLE OF CONTENT

1. INTRODUCTION.	1
1.1 Trace element analysis.	1
1.2 Spectrometric methods.	1
1.3 Atomic absorption spectrometry (AAS).	1
1.3.1 Instrumentation.	1
1.3.2 Measuring Absorbance.	2
1.3.3 THE graphite furnace.	4
1.3.3.1 Short history of graphite tube.	4
1.3.3.2 STPF concept	5
1.3.4 The temperature program.	6
1.4 Interferences in atomic absorption spectrometry.	7
1.5 Chemical modifiers.	8
2. THEORETICAL BACKGROUND KNOWLEDGE.	11
2.1 Types of graphite atomizers.	11
2.1.1 Two step-atomizer designed by Frech.	13
2.1.1.1 System description.	13
2.1.1.2 Features of the Frech system.	16
2.1.2 Two-step atomizer by Nagulin.	17
2.1.3 G. Schlemmer system.	20
2.1.4 Grinshtein system.	22
2.2 THE HIGH TEMPERATURE CHROMATOGRAPHY IN AAS.	28

2.2.1 High temperature chromatography system proposed by Grinshtein. ...	30
2.2.2 High temperature chromatography with modified two-step atomizer system.	35
3. AIM OF THE WORK.	38
4. METHODS AND EXPERIMENTAL.	39
4.1 AAS spectrometer description.	39
4.2 Graphite materials.	39
4.3 Hollow cathode lamps	40
4.4 Mass flow controller.	40
4.5 Water and nitric acid.	40
4.6 Standard solutions and certified materials.	41
4.7 Boronitride.	42
5 RESULTS AND DISCUSSION.	43
5.1 The new T-shaped graphite furnace.	43
5.2 The short time temperature program.	46
5.3 Optimization of the T-shaped furnace.	49
5.3.1 Optimization of dimensions.	49
5.3.2 Optimization of argon gas flow.	49
5.3.3 Optimization of the position	
5.3.3.1 Vertical position of furnace neck.	51
5.3.3.2 Horizontal position of the furnace neck.	57
5.4 QUANTITATIVE ANALYSIS WITH THE NON-PYROCOATED T-SHAPED GRAPHITE FURNACE IN THE HORIZONTAL POSITION.	59
5.4.1 QUANTITATIVE ANALYSIS OF ELEMENTS IN STANDARD SOLUTIONS.	59

5.4.1.1	QUANTITATIVE ANALYSIS OF HIGH VOLATILE ELEMENTS.	59
5.4.1.1.1	Cadmium.	59
5.4.1.1.2	Silver.	61
5.4.1.1.3	Bismuth.	63
5.4.1.2	ANALYSIS OF MIDDLE VOLATILEE ELEMENTS.	
5.4.1.2.1	Calibration curve for copper.	66
5.4.1.2.2	Calibration curve for Manganese.	68
5.4.2	ANALYSIS OF ELEMENTS IN URINE.	70
5.4.2.1	QUANTITATIVE ANALYSES OF HIGHLY VOLATILE ELEMENTS	
5.4.2.1.1	High temperature chromatography in analysis of cadmium.	70
	Analysis of cadmium using conventional AAS.	73
5.4.2.1.2	Analysis of Bismuth.	75
	Analysis of bismuth with conventional Shimadzu system.	77
5.4.2.2	DETERMINATION OF MIDDLE VOLATILE ELEMENS.	79
5.4.2.2.1	Analysis of Chromium using T-shaped graphite furnace. ...	79
	Analysis of chromium by using Shimadzu furnace.	82
5.4.2.2.2	Analysis of Manganese.	83
	Analysis of manganese using Shimadzu graphite furnace.	85
5.4.2.2.3	Analysis of Aluminium using T-shaped furnace.	86
	Analysis of aluminium using Shimadzu graphite furnace	89
5.4.2.2.4	Analysis of copper by non coated T-shaped graphite furnace.....	90
5.5	ANALYSIS WITH THE PYROCOATED T-SHAPED GRAPHITE	
	FURNACE.	92
5.5.1	ANALYSIS OF TRACE ELEMENTS IN URINE.	92
5.5.1.1	ANALYSIS OF HIGH VOLATILE ELEMENTS.	92
5.5.1.1.1	Analysis of cadmium.	92

5.5.1.2 ANALYSIS OF MIDDLE VOLATILE ELEMENTS.	94
5.5.1.2.2 Short time and conventional temperature program in analysis of manganese.	95
Analysis of Mn in urine sample using conventional temperature program.	95
Analysis of Mn in urine sample using short time temperature Program.	98
5.5.1.2.3 Analysis of of Aluminium.	103
5.5.2 ANALYSIS OF TRACE ELEMENTS IN BODY FLUIDS.	104
5.6 SUMMARY OF THE RESULTS.	109
5.7 CONCLUSION.	113
5.8 REFERENCES.	116

LIST FO FIGURES

Figure 1.1 Schematic construction of an atomic absorption spectrometer.	2
Figure 1.2 Relationship between light emission profile and absorption profile.	3
Figure 1.3 A conventional graphite tube with platform.	5
Figure 1.4 Transverse-heated furnace.	5
Figure 1.5 Heating profiles for the graphite tube walls (A), the inert gas (B), and the Platform(C).	6
Figure 2.1 First two-steop atomizer designed by Frech.	13
Figure 2.2 Graphite cup and side heated tube with integrated contacts.	14
Figure2.3 Furnace housing with installed cup and tube by Frech.	15
Figure .2.4 Normalized characteristic masses as a function of the gap distance for Cd and Pb.	15
Figure 2.5 Design of two-step atomizer by Nagulin.	17
Figure 2.6 Space-time structure of the signal of non selective absorption.	18
Figure 2.7 Integral signals of non selective absorption in (1) THGA and (2,3) TSA (2 evaporation; 3, atomization.	19
Figure 2.8 Schlemmer diagram of the two step atomizer.	20
Figure 2.9 Atomic and background signals of Cd (a) from bovine liver and standard solution.	21
Figure 2.10 TSAVP designated by Grinstein.	22

Figure 2.11 Schematic diagram of Two-step atomizer with vaporizer purging by Grinshtein.	23
Figure 2.12 Change of chemical interferences on Pb with T_{at} in different Atomizers.	25
Figure 2.13 Heated graphite tube with filter.	30
Figure 2.14 Filter furnace proposed by Grinshtein.	31
Figure 2.15 Delay of Cu signal (A) without filter and (B) with filter.	32
Figure 2.16 Atomic absorption signals with delay of different analytes.	32
Figure 2.17 Van deemter plot for gas chromatography.	34
Figure 2.18 Modified Grinstein system.	35
Figure 2.19 Determination of Cd in standard none diluted urine sample (1) Cd signal; (2) Urine signal.	36
Figure 2.20 Effect of protection gas on the transported sample.	37
Figure 5.1 Schematic diagram of T-shaped furnace.	43
Figure 5.2 Top view of T-shaped furnace.	44
Figure 5.3 The T-shaped furnace installed in horizontal position inside the spectrometer.	45
Figure 5.4 Diagram of conventional and short temperature program.	47
Figure 5.5 High temperature chromatography using T-shaped furnace and short time temperature program in analysis of Cd in urine.	48
Figure 5.6 Effect of argon flow on absorption signals of Cd in urine.	50
Figure 5.7 Vertical position of T-shaped furnace with side, front and top view of the furnace.	51
figure 5.8 Signal for Cd in urine sample using vertical furnace position.	53
Figure 5.9 Signals for chromium determination in acidified none diluted urine. sample with vertical non coated furnace.	54

Figure 5.10 Signals for copper analysis in standard urine using vertical non coated T-shaped furnace.	55
Figure 5.11 Signals for Bi analysis in non diluted urine sample.	56
Figure 5.12 Three dimensional diagram for T-shaped furnace in horizontal position.	57
Figure 5.13 Separated Cd signals in non diluted urine sample.	58
Figure 5.14 Absorption Signals for different standard solutions of Cd.	60
Figure 5.15 Calibration curve for Cd standard solution using non pyrocoated. T-Shaped graphite furnace.	61
Figure 5.16 Calibration curve signals for different concentration of Ag.	62
Figure 5.17 Calibration curve for silver standard solutions.	63
Figure 5.18 Signals for Bi calibration curve using none pyrocoated T-shaped furnace.	64
Figure 5.19 calibration curve for standard solution of Bi using none pyrocoated T-shaped furnace.	65
Figure 5.20 Signals for different concentrations of Cu standard solution.	67
Figure 5.21 Calibration curve for Cu determination in standard solutions.	67
Figure 5.22 Signals for Mn calibration curve using none pyrocoated T-shaped furnace.	69
Figure 5.23 Calibration curve for standard solution of Mn using none pyrocoated T-shaped furnace.	70
Figure 5.24 Signals for Cd (Red) determinations in standard and spiked urine sample using the none pyrocoated furnace.	72
Figure 5.25 Standard addition method for Cd determination in standard none diluted urine sample using short temperature program.	73
Figure 5.26 Analysis of Cd using original Shimadzu tube.	75

Figure 5.27 Signals for Bi determination in non diluted urine sample using non- pyrocoated T-shaped graphite furnace and conventional program.....	76
Figure 5.28 Calibration curve for determination of Bi in urine using standard addition method and T-shaped graphite furnace.	77
Figure 5.29 The analyses of Bi in diluted urine standard sample.	79
Figure 5.30 The calibration curve signals for Cr determination in standard urine sample.	80
Figure 5.31 Standard addition method for Cr determination in standard none diluted urine sample.	81
Figure 5.32 Signal for Cr determination using original shimadzu tube.	82
Figure 5.33 The calibration curve signals for Mn determination in standard non diluted urine sample.	84
Figure 5.34 Standard addition method for determination of manganese in standard none diluted urine sample.	85
Figure 5.35 Analysis of Mn by Shimadzu furnace using Shimadzu furnace.	86
Figure 5.36 Signal for standard addition method for determination of Al in urine sample using none pyrocoated T-shaped furnace.	88
Figure 5.37 Standard addition method for analysis of Al in standard none diluted urine sample using T-shaped graphite furnace.	88
Figure 5.38 Signal for Al determination using original shimadzu tube.	89
Figure 5.39 Signals for Cu determination in standard none diluted urine sample none pyrocoated T-shaped graphite furnace.	91
Figure 5.40 Standard addition method for determination of Cu in urine using none pyrocoated T-shaped graphite furnace.	92
Figure 5.42 Signals for analysis of Cu in standard urine sample.	95

Figure 5.43 Signals for Mn in non diluted non acidified urine sample	
Mn in non diluted urine sample.	96
Figure 5.44 Mn signals in standard urine sample Seronorm	
(Py = 800°C, 1200°C) and 2400°C.	98
Figure 5.45 Signals for Mn in non diluted urine (<3.5 ppb) using short	
temperature program.	99
Figure 5.46 Magnification of the signals in figure 5.37.	100
Figure 5.47 Signals for Mn determination in non diluted urine sample	
(Bio rad< 3.5ppb) using short temperature program.	101
Figure 5.48 Standard addition method for Mn determination in standard	
urine sample (Biorad <3.5ppb) using pyrocoated T-furnace and short	
temperature program.	102
Figure 5.49 Analysis of Mn in urine with short program and with pyrolysis	
step 1200°C.	103
Figure 5.50 Signals of Al in standard none diluted urine sample.	104
Figure 5.51 Signals for Cd in bovine liver using T-shaped furnace and short	
temperature program of 42 seconds.	105
Figure 5.52 Signals for Cd in bovine liver with different heating rates.	106
Figure 5.53 Signals for Mn in bovine liver using T-shaped furnace.	107
Figure 5.54 Absorption signals for Cr in bovine muscle.	107

LIST OF TABLES

Table 1.1 Temperature program used in conventional AAS systems with variable pyrolysis and atomization temperatures.	7
Table 2.1 Characteristic masses obtained by Frech.	16
Table 2.2 Peak absorbance values for Cd at 228.8 nm and background signal for 10-fold diluted sea water.	24
Table 2.3 Pb and Cd determination of spiked urine samples and recovery values of TSAVP in comparison with the platform atomization.....	26
Table 4.1 Hollow cathode lamps manufacturers, wavelength and current used for elements under investigation.	40
Table 4.2 Standard materials.	41
Table 4.3 certified materials.	41
Table 5.1 Short time temperature program for Cd in urine sample using T-shaped furnace and high temperature chromatography approach.	52
Table 5.2 Temperature program for cadmium determination in standard solution at the resonance line of $\lambda = 228.8$ nm.	59
Table 5.3 Temperature program for silver determination in standard solution at the resonance line of $\lambda = 328.1$ nm.	62
Table 5.4 short temperature program for Bi, $\lambda = 223.1$ nm determination in standard solution using T-shaped furnace and continuous flow mode.	64

Table 5.5 Temperature program for Cu determination in standard solution at the resonance line of $\lambda = 324.7$ nm.	66
Table 5.6 Temperature program for Mn determination in standard solution at the resonance line of $\lambda = 279.5$ nm.	68
Table 5.7 Short time temperature program for quantitative analysis of Cd in urine sample using non-pyrocoated T-shaped furnace.	71
Table 5.8 Temperature program for Bi determination in urine with non-coated T-shaped furnace and continuous flow analysis.	76
Table 5.9 Temperature program for Cr determination in standard solution at the resonance line of $\lambda = 357.8$ nm.	80
Table 5.10 Temperature program for determination of manganese $\lambda = 279.5$ nm in urine using T-shaped graphite furnace and continuous flow mode.	84
Table 5.11 Temperature program for determination of aluminium $\lambda = 307.3$ nm in urine using T-shaped graphite furnace and continuous flow mode.	87
Table 5.12 Temperature program for determination of copper $\lambda = 324.8$ nm in urine using T-shaped graphite furnace and continuous flow mode.	90
Table 5.13 Short time temperature program for quantitative analysis of Cd $\lambda = 228.8$ in urine sample using pyrocoated T-shaped furnace.	93
Table 5.14 Temperature program for determination of manganese in urine using pyrocoated T-shaped graphite furnace and continuous flow mode.	96
Table 5.15 Short time temperature program used for quantitative analysis of manganese in urine sample (Biorad Mn < 3.5 $\mu\text{g/l}$).	98
Table 5.16 Summary of characteristic masses (M_{ch}) values obtained for Cd and Bi and comparable values from literature.	109

Table 5.17 illustrates the M_{ch} values obtained for the Cr and Mn and the comparable values obtained from the literature survey.	110
Table 5.18 Characteristic mass, M_{ch} values obtained for Cu and Al and the comparable values obtained from the literature data.	111
Table 5.19 Values for trace elements analysis in standard non diluted urine sample and the certified values.	111

LIST OF ABBREVIATIONS

AAS	Atomic absorption spectrometry.
A	Absorbance.
BG	Background absorbance.
M_{Ch}	Characteristic mass.
GFAAS	Graphite furnace atomic absorption spectrometry.
HGA	Heated graphite atomizer.
RSD	Relative standard deviation
STPF	Stabilized temperature platform.
T	Temperature
T_{py}	Pyrolysis temperature
T_{at}	Atomization temperature
TSA	Two-step atomizer.
THGA	Transversely heated graphite atomizer.
TSAVP	Two-step atomizer with vaporizer purging.
τ	Transmittance.
Φ_0	Initial radiant flux.
Φ	final radiant flux.
λ	Wavelength

ABSTRACT

A new T-shaped graphite furnace for atomic absorption spectrometry (AAS) has been designed for kinetic analysis of trace elements. It is installed in heated graphite atomizer (GFA-EX7) connected with Shimadzu AAS system (AA6800). The furnace is installed in two different positions vertically and horizontally between the graphite electrodes. Good separations of analyte and matrix absorption signal were achieved for many elements with vertical position with some difficulties in sample injection procedure. Better results with horizontal position installation of the T-shaped furnace. The quality and performance of the new design was examined by creation of calibration curves for standard solutions of trace elements such as Ag, Cd, Bi, Mn, Cr, Al, and Cu..

High temperature gas chromatography approach using T-shaped graphite furnace with short time temperature program and continuous flow is tested for separation of analyte and background signals. Analysis of highly interfering matrix such as urine is performed using this approach. Quantitative analyses of many elements in standard urine sample (seronormTM Trace Elements Urine LOT NO2525) and urine from Biorad were done. Standard addition curves for quantifications of high, middle and low volatile elements in that urine sample were obtained with very small background signals.

More over standard bovine muscle and bovine liver were tested for application of high temperature chromatography in graphite and short time temperature program using T-shaped graphite furnace. All cases indicate the analyses of urine sample with high organic and inorganic matrix components and can be performed with less interferences and better accuracy. Excellent agreements between measured and certified values were achieved for analyzed elements in non diluted urine sample.

The working range, characteristic mass and RSD are comparable with the corresponding analytical data using conventional AAS system.

The new furnace design provides several advantageous features including:

- (1) Very low interference effects when analyzing samples with highly interfering matrix such as non diluted urine, which is not possible to analyze when using the other commercially available types of graphite furnaces.
- (2) Sampling volume up to 100 μ l without reducing the intensity of the incident beam.
- (3) Short time analysis causing higher sample throughput.
- (4) Low contamination risk.
- (5) Very simple design.
- (6) Application of high temperature chromatography with short temperature program is possible with highly interfering matrices.
- (7) T-shaped furnace can be simply installed in AAS-system.

1. INTRODUCTION

1. INTRODUCTION

1.1 TRACE ELEMENT ANALYSIS

Trace element analysis is a process where a sample of some material like, soil, waste water, drinking water, blood, urine, minerals or chemical compound is analyzed for its elemental composition. A trace element is the species that present in the sample with amount less than 0.1%. Species from 0.1- 1% is known as minor constituent, and components more than 1% treated as major compounds [1].

1.2 SPECTROMETRIC METHODS

Spectrometric methods are a large group of instrumental methods that deals with atomic and molecular spectroscopy. The most widely used spectrometric methods are that which based on the interactions of the electromagnetic radiations and the matter. Atomic absorption spectrometry uses the interaction of light with the analyte atoms to measure the absorption which related to the concentration of the analyte atoms in the gas phase.

1.3 ATOMIC ABSORPTION SPECTROMETRY (AAS)

Atomic absorption spectrometry is a quantitative method for measuring the amount of the individual analytes in the sample using a special light source at certain wavelength in the presence of the others. Since samples are usually liquids or solids, the analyte atoms or ions must converted into free atoms to be measured. The vaporized atoms absorb ultraviolet or visible light and are transfer into higher energy level. The quantity of light absorbed by the analyte atoms is proportional to the amount of that analyte in the sample.

1.3.1 INSTRUMENTATION

The general construction of an atomic absorption spectrometer is schematically shown in figure 1.1. The most important components are; (i) a radiation source, which emits the spectrum of the analyte element, (ii) an atomizer, in which the atoms of the sample to be

1. INTRODUCTION

analyzed are formed, (iii) a monochromator for the spectral dispersion of the radiation, (iv) a detector permitting measurement of radiation intensity, (v) amplifier and (vi) read out device that presents a reading.

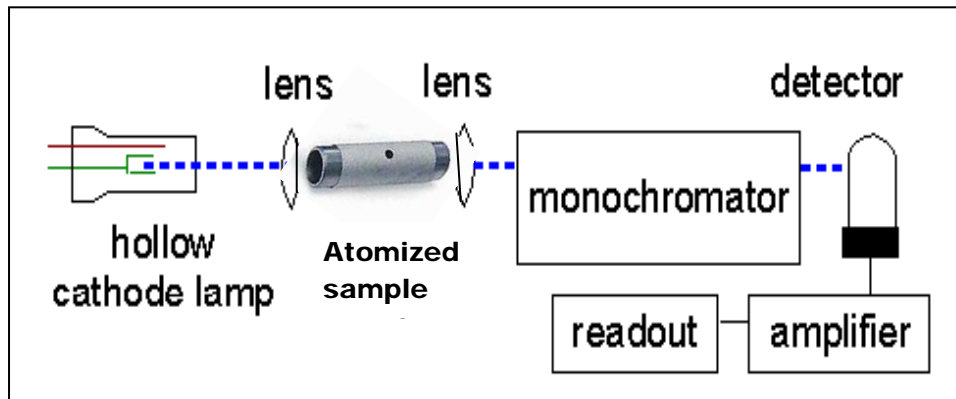


Fig .1.1 Schematic construction of an atomic absorption spectrometer

1.3.2 MEASURING THE ABSORPTION

When the light of radiation source of certain wavelength separated by a monochromator, and initial intensity is passed through a cell containing atoms in the gas phase in the electronically ground state, the intensity will decrease to a certain amount caused by radiation absorption of atoms in the cell. The absorbed radiation then directed to the detector where the reduced intensity is measured. The amount of light absorbed is corresponds to the amount of atoms in the cell and finally to the amount of element in the sample [2].

The usual quantity employed in normal absorption measurements is the radiant flux, Φ . The LAMBERT- BEER law which relates the absorbance to the concentration can be used in the following form

1. INTRODUCTION

$$A = \log \Phi_0 / \Phi = \log 1 / \tau \quad 1-1$$

where A is the absorption, Φ_0 and Φ are the initial and final radiant fluxes, and τ the transmittance.

Atomic absorption spectrometry is a relative method since linear relationship exists between the concentration of the free atoms in the measurement beam and their absorbance (Lambert-Beer law). The amount of analyte can be determined using calibration curve or standard addition method. The calibration curve is only linear within a certain concentration range of analyte, and then at higher amounts of the analyte deviation from linearity is observed. It is attributed to the shift in the absorption profile due the disordered thermal motion of the atoms and various collisions of the analyte atoms within each other and with atoms or molecules contained in the sample. This shift is shown in Figure 1.2.

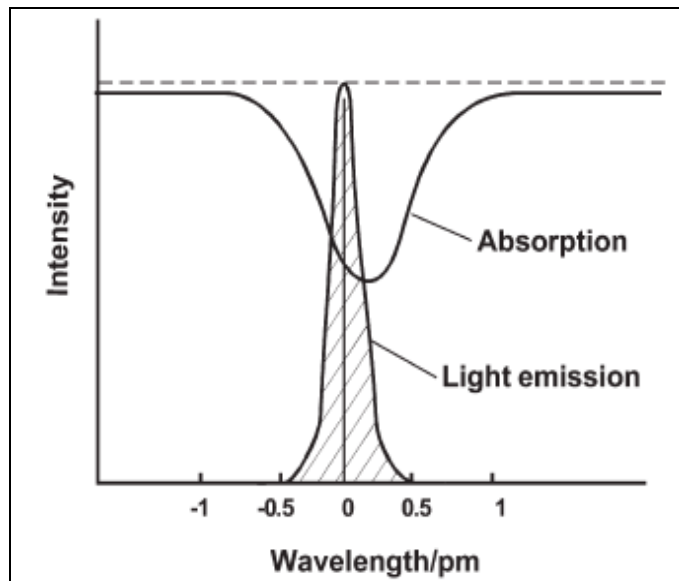


Fig.1.2 Relationship between light emission profile and absorption profile [3].

1. INTRODUCTION

1.3.3 GRAPHITE FURNACE

The emission spectrum of analyte element emitted from the radiation source is passed through an absorption cell in which a portion of incident radiation is absorbed by atoms produced by thermal dissociation in a flame or a heated tube made of graphite or tungsten. The most important function of this absorption cell is to produce analyte atoms in electronic ground state from ions or molecules present in the sample. It is the most difficult and critical process within the atomic absorption procedure.

The most advanced and widely used highly sensitive system for atomic absorption is graphite furnace [4]. In this technique, a tube of graphite is located in the compartment of the spectrometer, with the light beam passing through it. A small volume of sample solution is placed into the tube, normally through sample injection hole located in the center of the tube wall. The tube is heated electrically by running a specific heating program until the analyte present in the sample is dissociated into atoms and absorption occurs. As atoms are created and transferred out of the tube, the absorbance rises and falls forming a peak shaped signal. The peak height or integrated peak area is used as analytical signal for the quantitative determination.

1.3.3.1 SHORT HISTORY OF THE GRAPHITE TUBE

The use of the high-temperature furnace was firstly suggested by the Russian scientist B.L. Lvov in 1959. It had been developed by many workers. The most popular is the arrangement of massmann system [5], with graphite tube heated longitudinally between two electrodes and known as heated graphite atomizer (HGA). The temperature profile across the length of the tube was not symmetrical and the tube ends were usually at lower temperature than the centre of the tube. After several years of research, the geometry of the tube was finally optimized to a length between 20-30 mm and a diameter of 4-6 mm. Insertion of a platform into the tube was effective method because the platform was insulated electrically and thermally from the walls of the tube. The platform is heated by

1. INTRODUCTION

the radiations from the wall providing the required delay in atomization into the nearly stable thermal environment [2].

1.3.3.2 STABILIZED TEMPERATURE PLATFORM CONCEPT (STPF)

The insertion of a small platform inside the graphite tube was done by Slavin. The platform is a flat piece made of pyrolytically-coated graphite and placed near the bottom of the tube. A during the heating steps the tube walls heat firstly then the platform will be heated, thus the analyte will be atomized later and the gas inside the tube will reach to thermal stability before the atomization. This favors free atoms formation, maximizing sensitivity and producing a constant sensitivity regardless of sample matrix.

Figure 1.3 shows the picture of longitudinally heated graphite tube with platform, and the transverse-heated graphite atomizer (side heated) is shown in figure 1.4.



Fig.1.3 Conventional graphite tube platform,



Fig.1.4 Transverse-heated furnace

The heating profiles of the graphite tube walls, the inert gas, and the platform are shown in figure 1.5. From the profiles below, the atomization off the wall the sample volatilized

1. INTRODUCTION

at a time t_1 when the inert gas is still colder; while the sample volatilized with time delay and the inert gas is stabilized at higher temperature in case of platform t_3 [2].

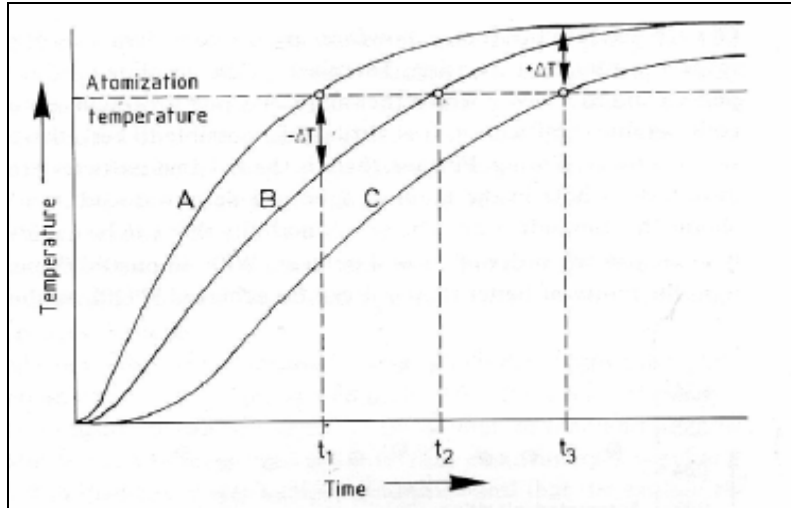


Fig.1.5 Heating profiles for the graphite tube walls (A), the inert gas (B) and platform(C) [2].

1.3.4 THE TEMPERATURE PROGRAM

The temperature program is composed of several steps, normally four steps, drying, pyrolysis, atomization and cleaning. Each step has its own temperature, holding time, heating rate and argon flow depending on the type of element wither it is high, middle or low volatile element and type of sample to be analyzed. Table 1.1 shows conventional temperature program with variable pyrolysis and atomization temperature depending on the type of sample and element under investigation.

1. INTRODUCTION

Table.1.1 Temperature program used in conventional AAS systems with variable Pyrolysis and atomization temperatures

Step	T (°C)	Time (s)	Mode	Argon flow (ml/min)
1	120	10	Ramp	500
2	120	20	Hold	500
3	variable	10	Ramp	500
4	variable	20	Hold	500
5	variable	variable	Hold	10
6	2400	4	Hold	500

1.4 INTERFERENCES IN ATOMIC ABSORPTION SPECTROMETRY

Interferences in graphite furnace atomic absorption spectrometry (GFAAS) can be classified into three classes, which are chemical, spectral and instrumental interferences. Interferences mostly arise because of escaping of the analyte off the furnace before atomization process takes a place. *Chemical interferences* are result of interactions of the analyte and the sample matrix components forming molecules. Formation of carbides, intercalation compounds and other reactions causing incomplete atomization of the analyte are the main types of chemical interferences.

Spectral interferences can be classified into three sub classes, broad-band background attenuation, structured interferences, and stray radiation. Broad-band background attenuation arises from molecular absorption and scattering of the primary source. Molecular absorption in the ultraviolet and visible regions of the spectrum can be caused by thermally stable molecules. Scattering interferences arises if some of the matrix components produce aerosol particles which lead to reduction of the intensity of the radiation source [6].

1. INTRODUCTION

Structured interferences arise when the absorption profile of the undesired element or molecular structure overlaps the band width of the primary or secondary radiation source.

Stray radiation is radiation with wavelength different from the analyte wavelength and occurs outside the spectral bandwidth of measurement. Stray radiation or stray light could be absorbed more or less by the sample causing an error.

Instrumental interferences arises if the instrument is not able to measure the analyte absorption accurately because of signals rapid and transient, hence the accuracy strongly depends on the timing associated with the instrument electronics.

In trace element analysis, the most important type of interferences is the chemical interference which has strong effects on the absorption signal of the analyte atoms. Some of matrices effects on the analysis are summarized in the next section.

Co-volatilization of trace elements with sodium chloride in the pyrolysis step leads to loss of sensitivity in the analysis of sea-water samples [8]. Karawowska et al found that halogenated organic solvents strongly depress iron signal due to the formation of volatile iron chloride [9]. Another group studied the effect of perchloric acid on the signal of lead [10]. Fuller discussed the same effect on the signals of thallium [11] and Koirtyohann et al. [12] showed that the signal of aluminum, gallium and thallium were reduced by 95 % due to the presence of perchloric acid. Vapor-phase interferences caused also known effects on the absorption signal in the trace element determination, such kind of interferences occurs during the atomization stage. Hutton [13] observed strong C_2 and CN molecular bands in the furnace when nitrogen was used as purge gas. Lvov and Pelievia reported that 30 elements formed monocyanides in presence of nitrogen. Lvov and Ribzyk reported the absorption spectrum of AlCN for the determination of aluminum with nitrogen as purge gas, Al_2C_2 molecular spectrum observed when using argon as purge gas [14].

1. INTRODUCTION

The thermal conditions of the graphite furnace played also of important rule. Frech et al. showed that the sample volatilized, while the furnace is still heating under non-isothermal conditions and a part of the analyte vapor phase escaped out of the tube before the atomization stage [15]. The use of stabilized temperature platform concept leads to more isothermal conditions and reduces to high extent the volatilization and vapor phase interferences. Special chemical compounds introduced into the sample solution or the graphite tube, called chemical modifiers have been found to enhance the sensitivity and reproducibility by stabilizing the analyte compounds and reducing the matrix effect.

1.5 CHEMICAL MODIFIER

The concept of chemical modifiers was introduced by Ediger in 1973 [16]. Chemical modifiers can be defined as compounds that are introduced into a graphite atomizer simultaneously with the test sample, and during the measurement it causes decreasing of matrix effects. The mechanism of action of most chemical modifiers consists of the removal of the sample matrix at the pyrolysis stage, this can be attained either by converting the matrix compounds into volatile compounds or by decreasing the volatility of the analyte, and gives the possibility to evaporate low volatile matrix components at temperatures above 1000°C. The use of the unsuitable modifier will not act as a modifier, but may act as an additional matrix compound and interferes with the analyte absorption.

Chemical modifiers can be classified into the following groups [17]:

- (1) Nitric acid and oxalic acids and corresponding ammonium salts ;
- (2) Metal nitrates (except platinum-group metals);
- (3) Ammonium phosphates;
- (4) High melting carbides;
- (5) Ascorbic acid, EDTA; and its salts;
- (6) Transition metals with higher oxidation states (W^{+4} , Mo^{+4} , Zr^{+4} , etc.).
- (7) The universal modifier (Pd/Mg nitrate).

During the last twenty years many workers studied the effectiveness of chemical modifiers in trace element analysis to reduce the matrix interference. Beinrohr et al. [18]

1. INTRODUCTION

studied the effect of ammonium fluoride on the determination of thallium. Shan [19] is the first one who improved the action of potassium dichromate as matrix modifier for determination of aluminium in urine. Holcombe studied the function of phosphate modifier in electrothermal atomizers [20]. The function of ascorbic acid in the determination of lead by atomic absorption spectrometry is discussed by Chakrabarti in 1989 [21]. Welz studied the effect of mixture of Pd and Ca on the determination of phosphorous [22]. The effect of various chemical modifiers, including nitrates of palladium, nickel, magnesium, calcium, lanthanum, europium and aluminium, on the analytical signal of selenium in a graphite furnace was studied by Docekal in 1991 [23].

Determination of antimony by graphite furnace atomic absorption spectrometry using five different matrix modifiers, nitric acid, copper, nickel, molybdenum and palladium, together with L'vov platform was also studied [24]. In 2005 Welz again investigated the interference of nickel chloride on the determination of copper by electrothermal atomic absorption spectrometry [25]. Campos studied the function of Iridium as a thermally deposited permanent modifier on the determination of lead by GFAAS [26]. Pd, Ir and Rh have been investigated as chemical modifiers for the simultaneous determination of As, Sb and Se by electrothermal atomic absorption spectrometry [27].

One can observe from the last short survey on the effectiveness of different chemical modifiers on the analyte under investigation that selection of the chemical modifier depends on kind of analyte, kind of matrix, temperature program and type of the graphite furnace used, which in turn means that there are many parameters taken in account for trace element analysis with GFAAS. Such kind of complex optimization procedure leads to increase analysis costs by increasing analysis time and instrument and material consuming.

In the next chapter we will describe many developments of graphite furnace within the last twenty years in order to reduce the matrix effect in the analysis as much as possible. Several furnace designs were made and materials rather than graphite such as tungsten is also studied.

2. THEORITICAL AND BACKGROUND KNOWLEDGE

2.1 TYPES OF GRAPHITE ATOMIZERS

The first analytical electrothermal atomizer for trace element determinations by atomic absorption spectrometry was the L'vov furnace [28]. This furnace was a two-step system and could be used at selected pressures. In this system, sample vaporization and atomization takes place in two clearly separated units, i.e. graphite electrode on which the sample is deposited and then vaporized and a heated tube where the sample vapour is atomized and the analyte concentration measured. This de-coupling of vaporization and atomization resulted in outstanding performance. At the same time this system was relatively complex constructed and therefore not suitable for routine work [29].

Due to this separation, this cuvette secured low interference levels and high sensitivity, but the sample volume was extremely small (1 μ l) which in contrast led to low sensitivity and reproducibility. These were the main reasons why the development of commercial atomizers moved in another direction and the principle of separating vaporization and atomization zones was neglected for certain period of time.

The Massmann type atomizer combines in the same graphite tube drying, pyrolysis, vaporization and atomization of the sample. But compared with the L'vov cuvette, reliability and sensitivity of the analysis decreases, and when analyzing samples with strongly interfering matrices several chemical interferences occur.

In order to overcome the drawback of the classical electrothermal atomizer, a new oven design was created, again taking idea of separating vaporization and atomization zone. One of the most successful solutions was the appearance of graphite furnaces with semi-separated vaporization and atomization zones in the form of graphite furnaces with different ballast bodies [30-33]. In this case the sample is injected onto or inside the ballast body placed in the furnace. The sample will be atomized with some delay if the ballast is in poor contact with the furnace body. STPF atomizer is the most well-known

2. THEORITICAL AND BACKGROUND KNOWLEDGE

version of a ballast body. Atomizers with different ballasts could solve analytical problems to some extent. More problems could be solved using different matrix modifiers [34] and transversely-heated graphite furnace with and without end capped graphite furnaces [35, 36].

The drawback of these furnaces is the limitation of the size and the shape of the ballast body depending on the size and the shape of the graphite tube itself, because the ballast body must never block the light beam. This limits the sample volume and hence the sensitivity of the measurement. Moreover noncomplete separation of vaporization and atomization zones does not provide the maximum possible atomization degree [37, 38]. A number of the so called filter furnaces were also developed [31].

In ultra trace determinations of metal impurities, Grinshtein et al. [39] demonstrated the separation of metal vapour by passing them through porous graphite inserted in the graphite tube.

Increasing the efficiency of the analyte determination and matrix effect reduction guide the researchers to think in the complete separation of vaporization and atomization zones, which could be done by creating two-step atomizer systems. A number of two-step atomizers have been developed by Frech and coworkers [40-45]. The first two-step atomizer suggested by Frech in 1983 is shown schematically in figure 2.1. This was complex design with four electrodes to acts as side heated tube.

2. THEORITICAL AND BACKGROUND KNWOLEDGE

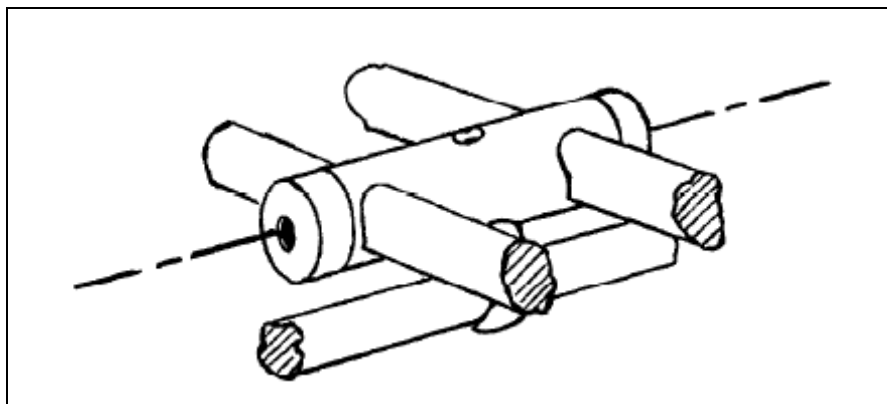


Fig.2.1 The first two-step atomizer designed by Frech in 1983 [45].

During atomization, spatially isothermal conditions were achieved by using side heated tube. Other two-step atomizers were carried out by different authors. This chapter will focus on the most important two-step atomizers within the last two centuries.

2.1.1 TWO STEP-ATOMIZER DESIGNED BY FRECH

Frech started in developing two-step atomizer systems 25 years ago. In this section we will describe the most effective system developed by him self in 2000.

2.1.1.1 SYSTEM DESCRIPTION

The two-step atomizer was consisted of two separated parts, one called cup and the other called tube (see figure 2.2). The system was installed in a modified Perkin-Elmer Analyst 700 with deuterium lamp background correction. The cup was used as vaporizer and a tube as atomizer. Heating of the graphite cup was controlled by the Analyst 700 and the tube heated by additional power supply and triggered by AA Win lab software.

Temperature was controlled by an in-house built control unit containing optical feed back allowed fast heating of the tube to selected temperatures [46].

2. THEORITICAL AND BACKGROUND KNWOLEDGE

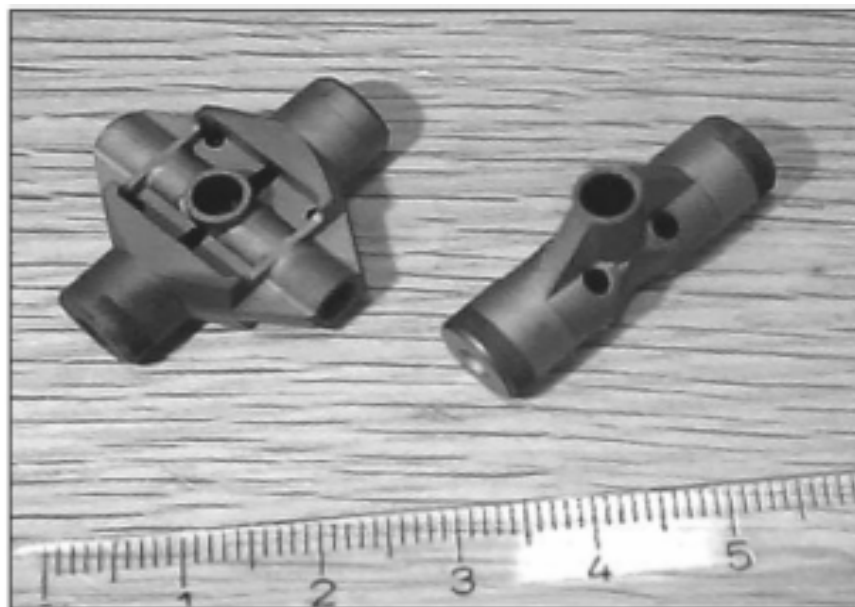


Fig.2.2 Graphite cup (right) and side heated tube (left) with integrated contacts [46]

Fig.2.3 shows the furnace housing, formed as a clamshell. In the upper part of the housing, the contacts of aside-heated graphite tube are clamped between a pair of graphite cylinders, pressed inside brass tubes, which in turn are tightly pressed into water-cooled brass blocks.

2.1.1.2 FEATURES OF THE FRECH SYSTEM

For determination of losses of sample vapour through the gap between the cup and the tube, Cd, Pb, and In standard solution were used. Sensitivity was monitored for cup to tube distances between 0.20 and 0.95 mm. These results were compared with that which were carried out for the same elements but with distance between 1.0 and 7.0 mm [47]. The relative signal for 1.0 and 2.0 mm were 1.00 and 1.01 respectively. For the gaps between 3.0 and 7.0 mm the peak area sensitivity decreased from 0.91 to 0.28. These results were explained by the presence of an inward convective flow in the gap region. Decreasing the distance between the cup and tube increase the linear velocity of the convective flows, and eliminate diffusion losses of vapour through the gap, which explains the practically unchanged sensitivity for the 1 and 2 mm gaps as shown in fig 2.4.

2. THEORITICAL AND BACKGROUND KNWOLEDGE

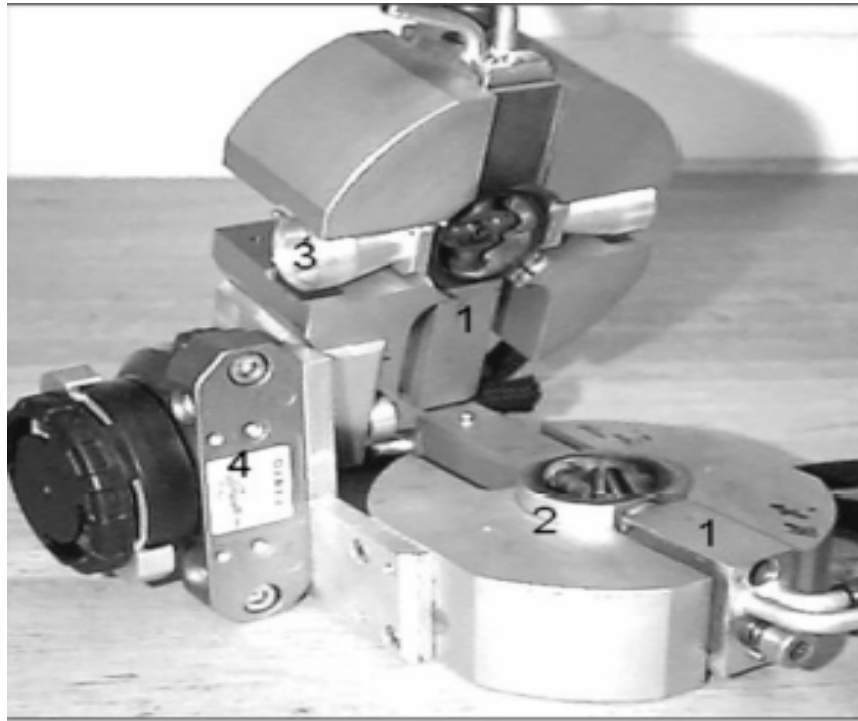


Fig.2.3 Furnace housing with installed cup and tube. (1) Water cooled contact block; (2) Lower brass housing; (3) holder for quartz windows; (4) pneumatically driven mechanism for opening and closing the furnace [46].

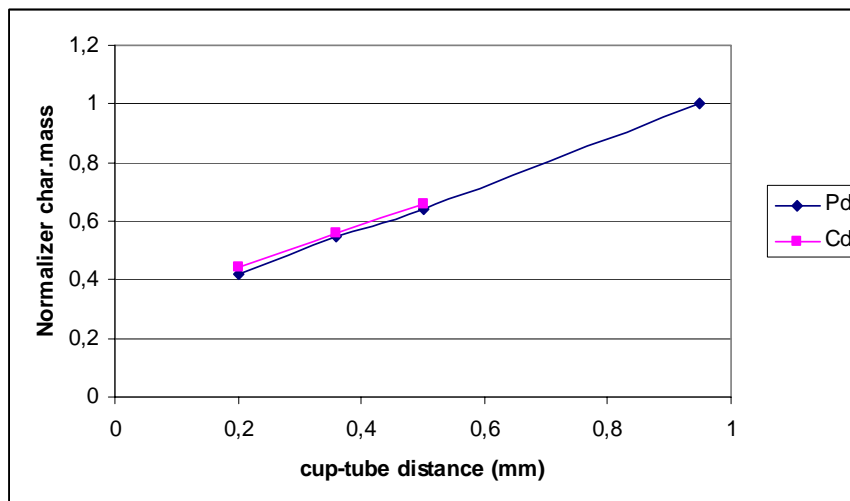


Fig.2.4 Normalized characteristic masses as a function of the gap distance for Cd and Pb [46].

2. THEORITICAL AND BACKGROUND KNOWLEDGE

The characteristic masses with different volatilities obtained with the two-step atomizer by Frech and the values for same elements obtained using transversely heated graphite furnace (THGA) are shown in table 2.1. Better characteristic masses were achieved with this system as compared with conventional system.

Table 2.1 Characterstic masses (M_{ch}) obtained by Frech TSA and THGA [46]

Element	TSA (pg)	THGA (pg)
Cd	0.3	1.3
Pb	7.4	30
In	18	80
Co	5.8	17
Al	14	31
Ni	7.6	20
Cr	1.8	7
Ag	1.9	4.5

The observed memory effects for Co as a function of the analyte mass introduced using the two atomizers for 10 ng of Co introduced, the THGA and two-step atomizer showed 0.5 % and 2 % carry over respectively.

Disadvantages of this system are that the analyte transfer from the atomizer to the vaporizer is only affected by normal diffusion. Signals of analyte are expected to be very broad and overlapped on each others in case of real samples. No application of this system to analysis of real samples has been reported. The loss of the analyte through the cup-tube distance was also unavoidable.

2.1.2 TWO-STEP ATOMIZER BY NAGULIN [48]

This work is created in the year 2003 by Nagulin and his research group. They tried to separate the lower and upper part of the furnace in order to create two-step atomizer in one furnace. The design is described in figure 2.5 standard tube atomizer (1) was divided into two parts, A gap was made in the side of the right contact and a mica bad for insulating the upper and lower part of the furnace was inserted (4).

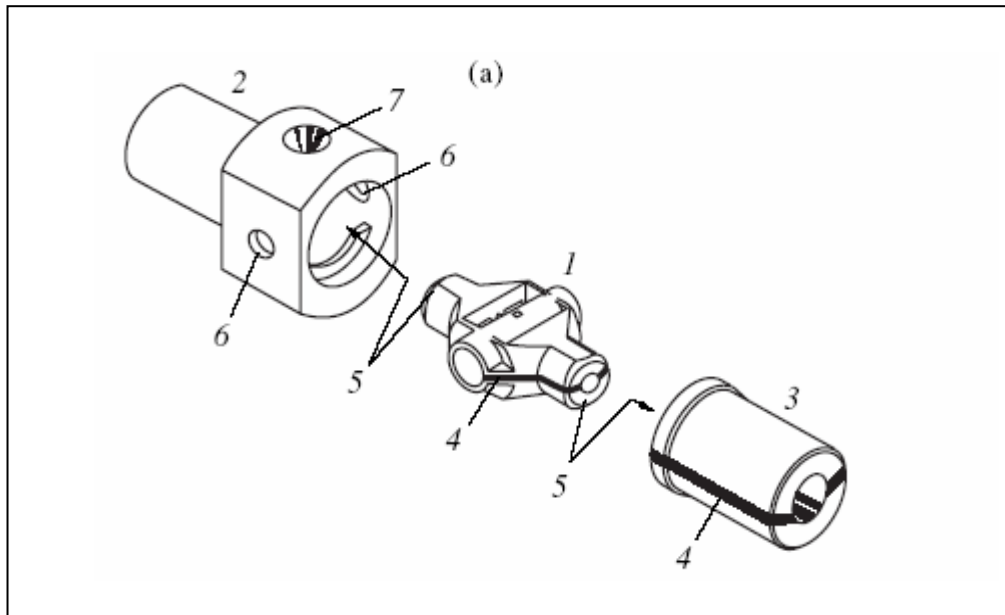


Fig.2.5 Design of two-step atomizer (1) graphite tube, (2,3) contacts, (4) mica separator, (5) contact surface, (6) light beam, (7) injection slit [49]

To apply the current to the tube, the right graphite contact was cut along the furnace and isolated with mica; such design offers two electrically and thermally isolated parts of the original tube. A special computer-driven power supply unit allows controlling the heating of the lower and the upper parts of the graphite furnace.

2. THEORITICAL AND BACKGROUND KNWOLEDGE

With this system it was possible to heat the sample firstly in the lower part and condensate it on the upper colder part of the tube, which could be heated later again up to the atomization temperature.

Nagulin studied the effect of sodium chloride matrix on the determination of highly volatile element (cadmium and lead) using the commercially available transverse-heated graphite furnace and two-step atomizer. He found that, for two step atomizer, the maximum allowable mass of sodium chloride for which the background at lead and cadmium lines could be adequately compensated was 17-30 times higher than that for the commercial atomizer. The effect of sodium chloride could be suppressed because of sample fractionation and distillation during its evaporation and condensation steps.

Figure 2.6 shows the signal of the nonselective absorption of the matrix at the cadmium absorption line (228.8nm) for two-step atomizer and transverse-heated atomizer

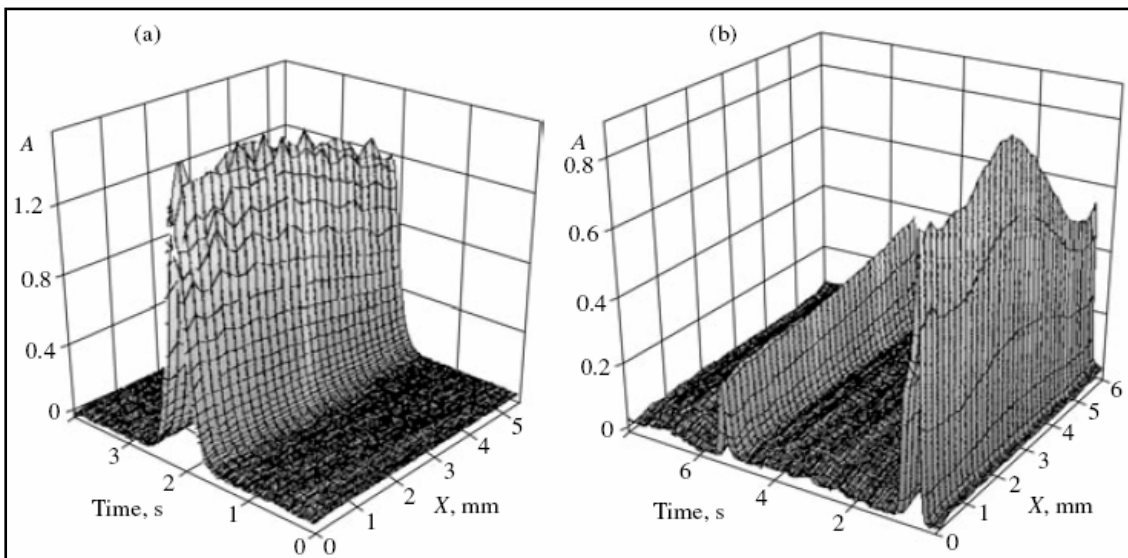


Fig.2.6. Signal of nonselective absorption of 18µg NaCl at Cd line (228.8nm) in (a) THGA with platform, (b) TSA [49]

2. THEORITICAL AND BACKGROUND KNOWLEDGE

The advantage of this system that it supports the arrival of the analyte element into a temperature stabilized atomizer volume (STPF), hence the sensitivity of the analyte increased and the matrix interference decreased compared with the transverse heated graphite furnace as shown in figure 2.7.

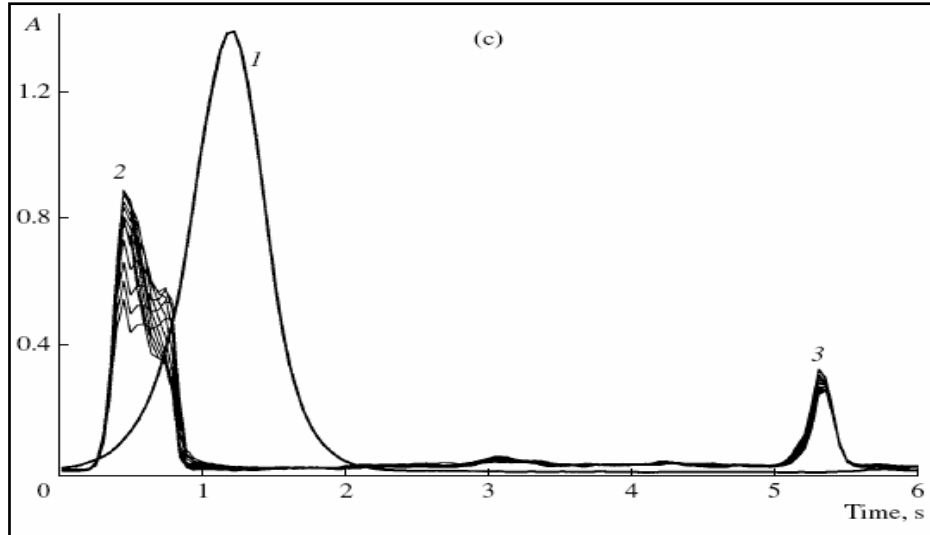


Fig.2.7 Integral signals of nonselective absorption in (1) THGA and (2,3) TSA (2 evaporation; 3, atomization)

More experiments should be done to improve this system, because there is no information about both middle and low volatile elements with highly interfering matrices such as urine, blood and waste water.

The upper part of the graphite furnace is not completely isolated and could be heated by radiation from the lower part, also because of the double vaporization of the sample, highly percent of the analyte will be lost through the injection hole of the furnace is expected. Further more the analyses were carried out along the furnace i.e. in all time measurements of both analyte and matrix occurs.

2. THEORITICAL AND BACKGROUND KNWOLEDGE

one. Comparable results have been achieved for the determination of magnesium, potassium, sodium, manganese and zinc in titanium oxide.

This system is practically the same as that designed by Frech [46]. The advantages of this system were the usage of highly efficient Zeeman-effect background corrector instead of the deuterium lamp background correction and the possibility of the solid sampling.

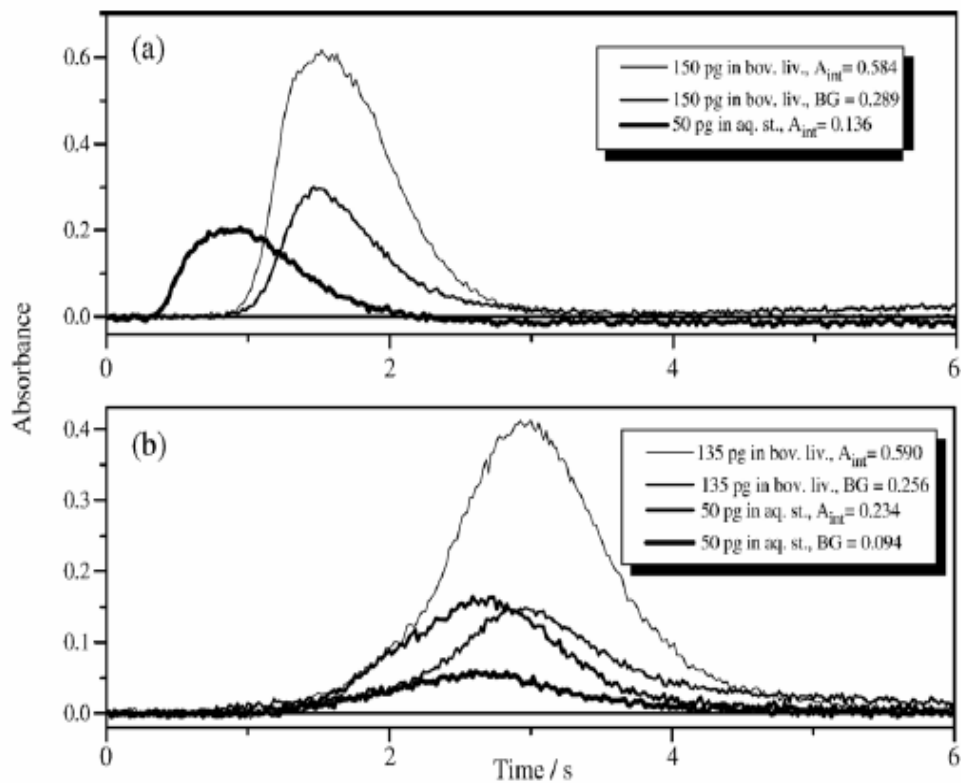


Fig.2.9 Atomic and background signals of Cd (a) from bovine liver and standard solution; (b) Bovine liver in presence of chemical modifier and pyrolysis [50]

This system is relatively new, and there is not enough information about the performance of the system for low volatile elements determinations and influences of highly interfering matrices such as urine. There is no argon flow through the vaporizer leads to broad peaks even for Cd (3 seconds) which is in fact a highly volatile element and gives

2. THEORITICAL AND BACKGROUND KNOWLEDGE

normally a very sharp peak (less than 1.5 seconds). This means that the sample transferred into the atomizer by normal diffusion, hence high memory effect in the determination of low volatile elements and very broad peaks of these elements are expected. No more information for other elements has been published up to now.

2.1.4 GRINSHTEIN SYSTEM

The two-step atomizer with vaporizer purging (TSAVP) consists of a longitudinal heated graphite atomizer-cuvette and transverse-heated graphite tube-vaporizer placed horizontally on the side of the cuvette-atomizer as shown in figure 2.10. The atomizer and vaporizer were heated independently by two power supply units [51]. The length of the atomizer and the vaporizer were 35 mm and 15-20 mm, respectively. Figure 2.11 shows a schematic diagram of the TSAVP proposed by Grinshtein and the process of transferring the sample from the vaporizer to the atomizer, and the double vaporization concept.

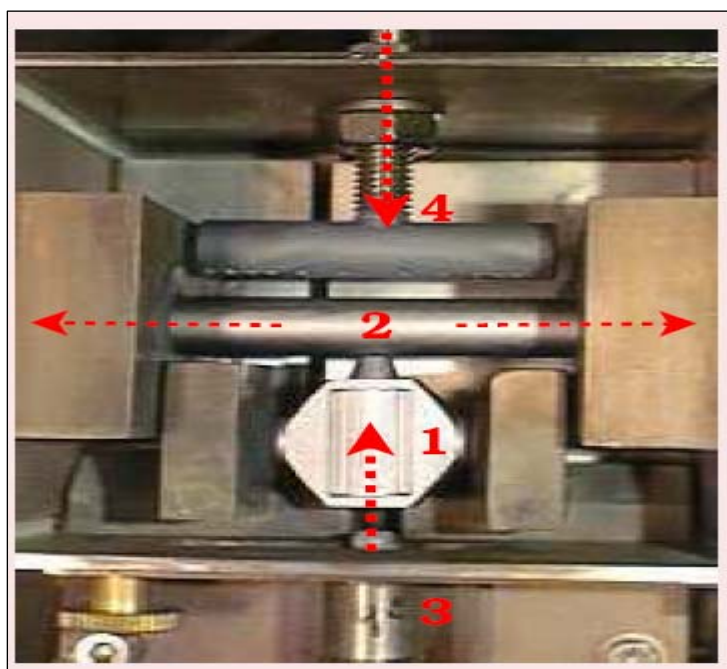


Fig.2.10 TSAVP designated by Grinshtein (1) vaporizer; (2) Atomizer; (3) purges gas; (4) outer argon.

2. THEORITICAL AND BACKGROUND KNWOLEDGE

The double vaporization concept based on vaporization of the sample two times, firstly sample is vaporized, transferred into atomizer and trapped in it then trapped sample re-evaporized gained in atomizer. This re-evaporization reduced the matrix interferences to some extent.

The sample vapour reaches the atomizer with the argon flow. Two different modes of vaporizer purging can be used, continuous mode, or gas stop mode. Mostly sample volume was 10 μl in the experiments other volumes some times were used [52].

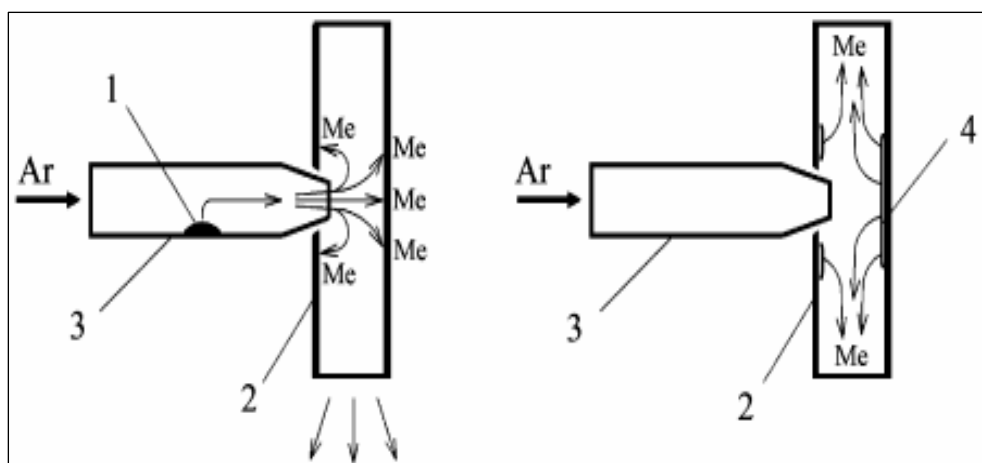


Fig.2.11 Schematic diagram of Two-step atomizer with vaporizer purging; 1 solid sample, 2 atomizer, 3 vaporizer; 4 condensed sample [51].

Grinshtein studied the dependence of the analyte and the background signals for sea water samples on the atomization temperature in three different atomizers using the two-step atomizer and the heated graphite atomizer (HGA) and conventional Hitachi graphite furnace system.

HGA showed the highest background signal even with five-fold diluted sample, the absorbance values were 3.0 for atomization temperatures between 2200 and 2800°C. TSAVP showed background absorbance readings between 0.8 and 1.3 which is the

2. THEORITICAL AND BACKGROUND KNWOLEDGE

lowest signal of the three atomizers with three-fold diluted sample. The values of the analyte absorbance and the background with different atomizer are shown in the table 2.1 below.

Table 2.2 Peak absorbance values for Cd 228.8 nm and background signal for 10-fold diluted sea water, sample volume was 10 μ l. (3.2 ± 0.3 ng/ml)

Atomizer	T _{at} (°C)	Absorbance signal	Background signal
TSAVP	1800	0.017	0.15
Hitachi (STPF)+M	2100	0.024	1.6
HGA-700 (STPF)	2000	-----	2.8

The STPF technique was used with HGA and Hitachi atomizers. In addition a Pd modifier was used with the Hitachi atomizer. In the case of the TSAVP the background value was small, in the case of Hitachi platform furnace with the matrix modifier very high. The HGA-700 platform furnace without modifier could not be used because the background signal was so high that Cd could not be determined.

The effect of the matrix on the absorption signal of Pb was studied by comparing the absorption signal of 0.5 ng of Pb in distilled water with the same amount of Pb in ten-fold diluted sea water in different atomizers at different atomization temperatures. The results are shown in fig 2.12. As can be seen from the figure at higher atomization temperatures the matrix effect is completely removed using TSAVP since the percent ratio of absorbance signals of Pb in water and sea water sample is 100%, while the same ratio is 80% when Hitachi and 60% when HGA-700 was used. The argon purge gas in TSAVP was 20 ml/min.

2. THEORITICAL AND BACKGROUND KNOWLEDGE

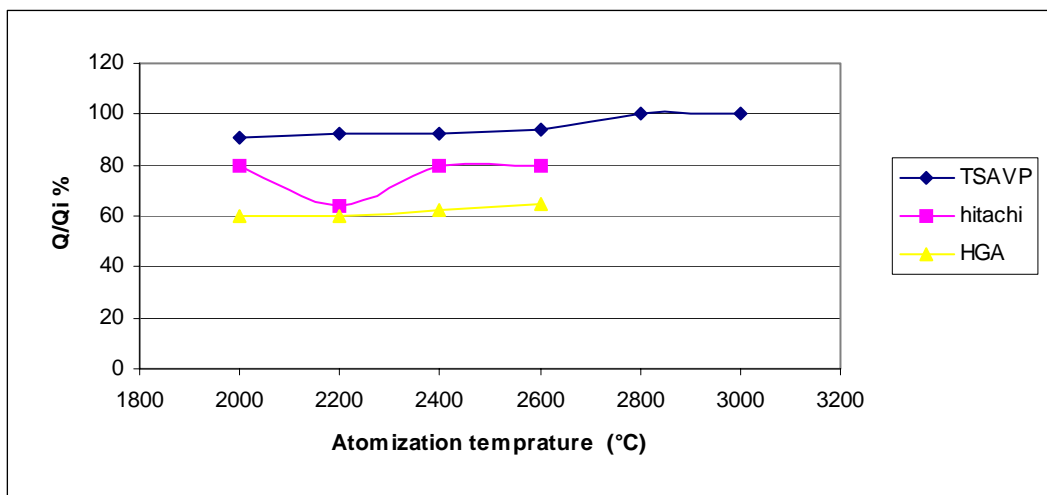


Fig.2.12 Change of chemical interferences on Pb with atomization temperature in different atomizers, Q_i is the integrated Absorbance of 0.5 ng Pb in distilled water, Q the same in ten-fold sea water.

Analysis of urine sample using stabilized temperature platform furnace STPF, rapidly heated graphite tube atomizer and chemical modifiers with the sample pretreatment provides interference free analysis [53-55]. Radzuik and Romanova [56] found that the STPF techniques cannot be fully free from interferences in the determination of Pb. The results of recovery measurements with two step atomizers with different ordinary modes and the conventional platform without modifier for Pb and Cd are shown in table 2.3 and 2.4.

With TSAVP, the deuterium background corrector was used, therefore diluted urine samples could only be measured in the ordinary operating mode because the non diluted urine samples showed higher than 0.6 absorbance values which are out of the working range of this corrector. For the double vaporization mode the background signal was reduced to less than 0.3 for Cd and 0.1 for Pb with recovery of about 100% for all samples under investigation.

2. THEORITICAL AND BACKGROUND KNOWLEDGE

Table.2.3 Pb and Cd determination of spiked urine samples and recovery values (R) of TSAVP in comparison with the platform atomization.

Element	Amount added (µg/l)	Platform atomization			TSAVP		
		found conc.(µg/l)		R ^b	found conc.(µg/)		R ^c
		Initial	spiked	(%)	Initial	spiked	(%)
Cd	1.00	0.14 ± 0.05	1.5 ± 0.05	105	0.2 ± 0.01	1.16 ± 0.05	96
	2.00	2.2 ± 0.05		136	2.2 ± 0.1		100
Pb	10.0	2.0 ± 0.5	10.0 ± 0.9	80	2.6 ± 0.17	12.9 ± 0.7	103

^a The number of replicates n = 7 .

^b The samples were threefold and fourfold diluted with water for Cd and Pb respectively.

^c R= (conc. in spiked sample– conc. in initial sample/Added conc.)×100%

With Grinshtein system and the double vaporization concept it was possible to measure the amount of some analytes in presence of highly interfering matrix such as sea water and urine. The characteristic masses and the recovery of this system are much better under these working conditions than for the transverse heated atomizer and stabilized temperature platform systems.

Table 2.3 Determination of Pb and Cd in seronormTM trace element urine reference sample and recovery values (R) for TSAVP double vaporization in comparison with platform.

Element	Known conc. (µg/l)	Platform atomization		TSAVP, double vap	
		Found conc. (µg/l)	R (%)	Found conc. (µg/l)	R ^c (%)
Cd	0.35	0.31 ± 0.07	89	0.36 ± 0.02	103
Pb	3.0	1.9 ± 0.2	63	3.12 ± 0.2	104

2. THEORITICAL AND BACKGROUND KNOWLEDGE

One of the disadvantages of Grinshtein system is the measurement of the analyte element along the atomizer tube. Spatially and temporally separation of the analyte and the matrix is not possible, because the matrix is also measured in the same time and position with the analyte.

Grinshtein proposed a method [57] using the same principle of the double vaporization to determine the concentration of Hg in the Russian drinking water using this system, because the conventional method of Hg determination is complicated and needs a reduction of the sample firstly by using reducing agent (contamination risk). On the other hand it is not possible to determine the Hg concentration in drinking water using HGA and THGA because of the low concentration of Hg, and the relatively high characteristic masses of Hg with both of them.

The main disadvantages of this system are:

- The complex design of the system (not available commercially).
- The measurement of the analyte concentration along the atomizer tube allows the matrix also to be measured with the analyte at the same moment.
- The atomizer housing is relatively large and not well protected with argon. This leads to a shorten life time of the tube.

Other authors tested atomizers manufactured from other materials rather than graphite in order to overcome the interference problems. Kiyohisa [58] studied the effect of using tungsten tube for atomic absorption spectrometry. Xiandeng Hou [59] used a tungsten-coil device for atomic absorption spectrometry, the limit of detection with this device were a factor of ten from that with the conventional AAS systems. Salido [60] determined Pb in blood samples using tungsten coil atomizer. Dagmar [61] discussed the action of tungsten atomizer as modifiers. Reid [62] Built and studied an improved version of a tungsten filament atomizer for atomic absorption spectrometry. Camero [63] studied the carbide forming elements using tungsten coil platform.

2. THEORITICAL AND BACKGROUND KNOWLEDGE

Williams [64] introduced commercial tungsten filament Atomizer for analytical atomic spectrometry. Atomization efficiencies for indium and tin in graphite furnaces from different atomizer surfaces, i.e. pyrolytically coated platform (PG), palladium modified pyrolytically coated platform (PdPG) and pyrolytically coated platform, modified with zirconium carbide (ZrPG), have been studied by Yang [65]. Boronitride platform has been used in electrothermal AAS for determination of Cd in sees water samples without chemical modification [66]. Reinaldo studied the use of silica and Nickel atomizer [67]. A direct determination of cadmium by electrothermal atomization atomic absorption spectrometry with a molybdenum tube atomizer has been investigated [68].

Many other Tungsten devices have been used in analytical atomic spectrometry for approximately 25 years [69].

2.2 THE HIGH TEMPERATURE CHROMATOGRAPHY IN AAS

As mentioned in previous sections in chapter one and two, many authors tried to overcome the matrix interference problems accompanied with the trace element analysis by GFAAS using matrix modifications, addition of ballast bodies inside the furnace, addition of materials to act as filters, different forms of furnaces (side heated with platform, graphite rod, tube in tube, graphite capsules,etc) and several two-step atomizer designs. The so-called *high temperature chromatography* using filter furnace is also used to overcome some of interference problems. In this section we will discuss briefly the most important studies in this new area of research.

The use of electrothermal atomizers with graphite filter provides additional possibilities in reducing matrix effect and metal vapour separation. High temperature chromatography could be applied within the graphite furnace after installation of graphite filters inside the graphite tube as mentioned before. The sample is injected in the zone which is separated from the measuring zone by the filter, heated atomized and the evaporated materials transferred into the measuring zone by passing it through the filter. The sample components penetrate the stationary phase of that chromatographic system (filter) with

2. THEORITICAL AND BACKGROUND KNOWLEDGE

different speed depending on their physical interactions with the stationary phase and the diffusion coefficient of the sample components. If the sample components travel with different speed they will be detected at different retention time. Thus components of the sample can be separated.

A number of publications about using of filter furnaces were published within the last two decades. As example the direct filtration through porous graphite for atomic absorption analysis of beryllium particulates in air was investigated [70]. Katskov proposed and discussed the filter furnace as a new atomization concept for electrothermal atomic absorption spectroscopy [71-77]. In 2003 the same author published the usage of transverse heated filter atomizer (THFA) in determination of Cd and Pb in urine, and its analytical performances were investigated using a PerkinElmer SIMAA 6000 atomic absorption spectrometer [71].

The filter furnace atomizer proposed by Katskov is shown in figure 2.13. The sample is injected into the filter, then dried, evaporized and atomized within the filter and transported to the measuring zone. But before measuring the urine sample should be firstly diluted 5-10 fold. The sensitivity of the determination is not good enough because the filter inserted inside the furnace reduces the original light path through the furnace as can be seen in figure 2.13.

The use of filter by Katskov was focused only on the reduction of matrix signal and not on separation of analyte and matrix from each other. Next section will focus on separation of analyte and matrices by mean of high temperature chromatography using graphite filter as stationary phase and measurement of the separated signals using atomic absorption spectrometry.

2. THEORITICAL AND BACKGROUND KNWOLEDGE

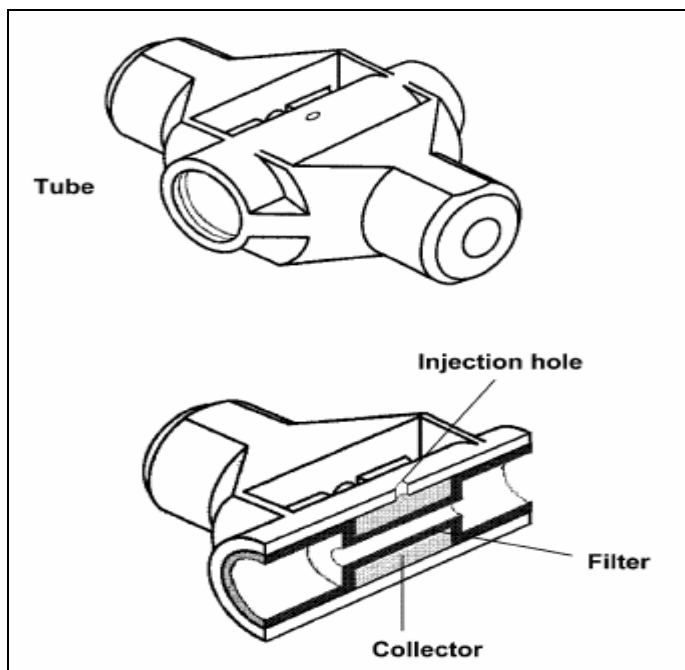


Fig. 2.13 Heated graphite tube with filter developed by Katskov [71]

2.2.1 HIGH TEMPERATURE CHROMATOGRAPHY SYSTEM PROPOSED BY GRINSHTEIN

In 1997 Grinshtein et al. studied the separation of different metal vapours for atomic spectroscopy by using high temperature chromatography on graphite and atomic absorption spectrometry as measuring method [39]. At high temperatures the porous graphite partition works as a stationary phase of a chromatographic column. The separation efficiency of graphite filter depends on the temperature of the column and on the carrier gas flow through the partition. Figure 2.14 indicates the filter furnace designated by Grinshtein. During the heating of these atomizers the sample vapours enter the analytical measurement zone after flowing through the porous graphite walls of the filter with the help of argon gas flow. At high temperatures different atomic vapours interact with the graphite material by different mechanisms. For example the atoms Cd, Pb, Tl, Ge, Sn, Sb, Bi, Se, Zn are practically inert. Atoms of Fe, Co, Ni, Mn, Cr, Cu, Ti,

2. THEORITICAL AND BACKGROUND KNOWLEDGE

Mo, V and some other metals interact chemically with carbon and form stable or metastable carbides or solid solutions or intercalation compounds [39].

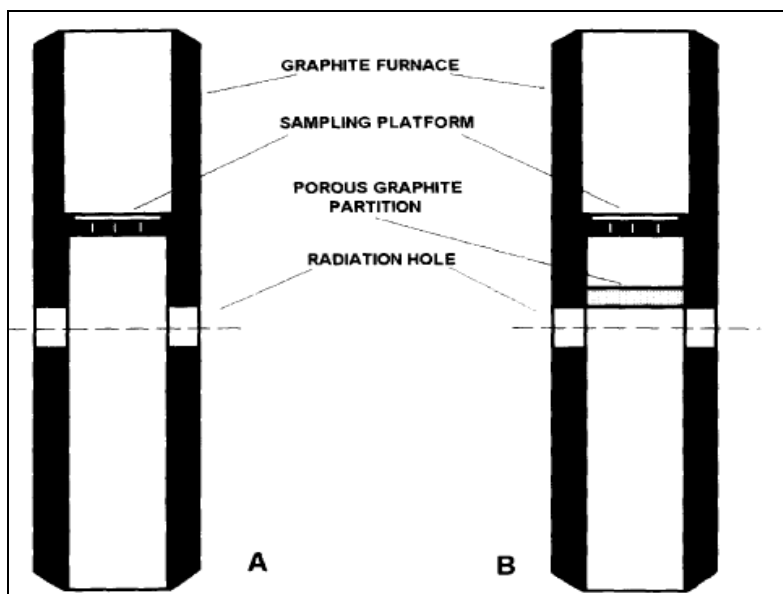


Figure 2.14 Filter furnace proposed by Grinshtein; A. without filter; B with filter [39]

Figure 2.15 indicates the difference in retention time or appearance time of Cu signal when using graphite furnaces with and without filter. As can be seen the retention time for Cu peak without chromatographic column (filter) is lower than that with graphite filter. The Cu signal appears after 2 seconds without filter, while 4 seconds in case of filter. The difference in appearance time could be used in separation of mixtures of metal vapors by using filter furnace. More elements were studied by the same authors. The separation of the absorption signals of the elements under investigation are shown in figure 2.16.

As can be seen from the figure, the high volatile elements appear first with less retention times, the middle volatile appear later with higher retention times. The separation occurs due to two main factors; the interactions of the metal atoms with the graphite materials

2. THEORITICAL AND BACKGROUND KNWOLEDGE

and the diffusion coefficient of metals through the graphite filter. More information still needed in case of body fluid sample analysis.

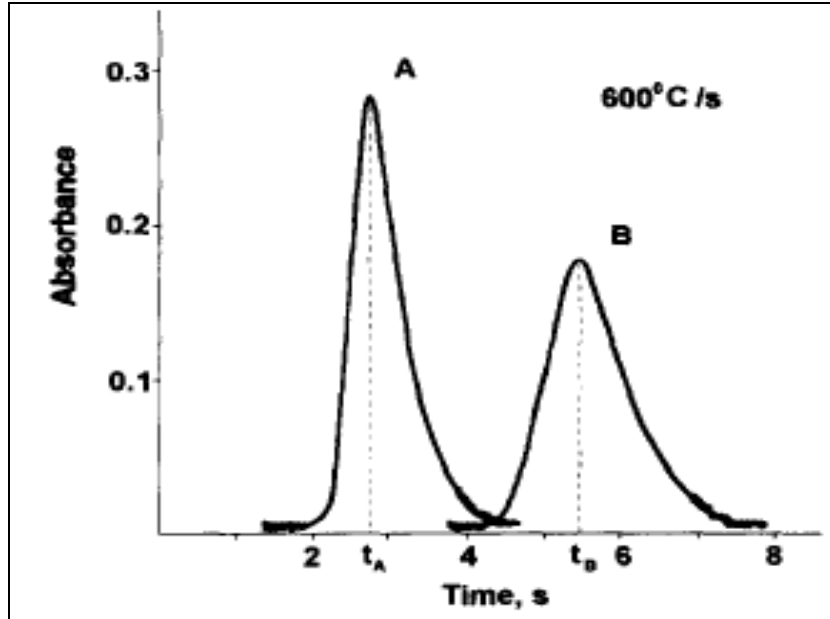


Fig.2.15 Delay of Cu signal (A) without filter and (B) with filter [39].

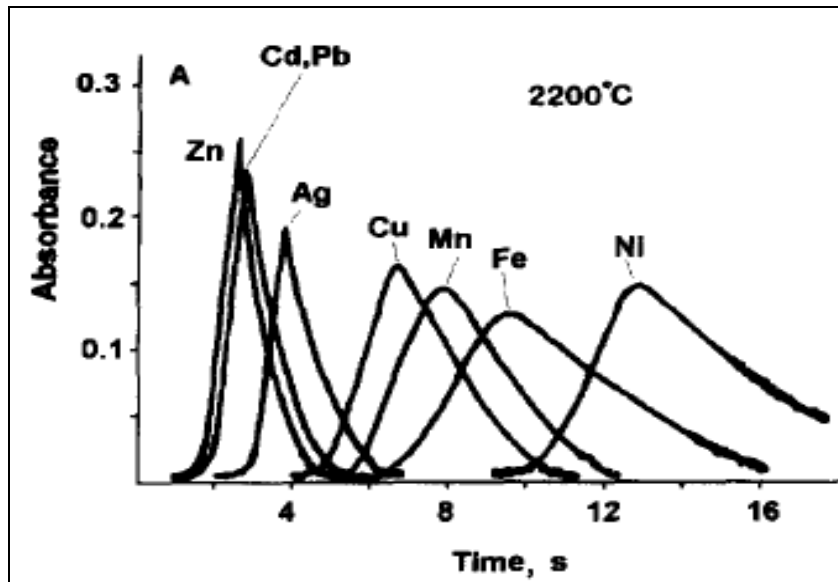


Fig.2.16 Atomic absorption signals for metals under investigation showing different retention times [39].

2. THEORITICAL AND BACKGROUND KNWOLEDGE

Since separation of two or more signals is possible using filter graphite furnace based on chromatographic principles and AAS detection system. One can calculate some important terms in chromatography such as separation factor and resolution. The separation factor (α) between two analytes permit the comparison between two adjacent solutes present in the same spectrum and given by the following equation [78]

$$\alpha = t_{R2} / t_{R1}$$

Where t_{R1} and t_{R2} are retention times for first and second components of the separated signals. The resolution factor between two peaks (R) can also be used for quantification of peaks separation and is given by the relation below

$$R = 2(t_{R2} - t_{R1}) / w_1 + w_2$$

Where w_1 and w_2 are peak widths of the two signals. Better resolution could achieve when the value of R is greater than 1. When $R = 1.5$ it is said that the peaks are baseline resolved.

Referring to figure 2.16, the separation factor between Zn and Cu is calculated from the figure ($\alpha = 2.8$), and the resolution factor $R = 1.5$, which means that the two peaks are baseline resolved. The same could be done fore another analytes with good separation factors.

Another chromatographic property could also be studied for high temperature chromatography in graphite furnace with AAS detection. The Van Deemter equation in chromatography relates the variance per unit length of a separation column to the linear mobile velocity by considering physical, kinetic, and thermodynamic properties of a separation. These properties include pathways within the column.

$$H = A + B/\bar{U} + C\cdot\bar{U} \quad (\text{Van Deemter equation})$$

2. THEORITICAL AND BACKGROUND KNOWLEDGE

A, B and C may be applied to the graphite furnace as a chromatographic column with stationary phase (graphite filter). The term A which is known as Eddy diffusion depends on the different paths used by analyte to pass through the column and it is related to the uniformity of the graphite filter and its density. The term B is known as the molecular diffusion and depends on the diffusion coefficient of the analyte in the mobile phase, the same behavior is also expected because this factor is controlled by the velocity of the carrier gas through the filter and the term C is known by resistance to mass transfer which is related to the number of equilibrations of analyte substance between the graphite wall and filter. The effect of these three factors is summarized in figure 2.17.

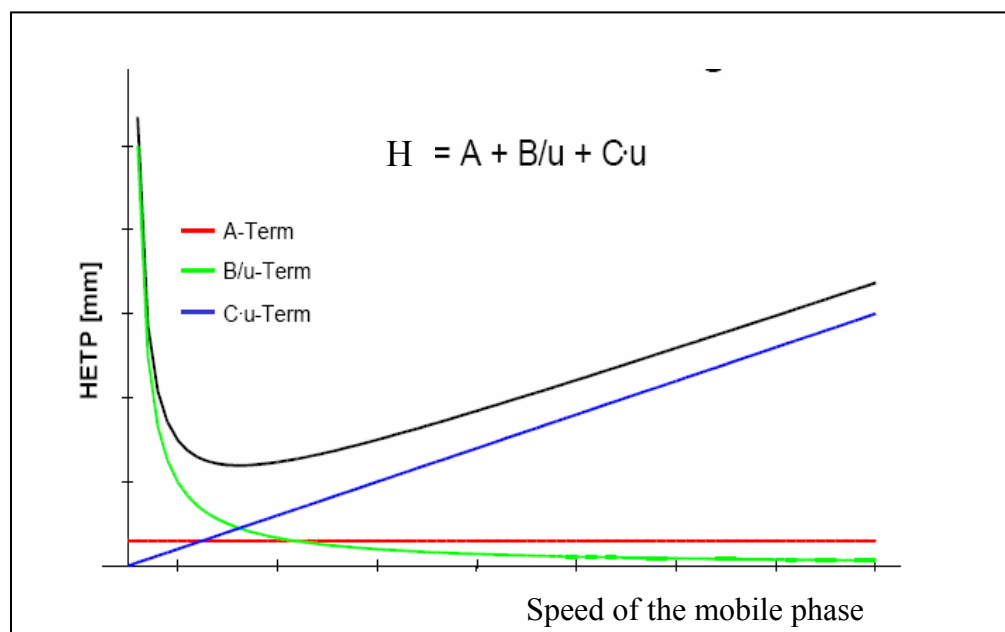


Fig.2.17 Van Deemter plot for gas chromatography [79].

The term H in equation is known as height equivalent of theoretical plate from which the number of theoretical plates within the chromatographic column can be calculated. As can be seen from figure 2.17 the factor H has optimum value with respect to velocity of the mobile phase. Temperature of furnace plays also important role in separation processes.

2.5.2 HIGH TEMPERATURE CHROMATOGRAPHY WITH MODIFIED TWO-STEP ATOMIZER [80]

The modified Grinshtein two-step atomizer system is shown in figure 2.18, the analyte is forced out of the atomizer with the help of the purge gas through a new exit slit (position No. 4 on the graph) adverse to the inlet slit of the atomizer as shown in figure 2.18. As can be seen from the figure, the atomized analyte atoms pushed into the atomizer direction and measured in a smaller measuring zone relative to that with the original Grinshtein system, then swept out of the atomizer from the new exit slit. With this modification the interference of the matrix with the analyte could be reduced.

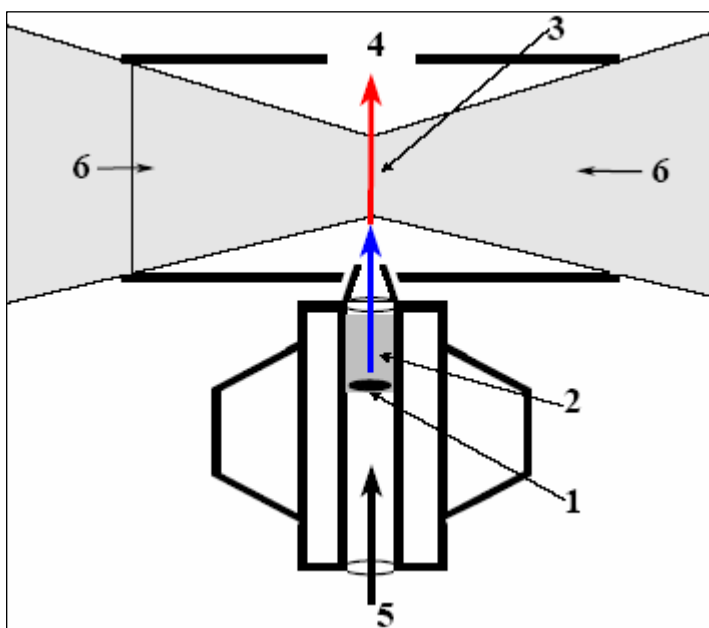


Fig 2.18 Modified Grinshtein system, (1) sample, (2) graphite filter (3) measuring zone, (4) exit slit, (5) purge gas (6) additional argon[80].

The application of high temperature chromatography was applied also by insertion of graphite filter (No.1 in fig. 2.18) in the vaporizer which increases the possibility of separation of the analyte and the matrix signal depending on the diffusion coefficient

2. THEORITICAL AND BACKGROUND KNOWLEDGE

difference of different sample compositions through the graphite filter and different reactions with graphite wall and filter (stationary phase).

The separation of the cadmium signal and the background signal in the determination of cadmium in urine which is highly interfering matrix using the modified Grinshtein system with filter is shown in figure 2.19.

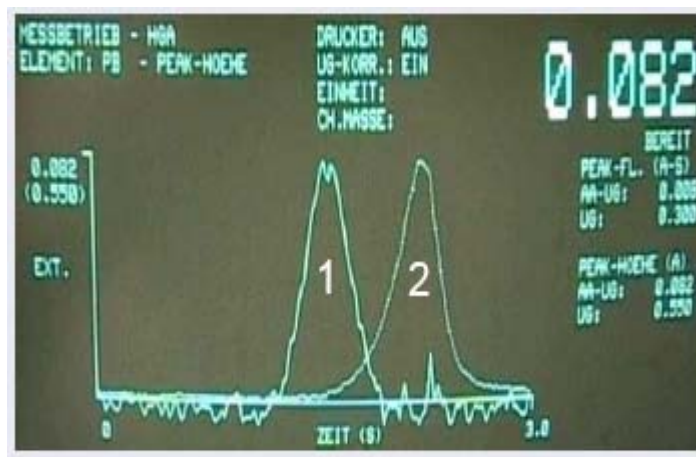


Fig.2.19 Determination of Cd in standard non diluted urine sample
(1) Cd signal; (2) Background signal [80]

The outer argon flow for system protection affected the sensitivity and the reproducibility of the measurements because it enhance the loss of the analyte vapour through the gap between the atomizer and the vaporizer with the so-called Venturi effect as can be seen in figure 2.20.

This system is based on the two-step atomizer system described by Grinshtein in section (2.4.1, Fig.2.10), which is complex design and had to be improved by further studies.

2. THEORITICAL AND BACKGROUND KNOWLEDGE

Figure 2.21 shows the real photo of the gap between the atomizer and vaporizer after a series of firings, which cause the transported sample compartments and analyte to escape from the high temperature regions into the lower temperature region with the help of outer argon gas as mentioned before.

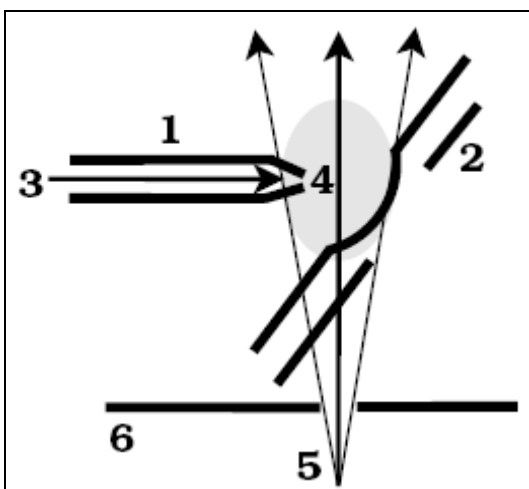


Fig.2.20 Effect of protection gas on the Transported sample



Fig.2.21 Real photo of the gap between atomizer and vaporizer [80].

Therefore, from the last survey on the history of the graphite furnace and the large number of articles in the field of development of this system as mentioned before more development still needed to separate and direct measuring of low amounts of trace elements in highly interfering matrices. Simple design with wide application was also target of many research groups.

3. THE AIM OF THE WORK

3 THE AIM OF THE WORK

The aims of this work are

- To get rid of the matrix interference during the analysis of samples with highly interfering matrices.
- To reduce the pretreatment steps as much as possible in the analysis of complex samples.
- To overcome the contamination risk accompanied with these pretreatment steps during the trace element analysis.
- To reduce the analysis time by reducing the number of pretreatment steps, hence increasing lifetime of the tube and reducing the analysis costs.
- To apply the high temperature chromatography method in AAS.
- To allow the possibility of direct analysis of solid samples.

4 METHODS AND MATERIALS

4.1 AAS SPECTROMETER DESCRIPTION

The spectrometer used our study is Shimadzu atomic absorption spectrometer (AAS6800), coupled with heated graphite atomizer (GFA-EX7). In this combination the instruments works on a maximum energy level and electronics double beam stability. The system operates in the wavelength range from 185-900 nm and includes a monochromator in Czerny Turner mounting with a holographic grating (1800 lines/mm).

The detector system consists of a photo-multiplier for the range from 185-600 nm and a Si detector from 600-900 nm and provides a maximum performance especially for the determination of ultra traces of elements. The optical double beam system guarantees longtime stability even in high temperature conditions. The spectrometer coupled with single ASC-6100 auto sampler. The "AA Wizard" software is installed in the system, which guide the user easily through a simplified parameter setup.

4.2 GRAPHITE MATERIALS

All graphite materials used for T- furnace manufacturing were bought from Schunk Kohlentchnik Germany. The properties of these materials are the same as for that material used in manufacturing graphite furnaces for AAS-systems. The specific properties of graphite materials are as follows:

- Specific electrical resistance $8.5 \Omega \text{ mm}^2 \text{ m}^{-2}$.
- Thermal conductivity $0.35 \text{ cal cm}^{-1} \text{ sec}^{-1} \text{ C}^{-1}$.
- Density 1.75 gm cm^{-3} .
- Machine ability Excellent.
- Maximum grain size $75 \mu\text{m}$.
- Porosity 13 %.
- Flexible strength 400 Kp cm^{-2} .
- Shore hardness 30.
- Melting point 3500°C .
- Linear expansion coefficient $4 \cdot 10^{-6}$.

4.3 HOLLOW CATHODE LAMPS

All lamps used during this study were hollow cathode lamps available in our laboratories from different companies as shown in table 4.1

Table 4.1 Hollow cathode lamps manufacturers, wavelength and current used for elements under investigation

Element	Company	λ (nm)	Current (mA)
Ag	Bachofer Reutlingen	328.1	6
Cd	Instrumental-laboratory England	228.2	4
Al	Instrumental-laboratory England	307.3	8
Cu	Bachofer Reutlingen	324.7	8
Bi	Varian-Techtron Australia	223.1	8
Cr	Unicam Analytical System	357.8	7
Mn	Shimadzu Japan	279.5	7

4.4 MASS FLOW CONTROLLER

The mass flow controller used for controlling the flow of purge gas was of type Brooks instrument Holland and with flow range of 0-100 ml/min.

4.5 WATER AND NITRIC ACID

All standard solutions were prepared using deionized water after purification by Elix3-MilliQ system (Millipore, USA). The containers (washing bottles, test tubes) used for all preparations were made of high purity polytetrafluoroethylene.

Nitric acid used from KFM (Laborchemie Handels GmbH) of purity 65%. Nitric acid is purified using quartz subboiling system (Kürner Analysentechnik, Germany).

4.6 STANDARD SOLUTIONS AND CERTIFIED MATERIALS

Table 4.2 shows the list of materials used in preparing standard solutions of elements under investigation and certified materials.

Table 4.2 Standard materials

Material	Company	Quality
AgNO ₃	Bernd Kraft Gmbh	AAS Standard
Cd(NO ₃) ₂	Merck- Darmstat	AAS Standard
Al(NO ₃) ₃	Bernd Kraft Gmbh	AAS Standard
Cr(NO ₃) ₃	Bernd Kraft Gmbh	AAS Standard
Mn(NO ₃) ₂	Merck- Darmstat	AAS Standard
Cu(NO ₃) ₂	Merck- Darmstat	AAS Standard
Bi(NO ₃) ₃	Bernd Kraft Gmbh	AAS Standard
HNO ₃	KMF	65%
Pd(NO ₃) ₂	Bernd Kraft Gmbh	ICP Standard
Mg(NO ₃) ₂	Merck- Darmstat	AAS Standard
(NH ₄) ₃ PO ₄	Bernd Kraft Gmbh	AAS Standard

Properties of certified reference materials used for quantitative analysis of trace elements are illustrated in table 4.3

Table 4.3 certified materials

Certified material	LOT. No	Company
Standard urine	2525	Sero norm TM
Standard Urine	69061	BIO-RAD
Bovine liver	SRM- 1577b	NIST
Bovine muscle	CRM-184	BCR

4.7 BORONITRIDE (BN)

Boronitride material from SINTIC Company, Germany, type BN7000 was with highest temperature capability, low thermal expansion, excellent thermal shock resistance and chemically inert.

Boronitride BN is non toxic material high temperature stability; the following table summarizes the most important properties of BN

Max use temperature in vacuum	3000°C
Density	1.8 gm cm ³
Dielectric constant	4.4
Dielectric strength	2000 J/kg.K

5 RESULTS AND DISCUSSION

5.1 THE NEW T-SHAPED FURNACE

All classical and newly suggested graphite furnaces try to separate matrix compounds from atom cloud. Background correction systems are not effective enough to ensure correct readings for complex samples. Therefore, separation should be attained at very high extent. Because separation of compounds in gas phase is the field of chromatography the new approach of chromatographic separation of evaporated gaseous compounds, atoms and molecules with following detection of atoms in the gas phase has been developed.

Berkhoyer [80] firstly published the first results using Grinshtein two-step atomizer system but opening the atomizer tube opposite to the introduction hole for the evaporation tube. The purge gas constantly flows through the evaporizer and atomizer tubes.

Following the idea of a real high temperature chromatographic system, it is not needed to use physically separated systems for evaporation and atomization. The new graphite tube has been designed in **T-form**. Figure 5.1 shows a schematic diagram and figure 5.2 presents a picture of the new T-shaped graphite furnaces and figure 5.3 shows a photo of the slightly modified Shimadzu graphite atomizer (GFA-EX7) with the new furnace and the connection with purge gas tube.

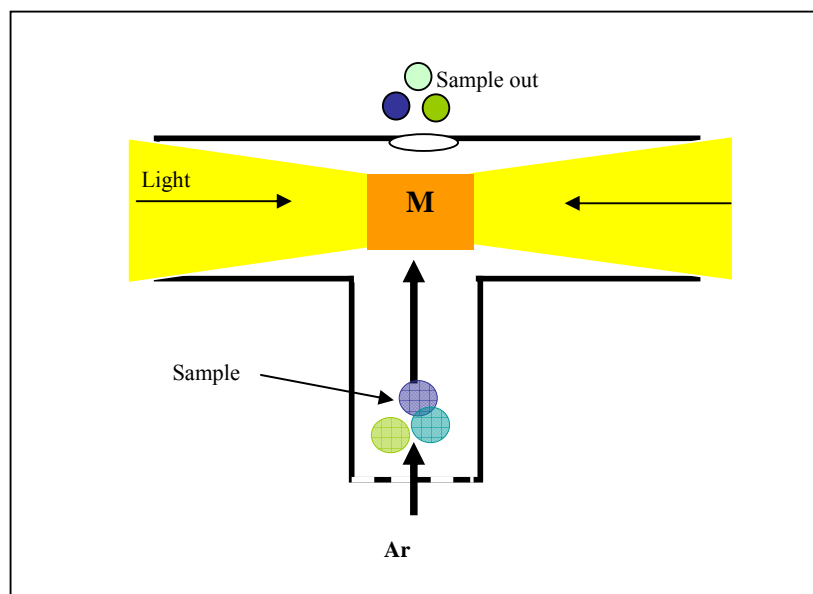


Fig.5.1 Schematic diagram of T-shaped furnace: M = measuring zone

The schematic diagram in figure 5.1 shows all features of a gas chromatographic system: sample injection, sample evaporation heating of sample injection system, carrier gas, separation column (diffusion and adsorption-desorption mechanisms of compounds on graphite), detector (measuring in perpendicular direction of the gas stream direction) (here AAS spectrometer) and gas exit.

Benefits of the new T-shaped furnace are firstly the separation of atom cloud and gaseous matrix components achieved because of different evaporation temperatures. The temperature of that part of the system is depending on both the temperature of the other part of the tube and the heating rate of that part. Secondly, at the time the relevant atom cloud appears in the measuring zone M (see figure 5.1) the amount of interfering species is dramatically reduced because the major part has already left the system through the exit hole or it is still in the evaporation process, hence the low volatile atoms are already transported by the carrier gas.

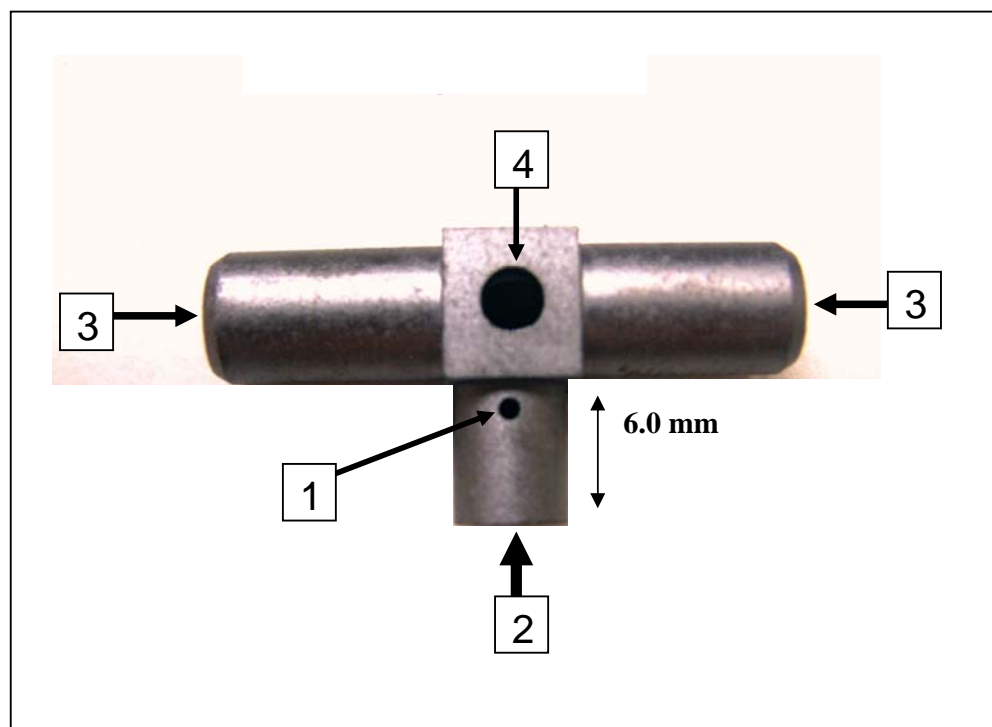


Fig.5.2 Top view of T-shaped furnace, furnace neck 6.0 mm length with sample injection hole (1) and *purge* argon (2). Longer part with *inner* argon gas of AAS system (3) and sample exit (4).

Figure 5.2 shows picture of T-shaped furnace, the sample injected from the small hole in the neck of the T-shaped furnace (position 1 in figure 5.2), then sample dried, pyrolysed, atomized and transferred to measuring zone by purging argon gas. Mass flow controller is used to control the amount of *purge* gas through the neck of the furnace (position 2 in fig.5.2). In order to concentrate the atom cloud of the atomized sample in the center of the furnace within the light beam, the argon mini flow mode of the Shimadzu system is used instead of conventional stop flow mode. A stream of 10 ml/min *inner* argon from both sides of the furnace along the light path (position 3 in figure 5.2) is used in the measuring step in all cases unless noted. One can say that the inner argon stream in the instrument is used to help in concentrating the sample in the central measuring zone (M) of the furnace, then to leave the furnace through the exit hole (position 4 in fig.5.2).

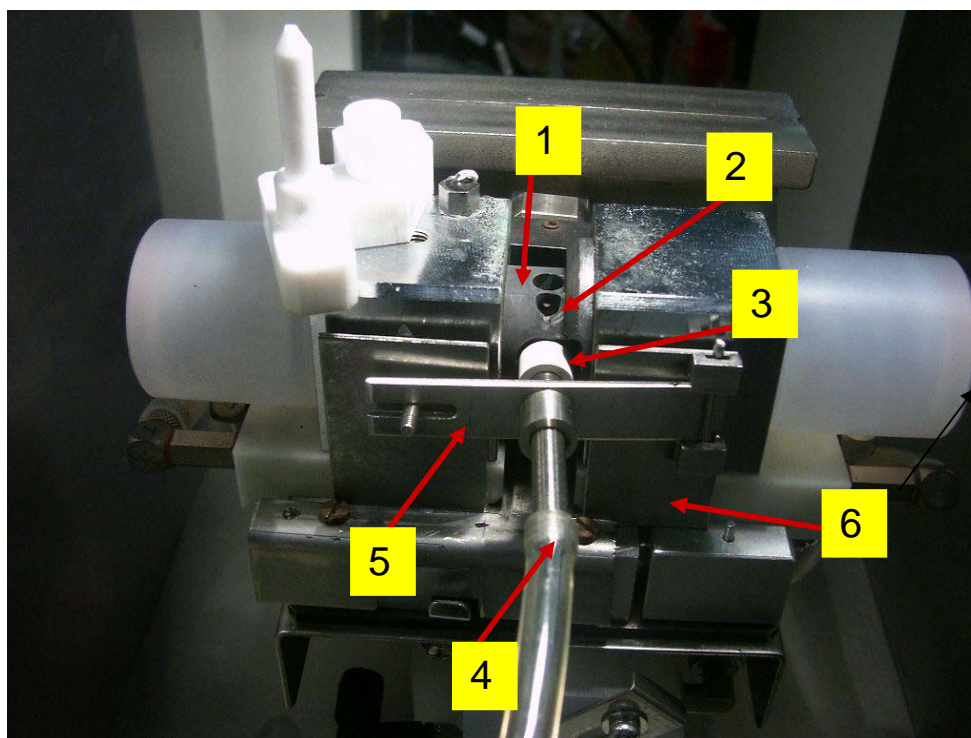


Figure 5.3 The T-shaped furnace installed in horizontal position inside the spectrometer:
1; graphite electrode, 2: sample injection, 3: boronitride connection, 4: metal tube for
purge argon, 5: metal door, 6: metal support.

Figure 5.3 indicates the components of modified furnace house of the Shimadzu spectrometer with all new parts needed for the complete installation of the T-shaped furnace. High temperature resistance and electrical insulating boronitride material (BN) used to connect the T-shaped furnace with the metal tube which provides the furnace with the additional purge argon is fixed in small metallic door. The metallic door itself is fixed on metal support which in turn fixed in the original furnace housing.

5.2 SHORT TIME TEMPERATURE PROGRAM

Separation between analyte and matrix compounds can be caused by:

- Evaporation temperature
- Evaporation kinetics
- Diffusion processes in gas phase
- Chemical reaction (homogeneous and heterogeneous)

The temperature program in AAS normally consists of mainly four steps, drying, pyrolysis, atomization and cleaning. In the drying step the solvent should be evaporated with suitable rate leaving the sample in a solid form (heaps or small crystals), drying time of 20 seconds ramp time plus 25 seconds hold time is suitable for a 20 μ l sample volume.

Setting of pyrolysis temperature depends on many factors such as the composition of the matrix and the nature of the element to be analyzed. The main purpose of the pyrolysis step is to reduce the amount of matrix as much as possible before the atomization step.

25 seconds ramp time plus 25 seconds hold time is suitable for pyrolysis step of some samples. Optimization of pyrolysis time and pyrolysis temperature is important for other samples with different elements, which is time and instrument consuming. Analyte maybe lost during the pre-treatment steps leading to erroneous measurement of the sample content if the pre-treatment steps were not will optimized.

The optimum atomization temperature depends on the element to be analyzed, for example 800 $^{\circ}$ C for cadmium, 1700 $^{\circ}$ C for chromium and 2700 $^{\circ}$ C for vanadium. The surface from which the atoms atomized also plays an important role. The atomization time is usually ranged from 2-7 seconds depending on type of the element. Cleaning step is about 5-8 seconds.

5. RESULTS AND DISCUSSION.

The short time temperature program shown in figure 5.4 composed of three steps; drying, atomization and cleaning step. The total time of short temperature program (blue curve) is between 35-50 seconds in stead of 150-250 seconds for the conventional temperature programs (red curve). The benefits of short time temperature program firstly, it has less time of analysis since it contains no pyrolysis step (red curve-line 2), secondly, atomization of sample with slow heating rate (blue curve-line 3) causes gradual evaporization of sample components depending on the vapour pressure of each component in the sample. The slow heating rate in short time temperature is comparable to temperature gradient in gas chromatography. Using the T-shaped graphite furnace with this chromatographic property allows the separation of analyte and matrix with good values for separation and resolution factor.

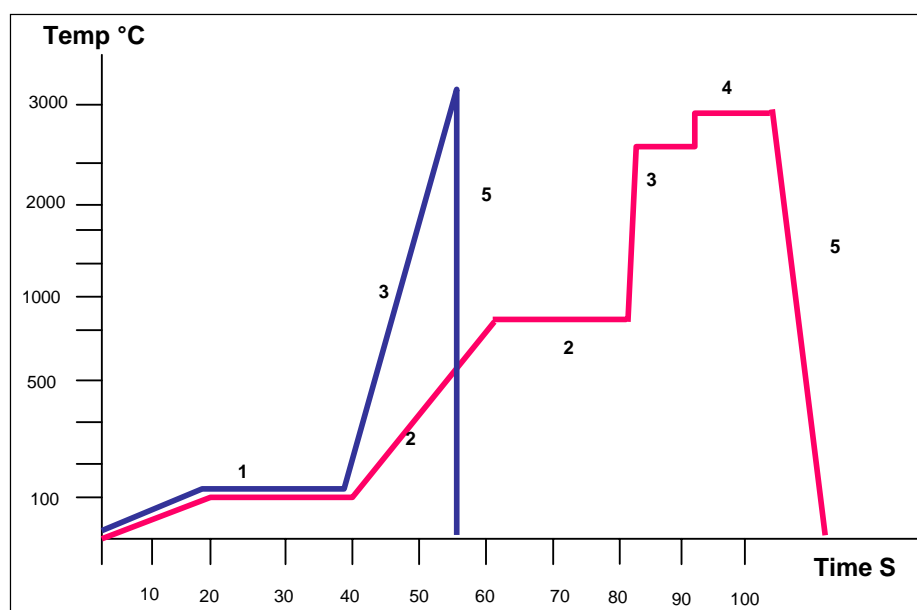


Fig.5.4 Diagram of conventional (red) and short (blue) temperature program with 1 drying, 2 pyrolysis, 3 atomization, 4 cleaning and 5 cooling step.

As an example for applicability of high temperature chromatography with T-shaped graphite furnace and short time temperature program, determination of analyte such as Cd in sample with highly interfering matrix (urine) is tested. The separated signals are illustrated in figure 5.5. As can be seen from the figure signals in urine the sample components are divided into three parts, the first part is the highly volatile organic components of the urine with lower

retention time (3.5s), the second one was the analyte with retention time of (4.5s) and the third part was the low volatile inorganic salts of urine sample with higher retention time (7.5s). In addition to reducing the analysis time using the T-shaped furnace, the analyses were done without pyrolysis step, which also reduces the analysis time since there is no need for optimization of the pyrolysis step. Analyte loss could also be avoided by cancelling this step from the temperature program.

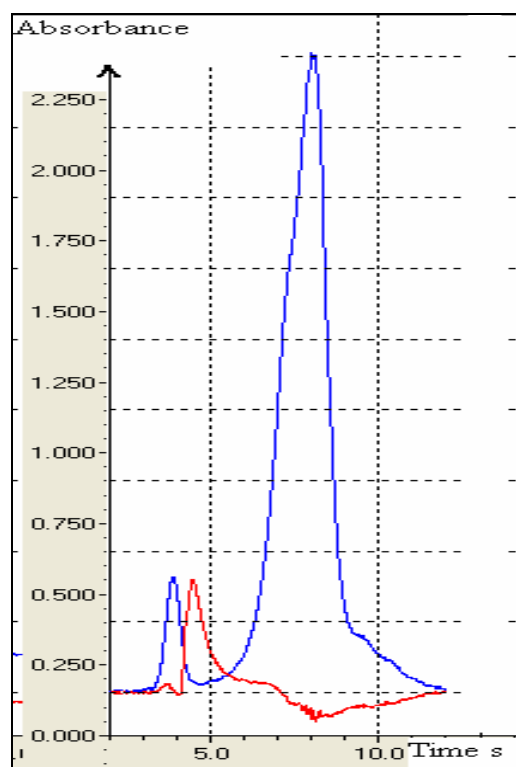


Fig.5.5 High temperature chromatography using T-shaped furnace and short time temperature program in analysis of Cd in urine (red-Cd and blue- high and low volatile components in urine)

The negative absorbance value of analyte at high absorbance of background indicates the over compensation phenomenon. More details on chromatographic separation and quantitative determination of different analytes in highly interfering matrices using T-shaped graphite furnace and short temperature program will be shown in the next chapter. Note that such quantitative determinations are impossible to be done using all conventional and developed AAS systems.

5.3 OPTIMIZATION OF THE T-SHAPED GRAPHITE FURNACE

The accuracy of the absorption measurements can be attributed to many sources, one of the most important parameters is the reproducibility and stability of the absorption signal, which in turn reflects the efficiency and the precision of the method developed. In addition to the design of the T-shaped graphite furnace described in the previous sections, many factors affected the absorption signal and hence the trueness and precision of measurement were studied. The effect of temperature program, direction of the furnace, additional purge gas flow rate, different furnace dimensions, different sample injection and types of matrices on analyte were tested. The first optimization part of the thesis was carried out using non pyrocoated graphite material.

5.3.1 OPTIMIZATION OF DIMENSIONS

The T-shaped graphite furnaces were manufactured at the mechanic workshop of the Duisburg-Essen university, the thickness of the furnace walls and furnace neck of 2.0, 1.5, 1.0 mm were tested, with 2 mm wall thickness the furnace was applicable with higher life time of the furnace in case of the highly and middle volatile elements such as Cd and Mn, but was not effective in case of the low volatile elements such as cobalt and chromium because of the relatively low heating rate which was not enough to volatilize these elements in a suitable time. Unsymmetrical furnace dimensions were also tested by manufacturing furnace with 1.5 and 2.0 mm path length wall thickness and 1.5, 1.0 and 0.6 mm wall for the neck of the furnace. Better heating rate was possible using thinner furnaces walls but shorter life time of the tube.

The sample exit slit was also tested, 3.0, 2.5, 2.0 mm diameter. Two effects were compensated, the internal gas flow and the suction system which pointed directly above the exit slit. 3.00 mm for exit slit diameter was optimum. Higher internal flow rate or larger exit slit diameter the analyte could no be measured because it is swiped out of the measuring zone faster than to be recorded.

5.3.2 OPTIMIZATION OF THE PURGE GAS FLOW

The inert purge gas flow has important role in heating graphite furnaces. The main function of this gas is to prevent the oxidation of carbon at higher temperatures by the hot atmospheric oxygen and corrosive sample components during the analysis period. In addition to it is

protective function, the argon gas removes the vaporized matrix component during the drying and pyrolyzing steps out of the radiation beam.

The effect of the flow rate of the argon gas flow rate on the absorption signal and separation is studied. The purge gas was used to move the sample from the atomization area into the measuring zone. The amount of the argon introduced to the furnace should be optimized in order to reach best sensitivity, good separation with low matrix interferences, reproducible measurements and laminar flow of the argon inside the furnace.

Argon flow rates between 20.0 to 70.0 ml/min had no remarkable effect on the absorption signal of cadmium in urine sample. This behaviour is expected to be similar with the other elements determinations. The signals overlapped and the absorption decreases as the flow rate increases. The effect of the argon flow rate on the absorption signal of cadmium in urine sample is illustrated in figure 5.6.

The background signal depends also on the additional argon flow rate, the peak height value decreases with increasing the flow rate of the purge gas.

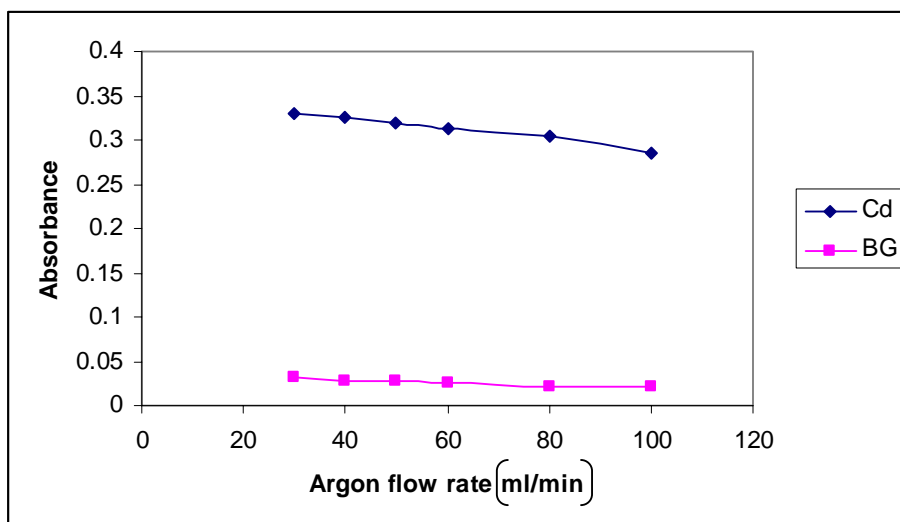


Fig.5.6 Effect of argon flow on absorption signals of Cd in urine sample (10 μ l of 5.5 μ g/l), BG = Background

As can be seen from figure 5.6 the optimum value of the argon flow rate in case of cadmium was 30.0 ml/min. The same argon flow rate is found to be optimum for all separations

measurements with other elements such as Mn, Cu, Cr, Al as will be shown in the next chapters. The original internal argon gas flow was also optimized; a flow rate of 10.0 ml/min from both sides of the furnace was suitable for all determinations.

5.3.3 OPTIMIZATION OF POSITION OF THE FURNACE

5.3.3.1 VERTICAL POSITION OF THE FURNACE NECK

Two ways of installing the furnace were examined. In the present case the neck of the T-shaped graphite furnace is positioned vertically below the light beam level and the sample exit slit was also used as sample injection hole. The sample was injected on a platform fixed at the lower part of the furnace neck so that the sample is dried, pyrolyzed and atomized away from the injection hole (about 8.0 mm) which reduces the loss of the analyte through the injection hole. Schematic diagram of furnace in vertical position is shown in figure 5.7

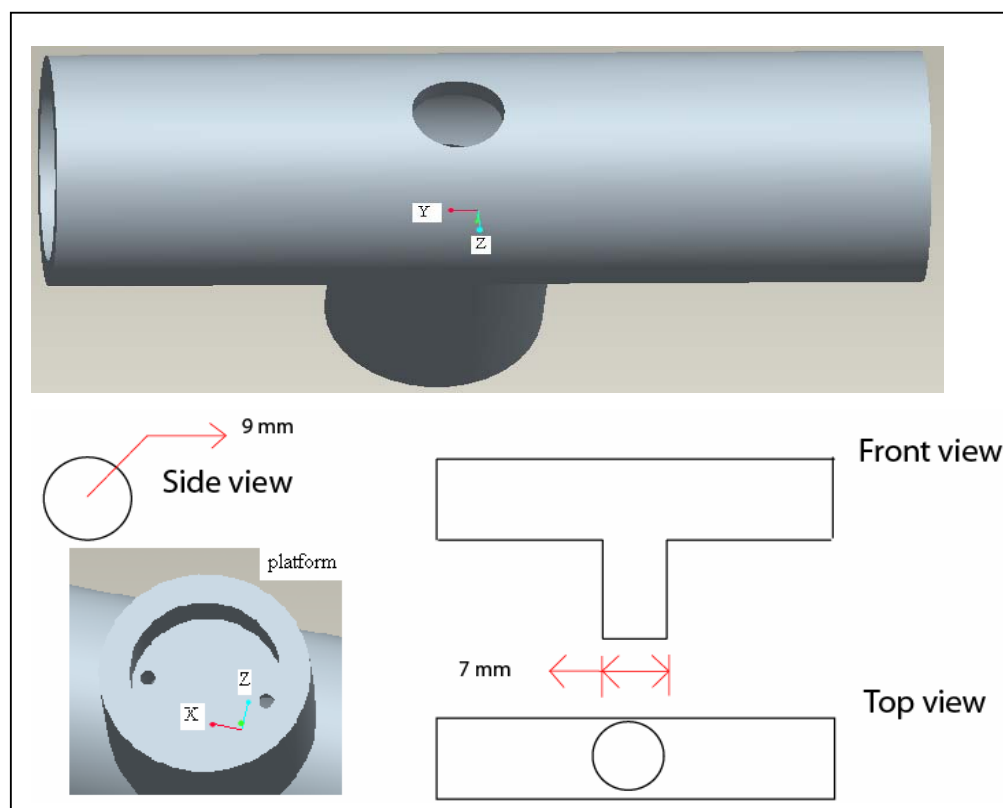


Fig.5.7 Vertical position of T-shaped furnace with side, front and top view of the furnace, and bottom view of platform, Y-horizontal and Z- vertical axis.

In the vertical position the sample is injected into the furnace using the auto-sampler through the opening at the top of the furnace shown in figure (fig.5.7 top view). The same injection position is used later as exit for the atomized sample after measurement. The additional argon gas introduced to the furnace from the lower part of the furnace neck (two small pores in the platform). The sample injected inside the furnace, since the tip of the auto-sampler goes deeply up to the plate form, which is fixed later at the end of the furnace neck. The sample injection process with vertical position was not so good because it was difficult to adjust the sampling tube tip in the right position inside the neck of the furnace.

Despite this drawback and after further optimization some repeatable measurements were achieved for chromatographic separation of analytes in presence of urine matrix. As can be seen in the figure 5.8, the Cd signal is separated to some extent from the non diluted urine matrix signal (blue), and by considering the peak height the reading could be considered as correct because the background signal is less than half of the analyte signal and can be corrected by deuterium background correction system. The advantageous of this furnace installation is the possibility of the separation of the matrix and analyte signal. It has been experimentally performed for a number of elements like Cd, Cu, Cr, Mn and Au.

Table 5.1 indicates the three steps used in short time temperature program for separation of Cd and urine matrix signals using high temperature chromatography with T-shaped graphite furnace and continuous argon flow

Table 5.1 Short time temperature program for Cd in urine sample using T-shaped furnace and high temperature chromatography approach.

Step	T (°C)	Heating mode	Time (s)	Inner argon (ml/min)	Purge argon (ml/min)
Drying	120	Ramp	15	500	30
Drying	120	Hold	20	500	30
Atomization	3000	Ramp	8	10	30
cleaning	3000	Hold	4	500	30

The program as mentioned before contains drying step followed by evaporation of sample with slow heating rate (8 seconds-Ramp). Since Cd is highly volatile element, thus Cd signal appears after organic part of urine matrix and before the low volatile part of urine.

Figure 5.8 shows the reproducibility of the cadmium determination in acidified urine sample using short temperature program, as can be seen from the figure the difference in appearance time of the high volatile part of the urine sample, cadmium atoms and low volatile part of the urine sample allows the separation of cadmium during the analysis of the non diluted acidified urine sample.

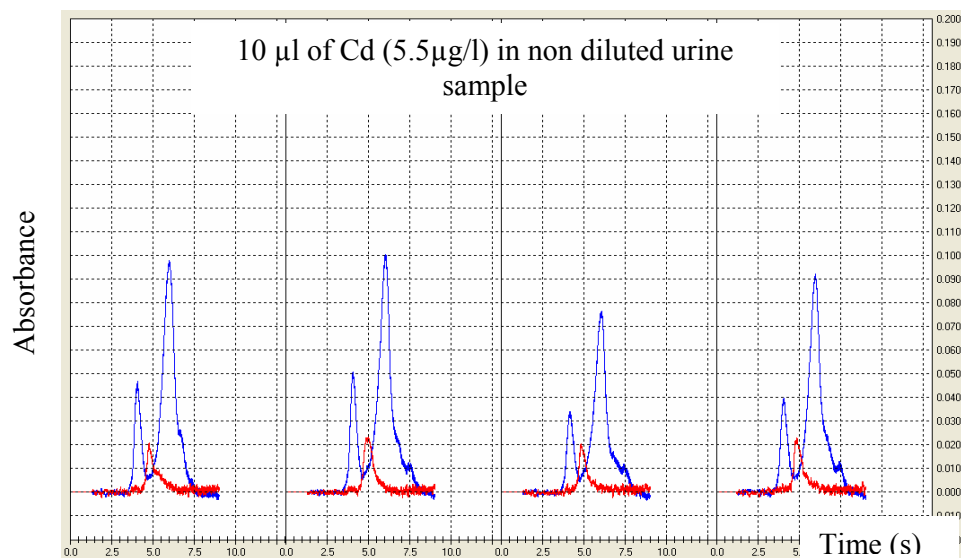


Fig. 5.8 signal for analyses of Cd (red) in non diluted acidified urine sample (blue) using non coated T-shaped furnace in vertical position

The appearance time of cadmium was less than 5 seconds and the total time required to complete atomization of strong urine matrix by short temperature program have been found to be about 8 seconds. These times varies with the platform thickness and hence since different of platform leads to different heating rate. In determinations of other elements this step should be optimized depending on the nature of element, for example high volatile elements in low matrix needs high heating rates and the reverse for low volatile elements.

The same short temperature program with atomization of 10 seconds hold time is used for analyses of middle and low volatile elements (because more heat needed be atomized) in highly interfering matrix using the same principle of high temperature chromatography with T-shaped furnace. Analysis of chromium in urine sample with T-shaped furnace using high temperature chromatography is shown in figure 5.9. As can be seen from the figure, the signals are reproducible with low relative standard deviation (RSD = 0.5%), and the separation of the analyte and matrix was also good in terms of peak height, the matrix evaporates first then analyte signal appears with delay (higher retention time).

The tailing of the analyte signals arises because of the higher tendency of chromium to react with the carbon of the non coated graphite tube forming chromium carbides which is stable carbide and needs longer time of atomization with higher heating rates. Care was taken by repeating the cleaning step in order to avoid the memory effect of chromium on the analysis of the next samples.

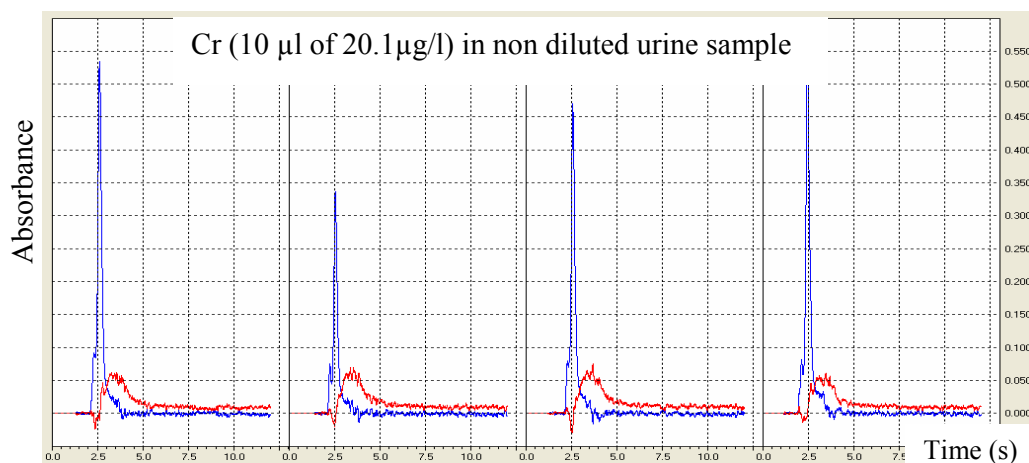


Fig.5.9 Signals for chromium determination in acidified non diluted urine sample (short temperature program) with vertical non coated furnace.

Absorption signals of Cu in standard non diluted urine sample is another example of separation of analyte and matrix signals by high temperature chromatography using short time temperature program with T-shaped graphite furnace installed in vertical position. Figure 5.10

illustrates the absorption signals of copper analysis in standard acidified non diluted urine sample. The short temperature program was used with out pyrolysis step, and with atomization with maximum heating rate (10 seconds hold time). The analysis time is shorter than that with the conventional systems since it excluding the pyrolysis step and the dilution of the sample.

Since Cu is also low volatile element, absorption signal of Cu appears as the same with that of Cr with higher retention time and matrix signal appears first

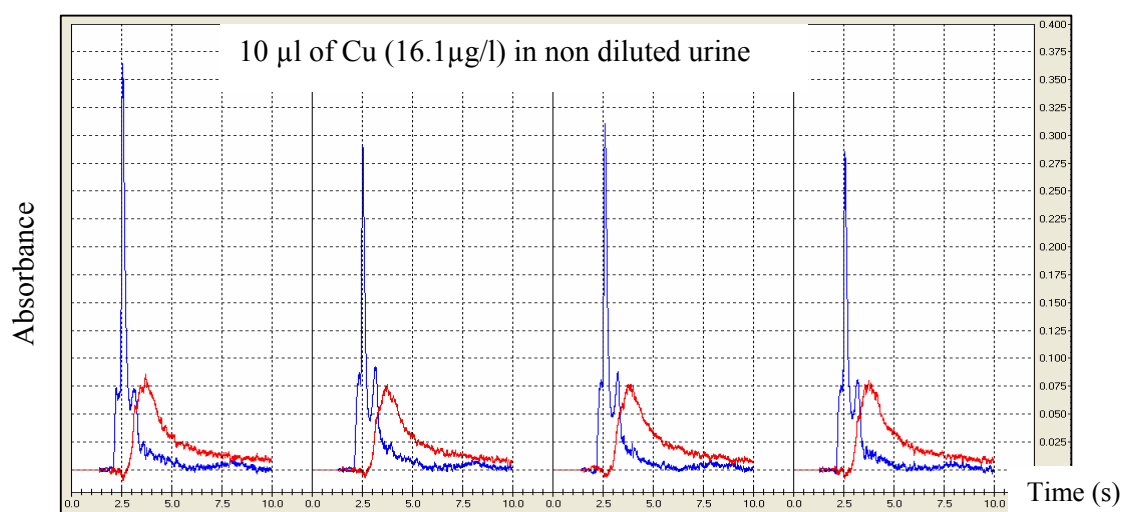


Fig.5.10 Signals for copper analysis in standard urine using vertical non-coated T-shaped furnace installed in vertical position.

The appearance time of copper was relatively higher than that of urine matrix; hence the separation of the analyte and urine matrices is possible. Comparing to the signal for chromium determination with vertical furnace position shown in figure 5.9 copper signals returns to the base line at 8 seconds because copper has fewer tendencies to react with the hot non coated graphite tube walls like chromium atoms

Since Cd is high volatile element and can be evaporized and separated from matrix signal using high temperature chromatography and Cd signal appears firstly with lower retention time than the signal of low volatile part of urine matrix. The case is inversed in case of low volatile elements such as Cr and Cu where their signals appear after urine matrix signal.

Therefore if there are elements with volatility lower than Cd and with volatility higher than Cr and Cu (i.e. about the same volatility of urine matrix). Overlapping of these analytes signals and urine matrix signal is expected. Bi is an example of this category of elements.

Analysis of bismuth in standard acidified non diluted urine sample was also tested with of the T-shaped graphite furnace in vertical position, the signals shown in figure 5.11 below. With vertical position the absorption signal of bismuth is highly influenced by the matrix because of the atomization temperature and the appearance time of both the analyte and the matrix are approximately the same, hence the separation in this case was not possible and the analysis could be done using the normal temperature program including the pyrolysis step. In figure 5.11.a the pyrolysis temperature was 800°C and 900°C in 5.11.b, less matrix effect with higher pyrolysis temperatures. At pyrolysis temperature more than 900°C, the absorption signal of bismuth decreases because of bismuth atoms losses in the pyrolysis step. The signals are acceptable and can be used for the determination and it is much better than the signals with original shimadzu tube as will discussed later in this chapter with quantitative determination of Bi in urine.

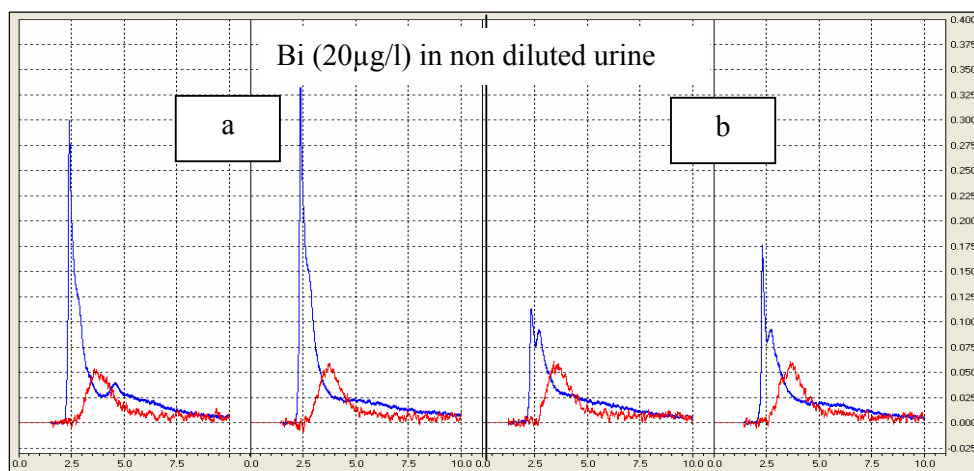


Fig.5.11 Signals for Bi analysis in non diluted urine sample; (a) $T_{py} = 800^{\circ}\text{C}$ and (b) $T_{py} = 900^{\circ}\text{C}$.

The installation of T-shaped graphite furnace as mentioned before is possible in vertical position and showed good separation properties of different analytes and urine matrix which

is known as highly interfering matrix and impossible to be analysed without dilution and chemical modifiers.

5.3.3.2 HORIZONTAL POSITION OF THE FURNACE NECK

Because sample injection inside the neck of the T-shaped furnace in vertical position was difficult, installation in horizontal position is suggested and used for quantitative analysis of trace elements in urine by applying high temperature chromatography and short time temperature program. Schematic diagram of T-shaped furnace installation in horizontal position is shown if figure 5.12. A new injection hole was created in the neck of the furnace.

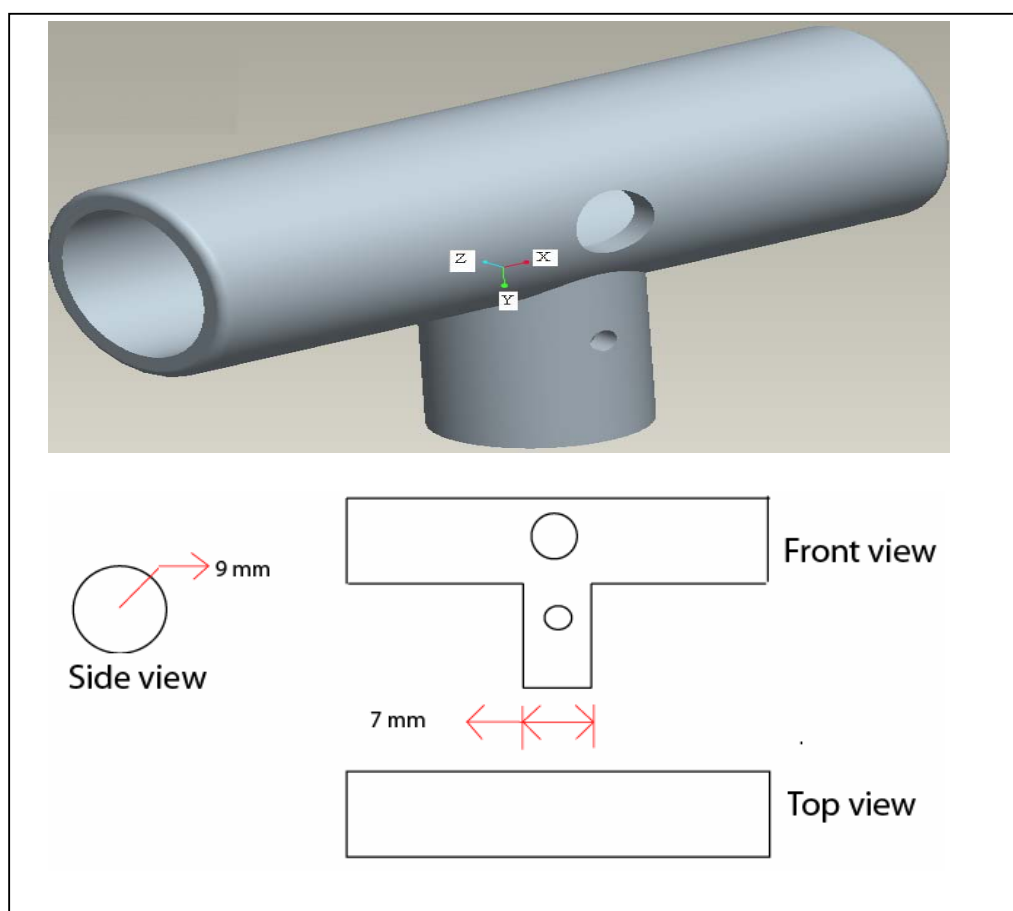


Fig.5.12 Three dimensional diagram of T-shaped furnace in horizontal position with side, front and top views.

non diluted urine sample using T-shaped graphite furnace in horizontal position and short time temperature program. Clear separation of analyte and matrix is achieved with appearance time of Cd signals between the high and low volatile parts of urine matrix; this behaviour is discussed before in case of vertical position of the furnace. This means that the furnace position has no remarkable effect on application of high temperature chromatography using T-shaped furnace. The signals are repeatable (note also the repeatability of matrix signals) with RSD of 1.2%. Such measurements are impossible to achieve with all conventional and developed AAS systems. The negative Cd signals at high absorbance value of matrix because of over compensation of the background correction system.

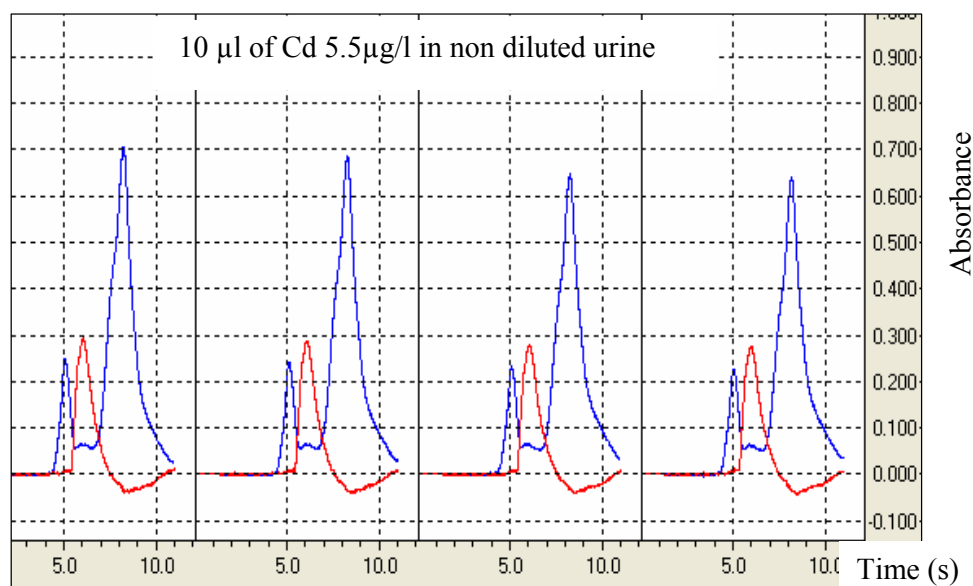


Fig.5.13 Cd signals in non diluted urine sample using the T-shaped furnace in horizontal position.

As can be seen from figure 5.13 the signals are stable, repeatable and separated. Further more automated introduction of sample inside the furnace neck in horizontal position is not so complicated like that with furnace in vertical position. Since high temperature chromatography with short temperature program can also be applied, we decide to continue quantitative analysis of samples with the T-shaped furnace in horizontal position. Another benefit of this furnace position, it allows the possibility of direct solid sample analysis.

5.4 QUANTITATIVE ANALYSIS WITH THE NON-PYROCOATED

T-SHAPED GRAPHITE FURNACE IN THE HORIZONTAL POSITION

Elements in AAS are classified into three main categories, highly, middle and low volatile elements depending on their behaviour inside the furnace during the pyrolysis and atomization stages. Elements of different evaporation properties were chosen as representative elements for each category. For the validation of the new design, element analyses were done firstly for standard solution of each element in the absence of any matrix effect, and then the effect of matrix was also investigated with different element analyses.

5.4.1 QUANTITATIVE ANALYSIS OF ELEMENTS IN STANDARD SOLUTIONS

Calibration curves of different elements were created by plotting the absorbance values of different concentration of each element against the amount of the element. In the absence of matrix less interferences is expected.

5.4.1.1 QUANTITATIVE ANALYSIS OF HIGH VOLATILE ELEMENTS

Cadmium and silver were chosen as elements of the high volatile elements category. Some difficulties normally accompanied the determination of cadmium with graphite furnace technique because of it is high diffusion coefficient.

5.4.1.1.1 Cadmium

The determination of cadmium was carried out at the resonance line of cadmium, $\lambda = 228.8$ nm, and hollow cathode lamp with a recommended current of 4.0 mA. The temperature program used is described in table 5.2.

Table 5.2 Temperature program for cadmium determination in standard solution at the resonance line of $\lambda = 228.8$ nm and lamp current intensity of 4.0 mA.

Step	T (°C)	Time (s)	Argon flow (ml/min)
1	120	10	500
2	120	20	500
3	400	10	500
4	400	20	500
5	2000	4	10
6	2400	4	500

Normal temperature program is used here to examine the behaviour of T-shaped furnace since no matrix be resolved in case of standard solution. Short temperature program may also be used as will discuss later in this chapter. The use of continuous inner argon flow mode during the atomization stage instead of stop flow mode leads to less sensitivity measurement. The purge gas in this determination was 30.0 ml/min.

In addition to the high volatility of cadmium, the loss of cadmium is also caused by the diffusion of cadmium atoms through the non pyrocoated graphite furnace walls since the non pyrocoated graphite contains a large number of cavities which can be occupied by cadmium atoms during the atomization stage leading to the decrease in sensitivity of the determination.

A series of different concentrations range of (1 - 7 ppb) of cadmium standard solution was measured using the new furnace design. Figure 5.14 shows the absorption signals of different cadmium concentrations using the non pyrocoated T-shaped graphite furnace; the signals as can be seen from the figure are typical absorption signal with sharp peak height at the centre of the peak.

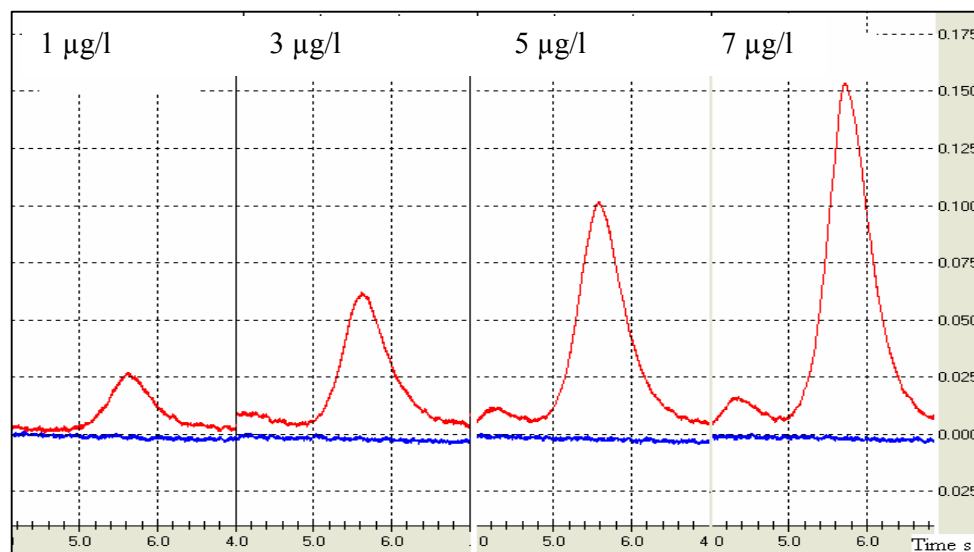


Fig.5.14 Absorption signals for Cd calibration curve in standard solution using T-shaped graphite furnace with continuous flow mode.

The calibration curve data were plotted as shown in figure 5.15. The linear working range for cadmium was up to (7 $\mu\text{g/l}$), and then at higher concentration the deviation from linearity takes place.

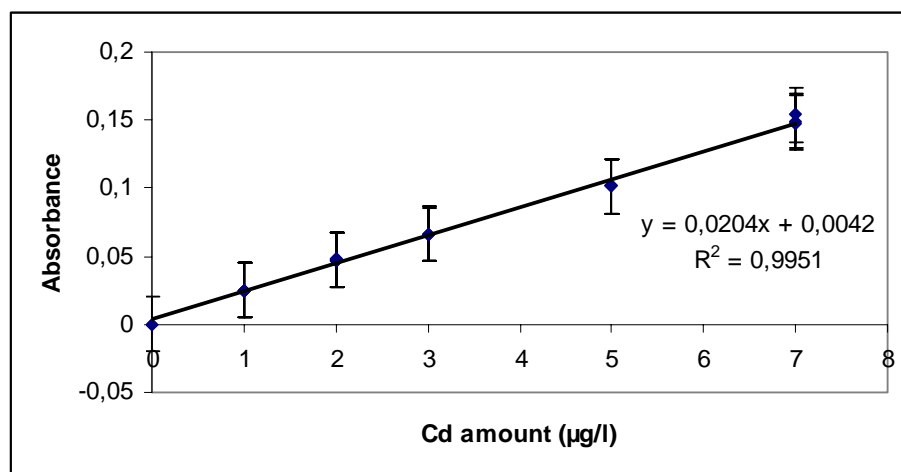


Fig.5.15 Calibration curve for Cd standard solution using non pyrocoated furnace (n = 5)

The calibration curve for standard Cd solution in 0.2M nitric acid shows linear relationship with correlation coefficient of 0.9975 and with excellent reproducibility and relative standard deviation (RSD) for n = 5 measurements in the range between 3-8 %. The characteristic mass of cadmium was calculated. The value is (1.6 pg), which is comparable with the cadmium determination using Perkin-Elmer pyrocoated furnace (1.3pg). The limit of detection is (3s = 0.0168 $\mu\text{g/l}$).

5.4.1.1.2 Silver

Silver calibration curve were carried out at the resonance line of $\lambda = 328.1$ nm and lamp current intensity of 6.0 mA. The temperature program used is shown below in table 5.3. conventional temperature program is also used for silver determination in standard solution since no matrix need to be resolved. Pyrolysis step with modifier is helpful in case of standard solution of high volatile element since it helps in analyte stability during pyrolysis and evaporation of all atoms together in evaporation step leading to best sensitivity for highly volatile elements. Short temperature program with high temperature chromatography will apply later in presence of highly interfering matrix. The inner argon stream used during

evaporizataion- determination step (step 5 in table 5.3) is 10 ml/min and the purge argon is constant with optimum value (30 ml/min) in all experiments within this thesis.

Table 5.3 Temperature program for silver determination in standard solution at the resonance line of $\lambda = 328.1$ nm and lamp current intensity of 6.0 mA.

Step	T (°C)	Time (s)	Argon flow (ml/min)
Drying	120	10	500
Drying	120	20	500
Pyrolysis	400	10	500
Pyrolysis	400	20	500
Atomization	2000	4	10
Cleaning	2400	4	500

Figure 5.16 illustrates the absorption signals of silver using the non pyrocoated T-shaped graphite furnace. The signals were also typical atomic absorption signals and sharp peak with zero background values.

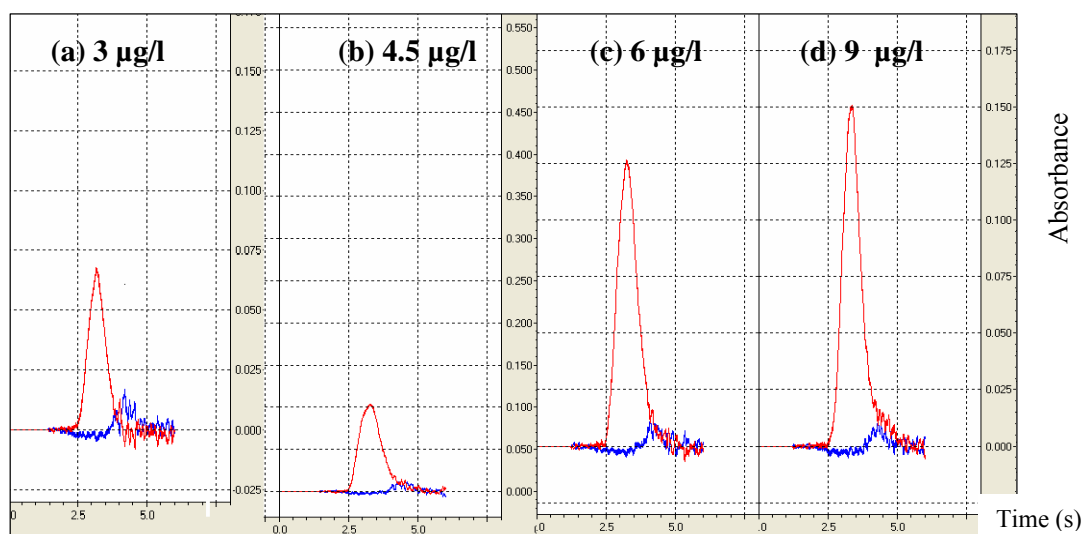


Fig. 5.16 Calibration curve signals for different concentration of Ag in standard 0.2 % nitric acid using T-shaped furnace in horizontal position

Figure 5.17 below illustrates the linear relationships between absorbance and amount of Ag in standard solution of 2% nitric acid using non pyrocoated T-shaped graphite furnace and continuous argon flow mode.

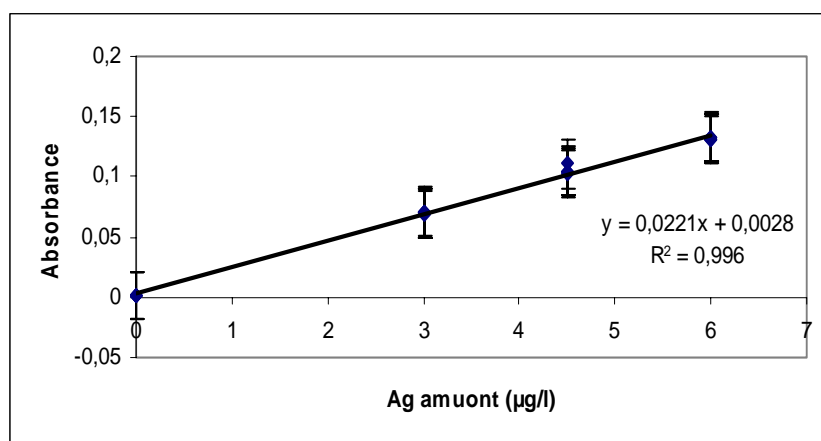


Fig.5.17 calibration curve for Ag determination in standard solution 2% nitric acid using non pyrocoated T-shaped furnace in horizontal position.

The maximum amount could be used within the linear range for silver determination is found to be 6.0 µg/l, at higher silver concentration (9 µg/l), the peak was also sharp but it was out of the linear range. As can be seen from figure 5.17, the calibration curve for silver shows linear relationship with Correlation coefficient of 0.998. The characteristic mass of silver under the described conditions was 1.90 pg, which is better than that obtained by Perkin-Elmer for silver (4.5 pg) although the measurement was done using the continuous flow mode and not the stop flow mode. The limit of detection for silver is found to be ($3s = 0.08$ µg/l).

5.4.1.1.3 Bismuth

Bismuth calibration curve were carried out at the resonance line of $\lambda = 223.1$ nm using series of different concentrations and suitable lamp current of 8.0 mA and slit width of 0.2 nm. Since Bismuth is the lowest volatile elements in this group, high atomization temperature than that in case of cadmium and silver, but the same argon flow rate condition. In all

5. RESULTS AND DISCUSSION.

measurement with short program the flow rate of inner argon is 10 ml/min and the purge argon gas flow is 30 ml/min.

Table 5.4 short temperature program for Bi, $\lambda = 223.1$ nm determination in standard solution using T-shaped furnace and continuous flow mode

Step	T (°C)	Heating mode	Time (s)	Inner argon (ml/min)	Purge argon (ml/min)
Drying	120	Ramp	15	500	30
Drying	120	Hold	20	500	30
Atomization	3000	Ramp	13	10	30
cleaning	3000	Hold	4	500	30

Figure 5.18 shows the absorption signals of standard solutions of Bi using the non coated T-shaped furnace. The signals were carried out using short temperature program with continuous argon flow as shown in table 5.4.

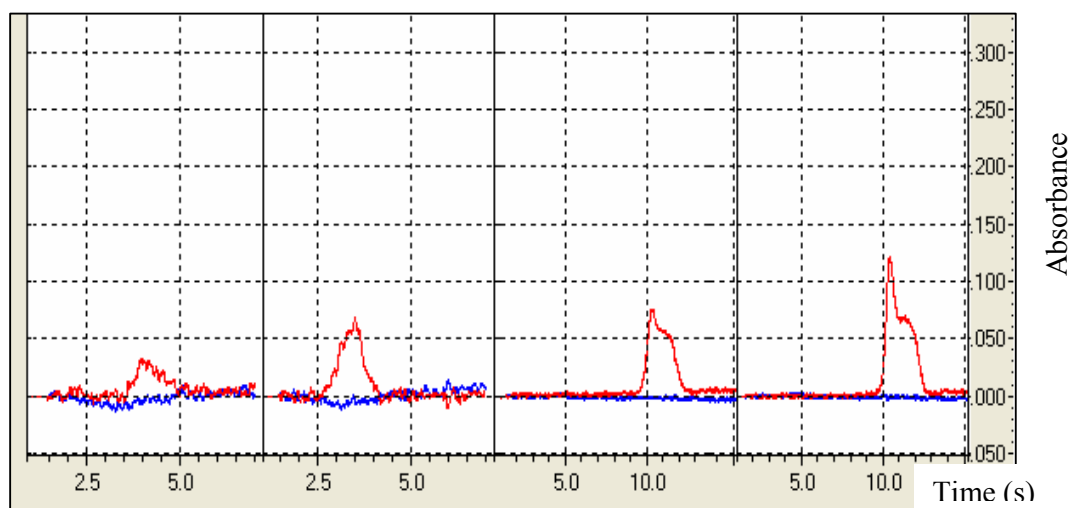


Fig.5.18 Signals for Bi calibration curve in standard nitric acid solution (2%) using non pyrocoated T-shaped furnace and short time temperature program.

5. RESULTS AND DISCUSSION.

The calibration curve data were plotted as shown in figure 5.19. The linear working range for bismuth is up to 300 $\mu\text{g/l}$, and then the deviation from linearity takes place at higher concentrations.

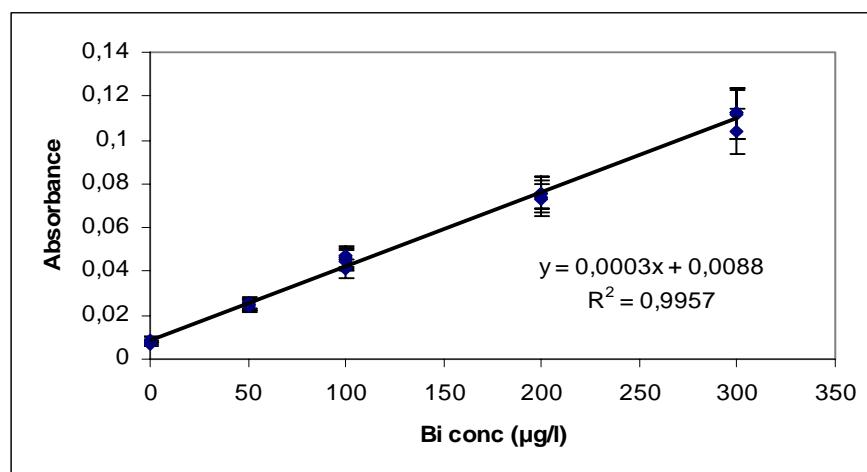


Fig.5.19 calibration curve for standard solution of Bi using non pyrocoated T-shaped furnace and short time temperature program.

The plot of the absorbance values against the amount of bismuth in the standard solution and it shows straight line with correlation coefficient of 0.997. The characteristic mass of bismuth was calculated. The value is equal to 90 pg, which is comparable with that for Perkin-Elmer of 60 Pg. The relative standard deviations for ($n = 5$) have been found to be between 2-11%. The limit of detection of Bi is equal to ($3s = 0.2 \mu\text{g/l}$).

From the previous section, one can say that the creation of calibration curve for the high volatile element group is possible using non pyrocoated T-shaped graphite furnace with conventional and short time temperature programs. All calibration curves are with good to excellent sensitivity and reproducibility. This means that the new furnace design should be applicable for the rest of the elements in this group.

5.4.1.2 ANALYSIS OF MIDDLE VOLATILE ELEMENTS

5.4.1.2.1 Copper

Copper was chosen as element of the middle volatile elements category, copper has less sensitivity as compared with silver and cadmium. Copper was determined at resonance line of $\lambda = 324.7$ nm and hollow cathode lamp current of 8 mA. Higher pre-treatment temperatures up to 1200°C could be used for copper in presence of 0.2 % nitric acid without losses of Cu atoms. The atomization temperature of copper was 2500° C, which is comparable with the atomization off L'vov platform (2300°C). The temperature program is shown in Table 5.5.

Table 5.5 Temperature program for Cu determination in standard solution at the resonance line of $\lambda = 324.7$ nm and lamp current intensity of 8.0 mA.

Step	T (°C)	Time (s)	Argon flow (ml/min)
Drying	120	10	500
Drying	120	20	500
Pyrolysis	900	10	500
Pyrolysis	900	20	500
Atomization	2500	10	10
Cleaning	2600	4	500

Figure 5.20 shows the absorption signals of standard solutions of copper, the absorption signals were sharp with appearance time of 3.0 seconds. The tailing in case of higher concentrations could be attributed to the formation of stable compounds, may be carbides at low heating rates and non pyrocoated graphite material of the furnace used.

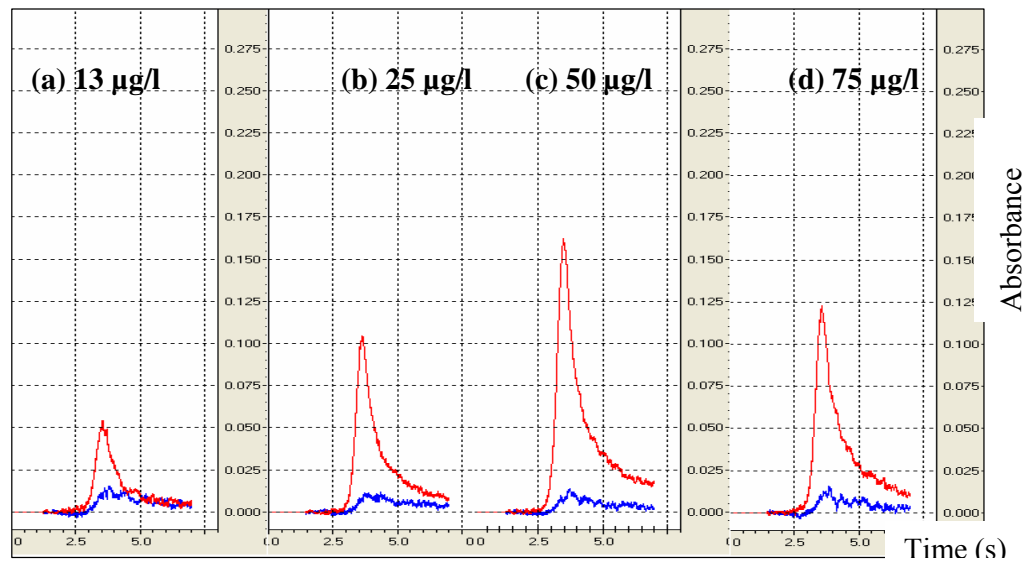


Fig.5.20 Signals for Cu calibration curve using non coated T-shaped furnace and
And continuous argon flow mode.

According to the expected sensitivity of the system, series of different copper standard solution concentrations were measured, the calibration curve is shown in figure 5.21.

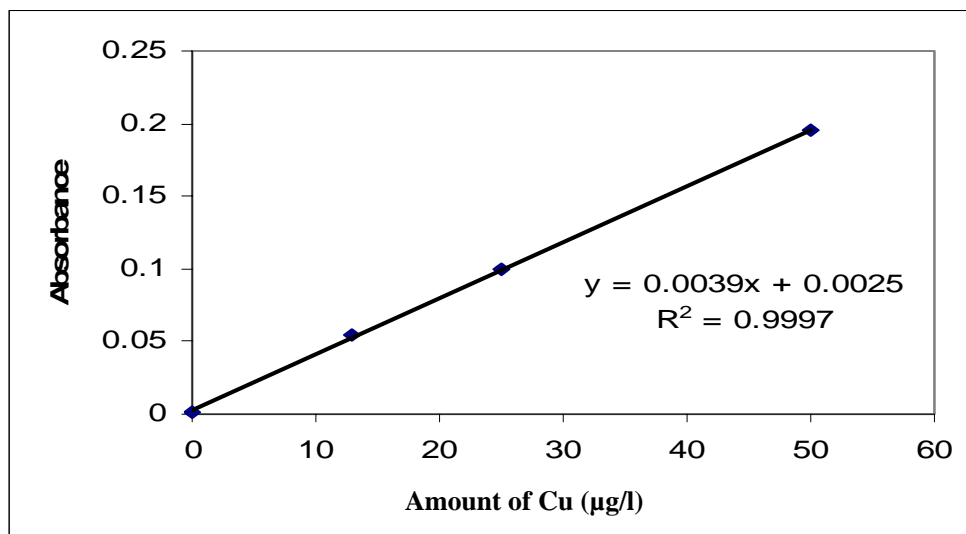


Fig.5.21 Calibration curve for Cu determination in standard solutions using
T-shaped graphite furnace and continuous flow mode.

The linear working range for copper was up to 50.0 $\mu\text{g/l}$, higher concentrations of 75.0 $\mu\text{g/l}$ shows deviation from linearity of the calibration curve the signal will returns to the original base line if higher heating rates, more atomization time and pyrocoated graphite used. The characteristic mass of copper was found to be 10.0 pg. the limit of detection for Cu is ($3s = 0.8 \mu\text{g/l}$).

As can be seen from the above calibration curve the absorbance increases directly with increasing concentration with correlation coefficient value of 0.999 and relative standard deviation of 3-9% for ($n = 5$).

The calibration is plotted using the mean value of absorbance after subtracting the mean value of the memory effect of copper in each case from the absorbance value obtained such that the percent error ranges are not shown in the calibration curve.

Copper is classified as one of the middle volatile elements group, but in case of using non-pyrocoated T-shaped graphite furnace copper atomizes at high atomization temperature because of forming thermally stable compounds which dissociates later and forms a tailing in the signal as mentioned above. Some of copper atoms stayed inside the furnace after atomization and cleaning step. This amount is treated as memory effect hence Copper maybe treated as low volatile element when using non pyrocoated furnace with lower heating rates.

5.4.1.2.2 Manganese

Manganese is known as an element in the middle volatile elements group. Manganese is measured at 279.5 nm with lamp current of 7.0 mA and with using 0.2nm slit width. The temperature program used for Mn determination is shown below in table 5.6.

Manganese atomizes easily from non-pyrocoated T-shaped graphite furnace as compared with the other elements in the same group such as copper and aluminium as can be seen from the figure 5.22 below. The absorption signals returns to the base line after time interval of maximum 10 seconds in case of high concentration sample. The determination carried out using temperature program with drying step followed by pyrolysis at 700°C then atomization of the sample at 2200°C.

Table 5.6 Temperature program for Mn determination in standard solution at the resonance line of $\lambda = 279.5$ nm and lamp current intensity of 7.0 mA.

Step	T (°C)	Time (s)	Argon flow (ml/min)
Drying	120	10	500
Drying	120	20	500
Pyrolysis	700	10	500
Pyrolysis	700	20	500
Atomization	2200	10	10
cleaning	2400	4	500

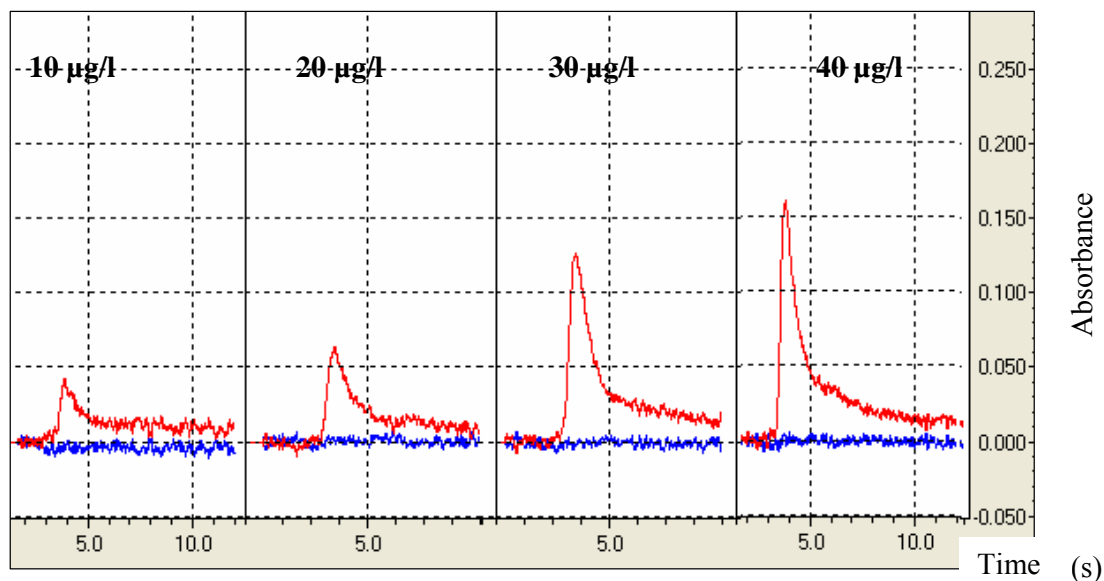


Fig.5.22 Signals for Mn calibration curve using non pyrocoated T-shaped graphite furnace in horizontal position.

Figure 5.23 shows the calibration curve for standard solution of Mn using non pyrocoated T-shaped graphite furnace. The data indicates linear relationship up to concentration of $40\mu\text{g/l}$ of manganese with correlation coefficient of 0.997 which is good correlation relationship and the relative standard deviation for $n = 5$ in the range of 3-11%.

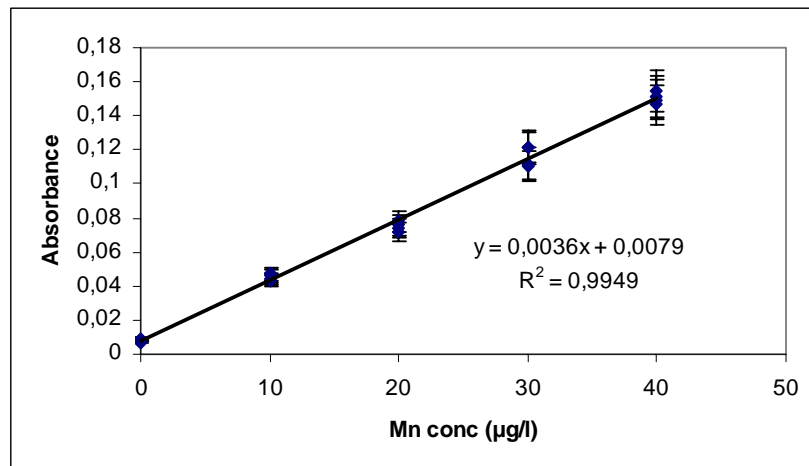


Fig.5.23 Calibration curve for standard solution of Mn using non-pyrocoated T-shaped graphite furnace.

The characteristic mass of manganese is found to be equal 11.0 pg, while it is 7.0 pg for Perkin-Elmer system. Our value is again comparable with the values found in literature. The limit of detection for Mn is equal to 0.8 µg/l.

5.4.2 QUANTITATIVE ANALYSIS OF TRACE ELEMENTS IN URINE

This chapter is much more important than the later one because calibration curves for standard solution without presence of any matrix can be created by all conventional AAS-systems but trace element analysis in presence of highly interfering matrix such as non diluted urine is a big challenge in this field.

Trace element analysis in non diluted urine sample is studied by applying principles of high temperature chromatography using T-shaped graphite furnace and short temperature program. Analysis of high, middle and low volatile elements in urine were done using standard addition method which is one of the most accurate methods for determination of analytes in different samples containing matrix that can influence the accuracy of the determination. it can be done by taking a number of replicate aliquot portions of the sample solution and adding to these solutions known quantity of the analyte to be measured (usually by using reference solution).

The series of the solutions obtained were used as a set for creating the calibration curve. By extrapolating the linear analytical line to the intercept with the negative X axis, the concentration of the analyte in the sample could be determined. As mentioned before elements of different volatilities such as Cd, Bi, Al, Cr and Mn were analyzed in urine using the standard addition method. The results are illustrated in the following sections.

All analyses using the non coated T-shaped graphite furnace were done with standard urine sample (Seronom No.2525). The result of each element determination was compared with the same analysis using the original Shimadzu graphite furnace.

5.4.2.1 QUANTITATIVE ANALYSES OF HIGHLY VOLATILE ELEMENTS

5.4.2.1.1 High temperature chromatography in analysis of cadmium

The direct determination of cadmium in standard non diluted urine sample was studied. Normally it is not possible to analyse any element in urine sample with out any pre-treatment because urine is known as highly interfering matrix, since it contains higher concentrations of organic and inorganic compounds.

In case of cadmium analysis using T-shaped furnace and short time temperature program the measurements will be more accurate if the sample is analysed directly without any pre-treatment because cadmium is very sensitive elements and the contamination risk in analysis is very high. T-shaped furnace as central experimental part for high temperature gas chromatographic quantitative determination of cadmium in urine allows the direct analysis of cadmium in non diluted urine using standard addition method. The short time temperature program of high temperature gas chromatography for Cd is shown in table 5.7.

Table 5.7 Short time temperature program for quantitative analysis of Cd in urine sample using non-pyrocoated T-shaped furnace.

Step	T (°C)	Heating mode	Time (s)	Inner argon (ml/min)	Purge argon (ml/min)
Drying	120	Ramp	15	500	30
Drying	120	Hold	20	500	30
Atomization	3000	Ramp	11	10	30
cleaning	3000	Hold	4	500	30

Chromatographic separation of cadmium from that for urine matrix (two blue signals) is possible using operation condition of high temperature gas chromatography and short time temperature program with continuous flow of purge argon as mentioned before.

Figure 5.24 illustrates the signals for quantitative determination of cadmium in standard non diluted urine sample using standard addition method. As can be seen from the signals, the cadmium could be analysed with very low matrix interferences since the urine matrix (Blue) composed of two main parts, organic part which was atomized firstly before atomization of cadmium and inorganic part which is atomized later after the appearance of the cadmium signal. In addition to the direct determination and matrix separation of the analyte and standard urine sample, the shorter time temperature program is also used. This program decreases the time of analysis since it contains only drying and atomization step. Complete evaporation and separation of cadmium and urine matrix as discussed before could be attained in 12 seconds. Since peaks are sharp and symmetric one can use peak height values to determine the amount of cadmium in the sample, it is a benefit of T-shaped furnace with high temperature chromatography since it is impossible to measure cadmium in non diluted urine without pre-treatment, dilution and use matrix modifier.

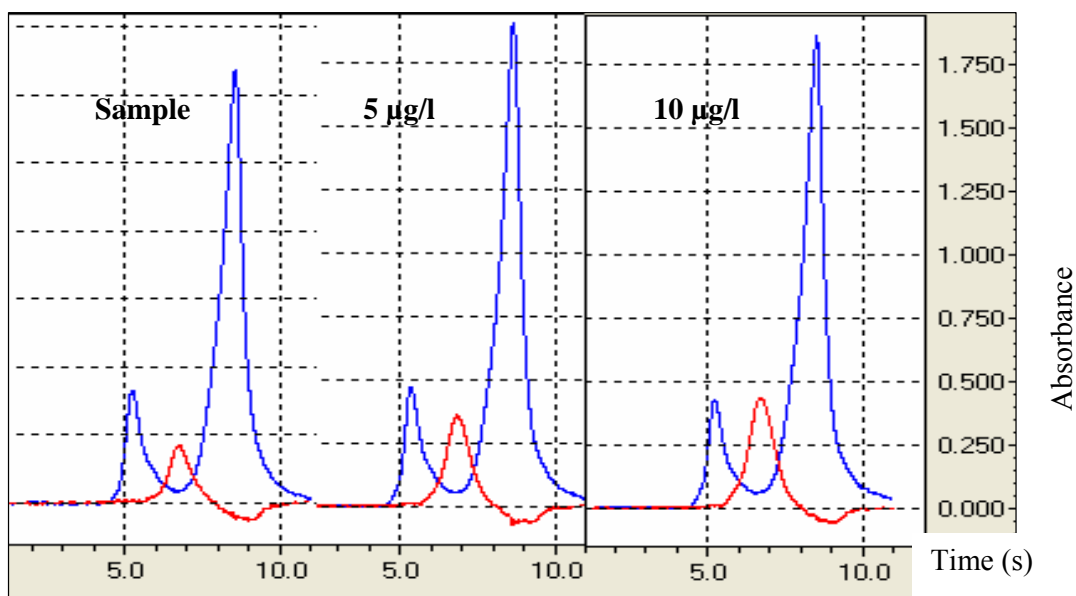


Fig.5.24 Signals for Cd (Red) determinations in urine sample (seronorm) using the non pyrocoated furnace and short time temperature program.

5. RESULTS AND DISCUSSION.

The average of the absorbance values were 0.195, 0.3373 and 0.465 for standard urine sample, first spiked with 5 $\mu\text{g/l}$ samples and second spiked with 10 $\mu\text{g/l}$ samples respectively. The relative standard deviation (RSD for $n = 5$) values were ranged from 3.5 – 10 % which excellent percent is considering the non pyrocoated graphite and peak height measurements.

The standard addition method for cadmium determination is illustrated in figure 5.25, linear relationship between the absorbance and concentration of the standard and spiked samples, with correlation coefficient of 0.998 as shown in the figure below.

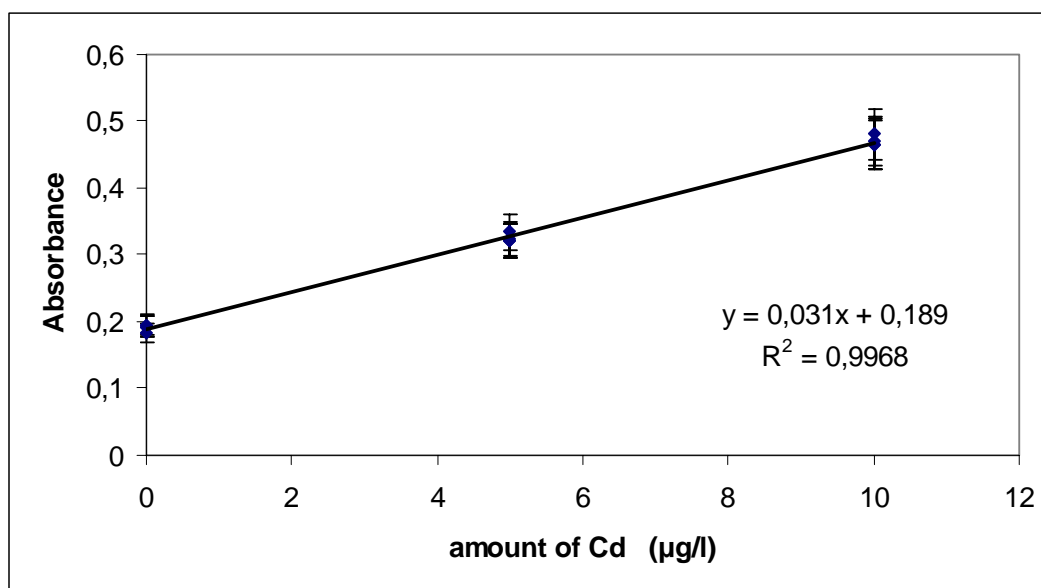


Fig.5.25 standard addition method for determination of Cd in urine using short time temperature program high temperature chromatography with T-shaped furnace

The characteristic mass is found to be 1.7 pg using non-pyrocoated T-shaped furnace with high temperature chromatography and continuous flow mode which is comparable with the characteristic mass value calculated by Perkin-Elmer using pyrocoated furnace with stop flow mode in standard cadmium solution (M_{ch} = found to be 1.3 pg, which is comparable with the value (1 – 2 pg described by Perkin-Elmer AAS, and 0.4 with TSAVP developed by

Grinshtein [30]). The agreement of both values enhances the applicability of high temperature chromatography method. The calculated value for amount of Cd in urine using this method is 5.7 $\mu\text{g/l}$, which also in good agreement with certified value (5.2 $\mu\text{g/l}$).

Analysis of cadmium using conventional AAS

For demonstrating the very positive features of the new approach, high temperature chromatography with AAS detection the results attained by the new system will be compared with conventional determinations of elements in the same sample solution by the classical Shimadzu AAS-System.

Figure.5.26 describes briefly the effect of urine matrix on the determination of cadmium using different conditions, for example, figure 5.26.A shows very high cadmium and background signal (Absorbance > 2.5), which out of the linear working range and the working range of the background corrector. This result arises when using the direct determination method (short program without pyrolysis step), and Pd as chemical modifier to stabilize the analyte atoms. Figure.5.26.B was done using typical temperature program recommended by Shimadzu without using any chemical modifiers assuming that the modifier stabilizes the matrix and not the element, no cadmium signal could be detected at pyrolysis temperature of 1000°C as can be seen from the figure below. Figure 5.26.C illustrates the signals when higher pyrolysis temperature was used (1300°C) with Pd modifier, the signal of the background was also very high (absorbance = 1.25), superimposed on the analyte signal hence impossible to be corrected. Ammonium phosphate modifier was also tested instead of Pd, the signal was unacceptable as mentioned before, and this case is shown in figure 5.26.D.

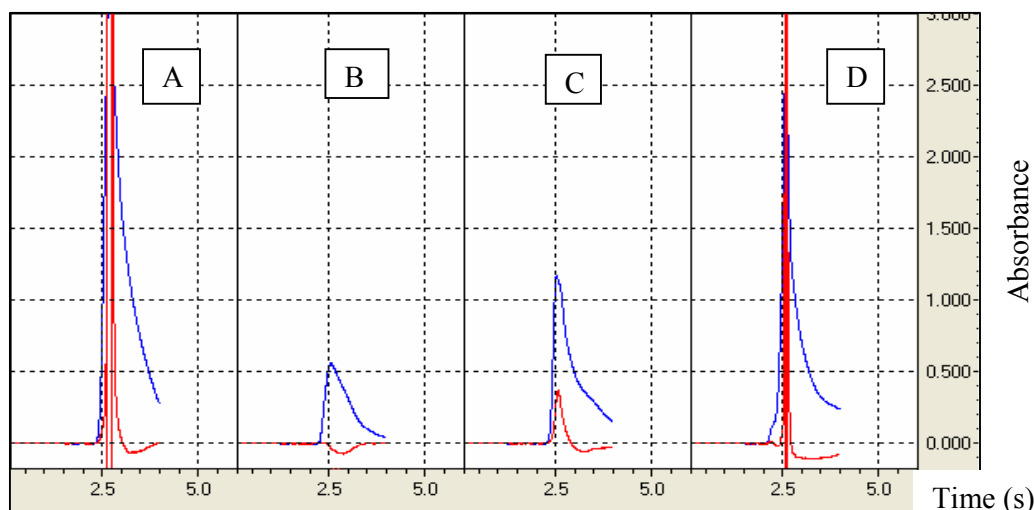


Fig.5.26 signals for Cd in urine (5.5 $\mu\text{g/l}$) using original Shimadzu tube
A; Pd short program, B; 1300°C, C; 1000°C and D; ammonium phosphate.

From the previous section, the results of cadmium determination in standard urine sample using a conventional high quality AAS-systems with different temperature programs and different chemical modifiers are not acceptable.

5.4.2.1.2 Quantitative analysis of Bismuth

The direct determination of Bi in standard urine sample at $\lambda = 223.1$ nm by using standard addition method and T-shaped graphite furnace was done. The standard and spiked sample was injected directly into the furnace, and the absorbance signals were measured. Table 5.8 shows the temperature program used in this determination of Bi. It is the same with the conventional program with drying the sample up to 120°C, pyrolysis step with 600°C and atomization was at 2200°C. Short temperature program could not be applied in case of Bi, because Bi is evaporized exactly with the urine matrix, but still we have the benefit of it is determination in nin diluted urine sample with small background values as compared with background values with conventional systems.

Table 5.8 Temperature program for Bi determination in urine with non-coated T-shaped furnace and continuous flow analysis.

Step	T (°C)	Time (s)	Argon flow (ml/min)
Drying	120	10	500
Drying	120	20	500
Pyrolysis	600	10	500
Pyrolysis	600	20	500
Atomization	2300	4	10
Cleaning	2600	4	500

The absorption signals of standard and spiked urine samples are illustrated in figure 5.27. Pyrolysis step is used in case of bismuth in urine because bismuth and urine matrix have the same retention time (short time temperature program is not possible), but the use of continuous flow mode allow the determination of bismuth with very low background signal, although it was not possible using conventional AAS-systems as will describe latter in case of analysis of bismuth using original Shimadzu tube.

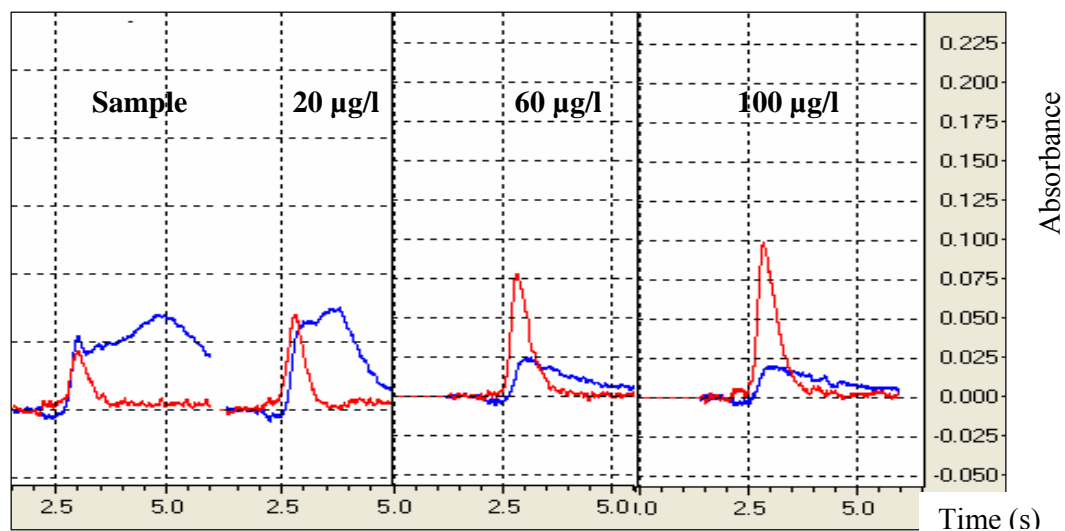


Fig.5.27 Signals for Bi determination in non diluted urine sample using non-pyrocoated T-shaped graphite furnace and conventional program

The absorbance data are plotted as shown in figure 5.28. The function was linear with correlation coefficient of 0.997 ($R = 0.998$). The sample content of Bi is found to be $19.5 \mu\text{g/l}$, which is in very good agreement with the certified value ($20.1 \pm 1 \mu\text{g/l}$).

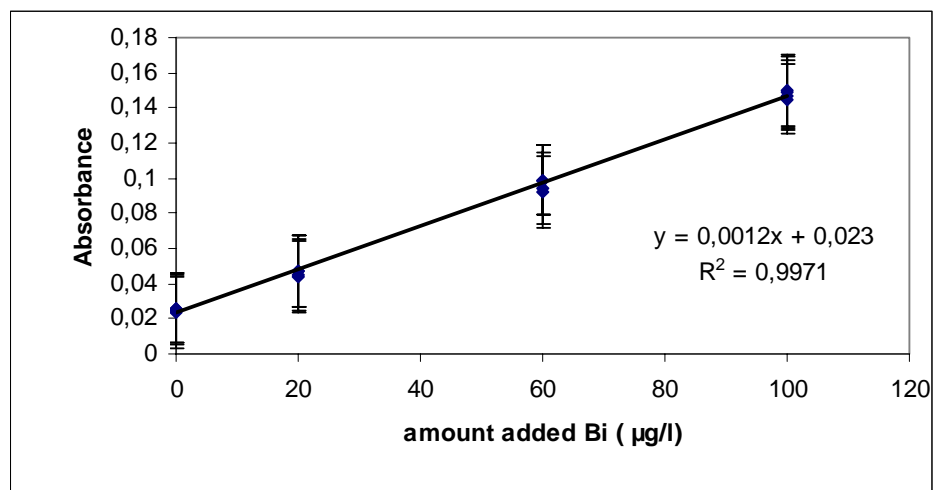


Fig.5.28 Standard addition method for determination of Bi in urine using non coated T-shaped graphite furnace and continuous flow mode.

The characteristic mass of Bi with the non coated T-shaped graphite furnace under these working conditions is found to be 30. pg, which is comparable with the value, calculated by Nunes [85] for Bi in case of atomization off furnace wall, the value is found to be 29.3 pg. The characteristic mass is found to be 60.0 pg by Perkin-Elmer [86].

Analysis of bismuth with conventional Shimadzu system

The temperature program used here was the same as that one used normally with the conventional AAS systems, the advantage of the our system is the possibility of the direct measurement of the non diluted urine sample, while in Germany, Bi medication is available without prescription and it is used for the treatment of different gastrointestinal symptoms and

disorders such as gastric ulcers, and over doses of Bi can cause severe myoclonic encephalopathy, hence Bi should be detected in urine at low concentrations. If the sample diluted three or four times as what usually done using the conventional AAS systems, the amount of Bi to be analysed is very low then it can not be detected. Additionally Bi is known as one of the most difficult elements to be analysed in the presence of urine matrix because of highly interfering effect of this matrix at absorption line of Bi 223.1 nm. This could be clarified within the following section. The analysis of real urine samples is even worse than the standard once. Analyses of Bi in urine using the original Shimadzu graphite furnace were done with different conditions (temperature programs and modifier) and three times dilution with 0.2% HNO₃. These analyses were summarized in figure 5.29.

In figure 5.29.A, the diluted standard urine sample was dried, and then atomized directly with short temperature program. The background absorbance was about 8-times greater than the Bi signal and could not be corrected as mentioned before.

The use of pyrolysis step and Pd as chemical modifier to get arid of the highly interfering matrix was tested and plotted in figure 5.29.B and C, In graph B the pyrolysis temperature was higher (1300°C) than that in graph C which was 1000°C, This difference in the pyrolysis temperature affects both, the analyte and matrix and higher amount of analyte lost in the higher temperature case and the interference of matrix is still present. The last graph figure 5.29.D, was carried out with pyrolysis but without using chemical modifier, complete loss of Bi as can be seen from the graph. The negative value of Bi in the case D is attributed to the

Spectral interferences of the urine matrix which indicates that, even when the Background signal could be corrected by the background corrector, the analyte signal appears with erroneously reduced value because of the spectral interference effect.

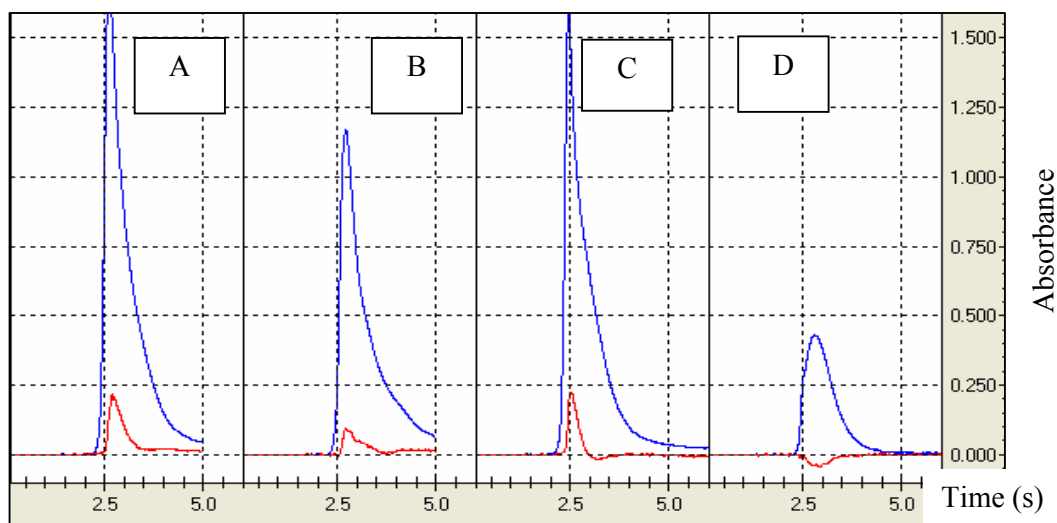


Fig.5.29 The analyses of Bi in diluted urine standard sample A: direct atomization; B and C: Pyrolysis (1300 and 1100°C) And D: without modifier.

From the previous studies, one could note that the determination of Bi in urine sample is more difficult as compared with Cd, because Cd could be analysed easily if the sample is diluted and pre-treated with pyrolysis and chemical modifier.

5.4.2.2 QUANTITATIVE DETERMINATION OF MIDDLE VOLATILE ELEMENTS IN URINE

5.4.2.2.1 Analysis of Chromium using T-shaped graphite furnace

Chromium was chosen as an element of the middle volatile elements group. The problem accompanies analysing chromium in highly interfering matrix such as urine is the insufficient radiation intensity of the deuterium lamp at the chromium resonance line 357.8 nm. Because of this reason the relatively higher background signals could not be easily corrected. It is possible with the new furnace design and the new analysis approach with continuous flow analysis. It is possible to reduce the effect of matrix so that chromium could be measured. Table 5.9 indicates the temperature program used in quantitative analysis of chromium in urine sample.

Table 5.9 Temperature program for Cr determination in standard solution at the resonance line of $\lambda = 357.8$ nm and lamp current intensity of 6.0 mA.

Step	T (°C)	Time (s)	Argon flow (l/min)
Drying	120	10	500
Drying	120	20	500
Pyrolysis	900	10	500
Pyrolysis	900	20	500
Atomization	2400	6	10
Cleaning	2600	4	500

Figure 5.30 shows the signals for chromium determination in urine sample by standard addition method. Memory effect during determination of chromium using non pyrocoated graphite furnace was observed, because of the presence of large number of active sites within the structure of non pyrocoated graphite which allows the reaction of chromium with graphite carbon forming stable carbides.

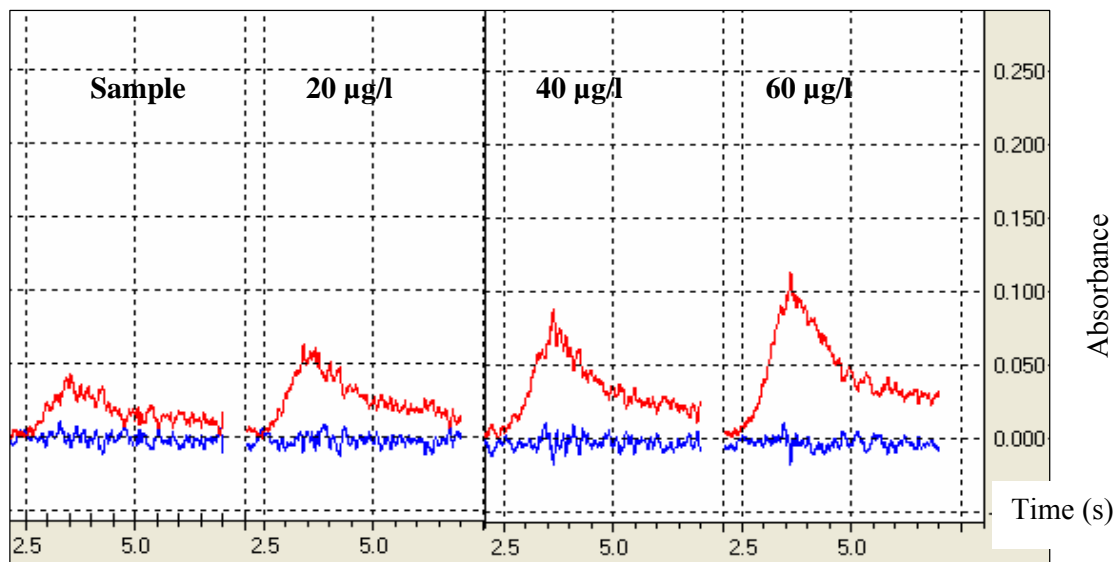


Fig.5.30 The calibration curve signals for Cr determination in urine sample (seronorm) using standard addition method and T-shaped graphite furnace

The memory effect value was with value of 0.02 absorbance. Hence this value was taken in account during the plotting of the standard addition method as can be shown later. The average memory effect value should be subtracted from the average value of each absorption signal before plotting the linear relation between absorbance and the added amount of chromium. The absorbance value after subtraction was used to plot the curve. Figure 5.31 illustrates the plotting of the absorbance value of chromium during the determination in standard urine sample by standard addition method.

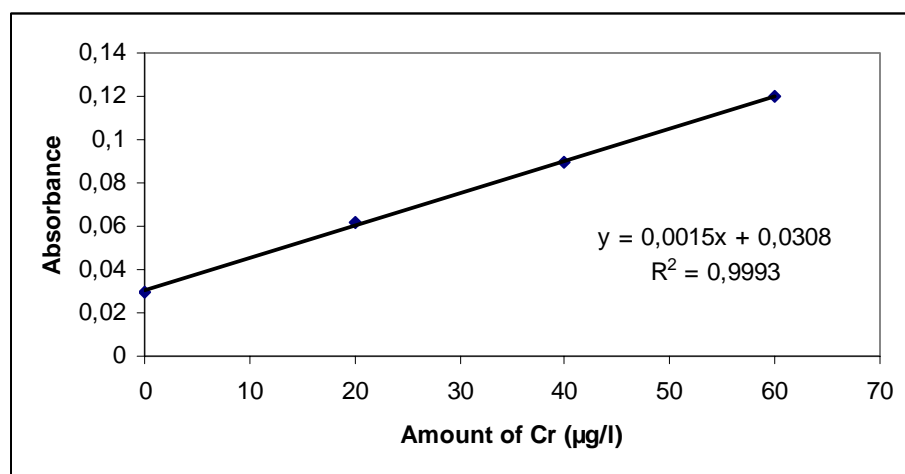


Fig.5.31 Standard addition method for Cr determination in standard urine sample using non coated T-shaped furnace and continuous flow mode.

The relation was linear correlation coefficient of 0.999 ($R = 0.999$) and the quantity of chromium in standard urine sample was found to be 20.5 µg/l, which is good agreement with the certified value is $20.1 \pm 1\mu\text{g/l}$ with respect to the difficulty of direct chromium determination in presence of highly interfering matrix such as urine. The characteristic mass was equal to 24 pg which is relatively high as compared with the value determined by the other systems (SIMAA6000 $M_{\text{ch}} = 7$ pg); this is because of determinations using the T-shaped graphite furnace and the use of continuous flow mode during atomization stage instead of stop flow.. This is well known effect which decreases the sensitivity of the measurement by decreasing the residence time of the analyte atom cloud in the measuring zone. The second is the effect of the non pyrocoated graphite material.

Analysis of chromium using Shimadzu furnace.

Determination of chromium was also studied using the original pyrocoated Shimadzu graphite furnace under different conditions. The absorption signals of different temperature programs are shown below in figure 5.32. The signal A in the figure represents the determination of chromium in standard non diluted urine sample at pyrolysis temperature of 800°C, it is not possible to determine chromium under this working conditions as can be seen from the signal, the spectral interferences could be indicated by the negative value of the analyte signal and higher value of the background at the same appearance time.

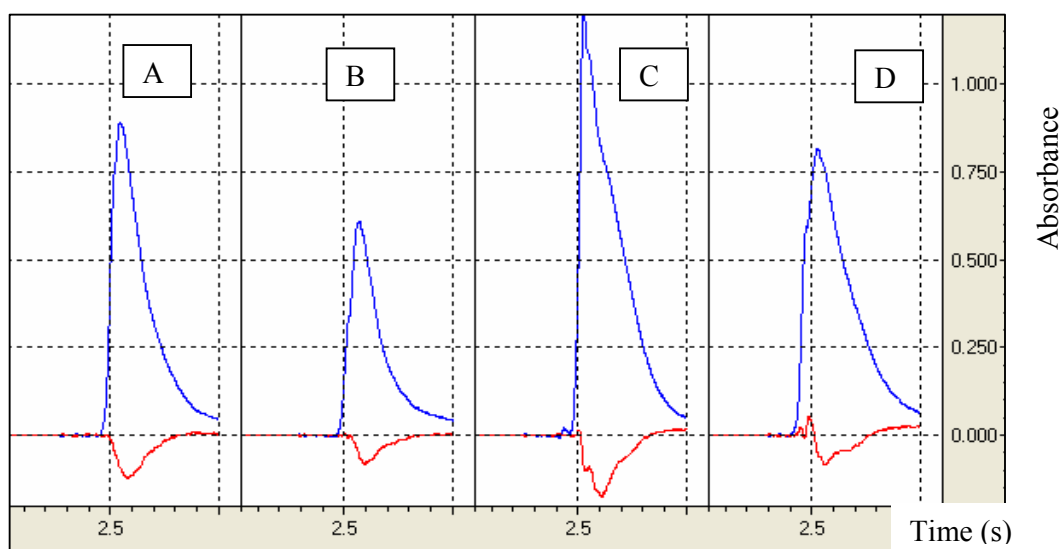


Fig.5.32 Signal for Cr determination using original shimadzu tube, A. Pyrolysis at 800°C, B. Diluted sample ($T_{py} = 800^{\circ}\text{C}$), C. Direct atomization, D. Pd modifier ($T_{py} = 1200^{\circ}\text{C}$).

Then the sample was diluted four times and measured with the same program, the result presented in the signal B, signal C shows the direct atomization (without pyrolysis step) of the diluted sample, and the signal D was obtained with pyrolysis temperature of 1200°C and Pd as chemical modifier for the diluted urine sample, a small chromium signal could be detected but accompanied with high background signal, spectral interference is also present.

To determine chromium in highly interfering matrix such as urine, a lot of pre-treatment should be done, optimization of the pyrolysis and atomization temperature and the selection

of suitable modifier for each kind of sample, dilution can cause problem in the detection of low concentrations of analytes, all the previous treatment is time and instrument consuming and increasing the cost of the analysis. There for analysis of chromium in presence of high interfering matrix such as urine is impossible to be done without pre-treatment steps using all conventional and developed AAS-systems.

Comparing with the conventional AAS-systems, T-shaped furnace in vertical position with applying the new approach of high temperature gas chromatography with AAS detection as mentioned before can be applied also for quantitative determination of chromium in non diluted sample with low background value because less amount of matrix being at same time with chromium in the measuring zone.

5.4.2.2.2 Analysis of Manganese with non coated T-shaped furnace

Manganese is an example of middle volatile elements is tested with non pyrocoated T-shaped furnace. With all conventional systems, quantitative analysis of manganese in non diluted urine samples without interfering of the matrix component was not possible, spectral interference are very well known in this determination.

Our measurement were carried out with continuous argon flow in all temperature program steps, in the atomization step the original argon flow from both sides of the T-shaped furnace through the light path was reduced to 10 l/min instead of stop flow mode which is normally used in the conventional systems. Additionally the argon was also purged through the sample port in order to push the atom cloud from the neck of the furnace to the measuring zone as shown in the schematic diagram (fig.5.1).

The determinations were carried out using normal temperature program as shown in table 5.10 composed of drying, pyrolysis at 1000°C, atomization at 2300°C and cleaning step. There is no analysis time reduction in the temperature program, but the determination is completely free from interferences even with highly interfering matrix such as urine which is not possible with all conventional AAS-system.

Table.5.10 Temperature program for determination of manganese $\lambda = 279.5$ nm in urine using T-shaped graphite furnace and continuous flow mode

Step	T °C	Time (s)	Mode	Inner argon (ml/min)	Purge argon (ml/min)
Drying	120	10	Ramp	500	30
Drying	120	20	Hold	500	30
Pyrolysis	1000	20	Ramp	500	30
pyrolysis	1000	20	Hold	500	30
Atomization	2600	6	Hold	10	30
Cleaning	2600	3	Hold	100	30

Figure.5.33 shows the signals of manganese determination in non diluted Seronorm urine sample, the signals represents the non spiked non diluted urine sample spiked samples for quantitative determination of manganese in non diluted urine using T-shaped furnace and continuous flow mode high temperature chromatography.

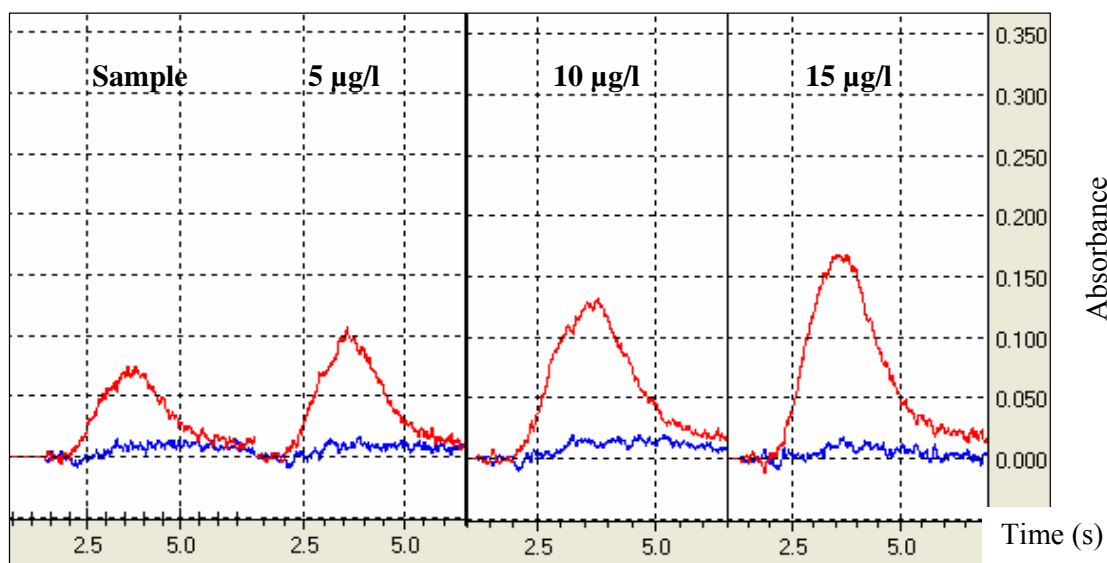


Fig.5.33 The calibration curve signals for Mn determination in standard non diluted urine (Seronorm 11.5 $\mu\text{g/l}$) sample by non-coated T-shaped furnace.

Plotting of the absorbance data against the amount of manganese added shows linear relationship and correlation coefficient with value of 0.997, hence the absorbance increasing with concentration with acceptable linear relation as shown in figure 5.34.

The relative standard deviation for (n =5) is found to be with maximum value of 3 -7%, which indicates good reproducibility of the measurements.

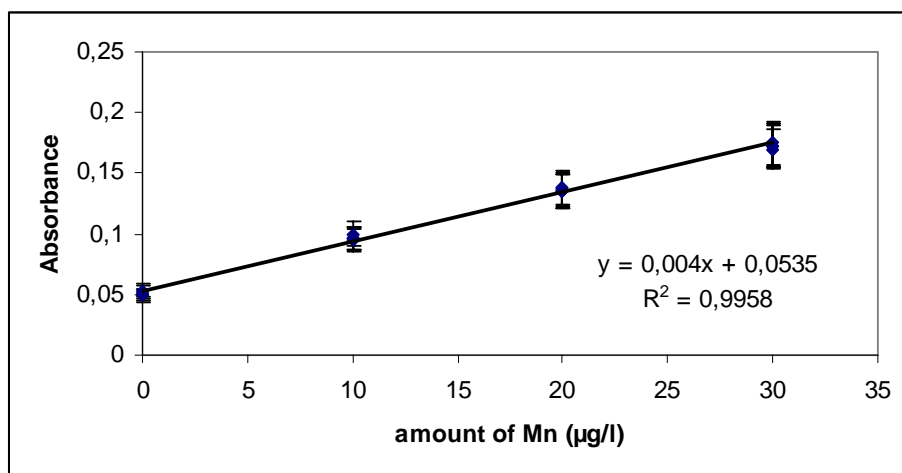


Fig.5.34 Standard addition method for determination of manganese in standard non diluted urine sample using T-shaped furnace.

Finally the amount of manganese found in the sample using standard addition method is found to be 12.5 µg/l, which is in good agreement with the certified value of 11.2±1 µg/l. The characteristic mass of manganese is found to be 6.8 pg, which very good value compared with that obtained by perkin-Elmer Simaa 6000, where the value is 6.3 pg using pyrocoated transverse heated graphite atomizer equipped with platform and atomization from standard solution.

Analysis of manganese using Shimadzu graphite furnace

Analysis of manganese in non diluted urine sample using original Shimadzu graphite tube is also done under different working conditions. Figure 5.35 shows absorption signals obtained with this system. As can be seen from all signals (A, B and C) the analyte signal is with negative value, which means that analyte evaporation and determination is highly affected

by strong urine matrix. In figure 5.35A analysis is done using 1000°C for pyrolysis step and recommended 2000°C for atomization step in presence of palladium nitrate as chemical modifier, high matrix signal with negative analyte signal is obtained. Figure 5.35B shows the signals obtained using the same temperatures in case A but with 2-times diluted sample and chemical modifier. Finally if the pyrolysis temperature is decreased to 700°C with the same atomization temperature, very high matrix signal is observed, and the negative analyte value is decreased. This means that there is possibility to determine manganese also in non diluted sample even under many different conditions. This adds another benefit to the analysis of trace elements in non diluted urine by T-shaped graphite furnace and high temperature chromatography.

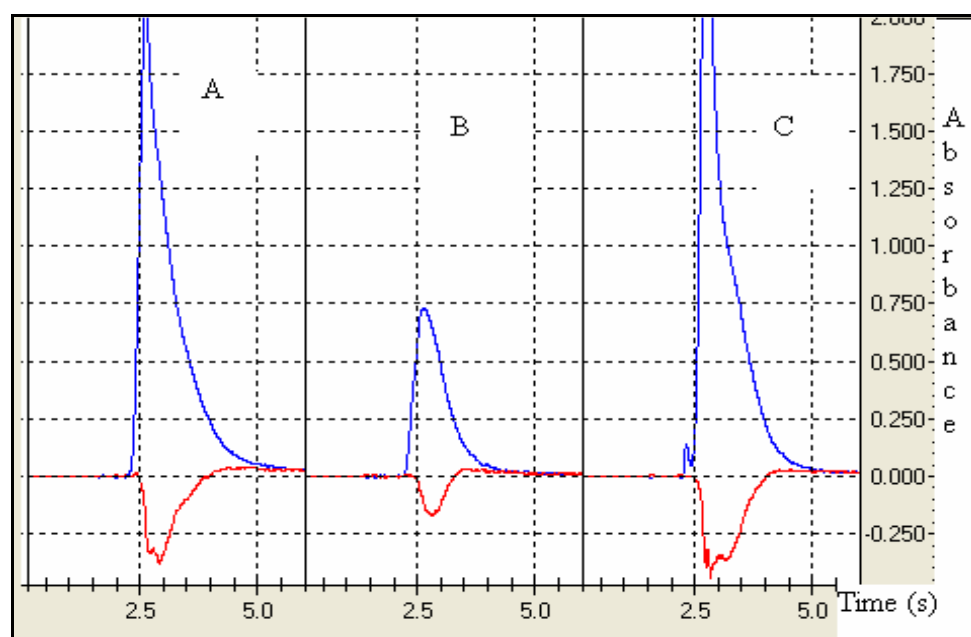


Fig.5.35 Analysis of Mn by Shimadzu furnace A: A. Pyrolysis at 1000°C, B. diluted sample ($T_{py} = 800^{\circ}\text{C}$), C. Pd modifier ($T_{py} = 700^{\circ}\text{C}$).

5.4.2.2.3 Analysis of Aluminium using T-shaped furnace

Aluminium calibration curve were carried out at the resonance line of $\lambda = 307.3$ nm using series of different concentrations and suitable lamp current of 10mA and slit width of 0.5 nm. Aluminium has volatility less than manganese within the middle volatile elements group, but

it is more volatile than copper thus high atomization temperature than that in case of cadmium, silver and manganese using the same argon flow rate condition.

Table 5.11 shows the temperature program used for quantitative determination of aluminium in non diluted urine sample using T-shaped graphite furnace and high temperature gas chromatography approach.

Table.5.11 Temperature program for determination of aluminium $\lambda = 307.3$ nm in urine using T-shaped graphite furnace and continuous flow mode

Step	T °C	Time (s)	Mode	Inner argon (ml/min)	Purge argon (ml/min)
Drying	120	10	Ramp	500	30
Drying	120	20	Hold	500	30
Pyrolysis	1100	20	Ramp	500	30
pyrolysis	1100	20	Hold	500	30
Atomization	2300	6	Hold	10	30
Cleaning	2500	3	Hold	1.0	30

The signals for analysis of aluminium in non diluted urine sample using non coated furnace are shown below in figure 5.36 as can be seen from the figure, the absorption signals are sharper as compared with that for copper. The tailing in the signal as mentioned before caused because thermally stable compounds are formed by the interactions of aluminium with the hot graphite walls of non pyrocoated furnace. The determination is carried out using the conventional temperature program with drying step, pyrolysis step at 1100°C using magnesium nitrate as modifier, atomization step at 2300°C and cleaning at 2500°C. The absence of the background signal in all cases indicates that all matrix concomitants are removed because of effect of the matrix modifier and the high temperature gas chromatographic separation with continuous flow measurement using the new T-shaped furnace design. The same effect of the furnace design can be seen in the former cases with manganese and chromium.

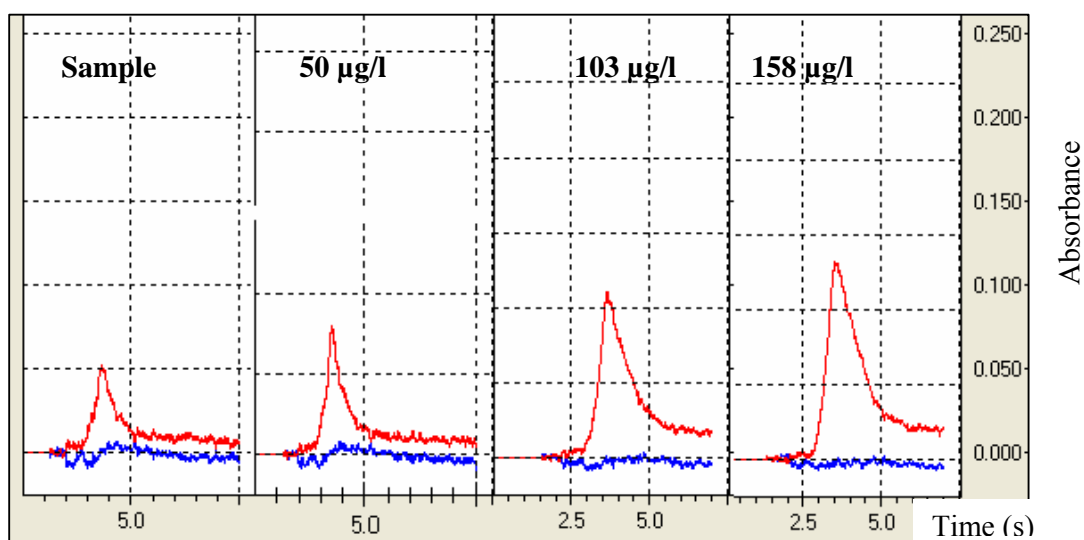


Figure 5.36 Signal for standard addition method for determination of Al in non-diluted urine sample using non-pyrocoated T-shaped furnace.

Figure 5.37 indicates the linear relationship of the absorption signals of aluminium in urine and the amount of aluminium spiked to the sample. The curve shows straight line with correlation coefficient of 0.997 which is known as good linear relation.

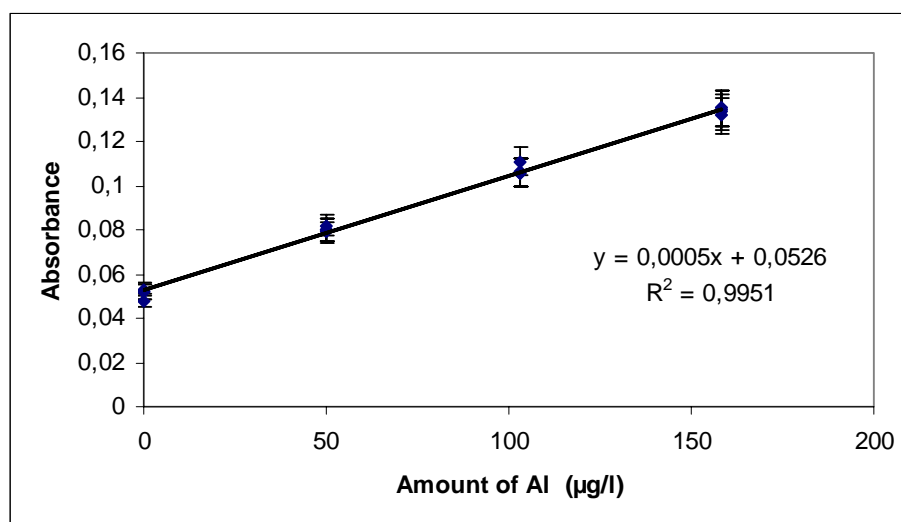


Fig.5.37 Standard addition method for analysis of Al in standard non diluted urine sample using non coated T-shaped graphite furnace.

Finally the amount of aluminium found in the sample using standard addition method and non pyrocoated T-shaped furnace with continuous flow mode is $105.2 \mu\text{g/l}$, which is in very good agreement with the certified value of $105.0 \pm 4 \mu\text{g/l}$. The characteristic mass of Al is found to be 19.0 pg , which good value compared with that obtained by Frech where the value is 14.0 pg and by THGA is 31.0 pg using the pyrocoated transverse heated graphite atomizer equipped with platform and atomization from standard solution [51].

Analysis of aluminium by conventional AAS-systems

To study the behaviour of non diluted urine sample during analysis of aluminium, different measurement conditions were tested using original shimadzu furnace and summarized in figure 5. 38. The same case arises as mentioned before with the former elements where the analysis of aluminium in urine sample is not possible without pre-treatment steps and dilution of the sample. Figure 5.38;a shows the signal for analysis of direct analysis of urine sample at pyrolysis temperature of 1000°C , the analyte signal (red) is very small as compared with the background, such absorbance value is incorrect and must be treated further. The signal in figure b belongs to the five times diluted urine sample, no valuable change under these working conditions because the overlap of the analyte and matrix signal is still present.

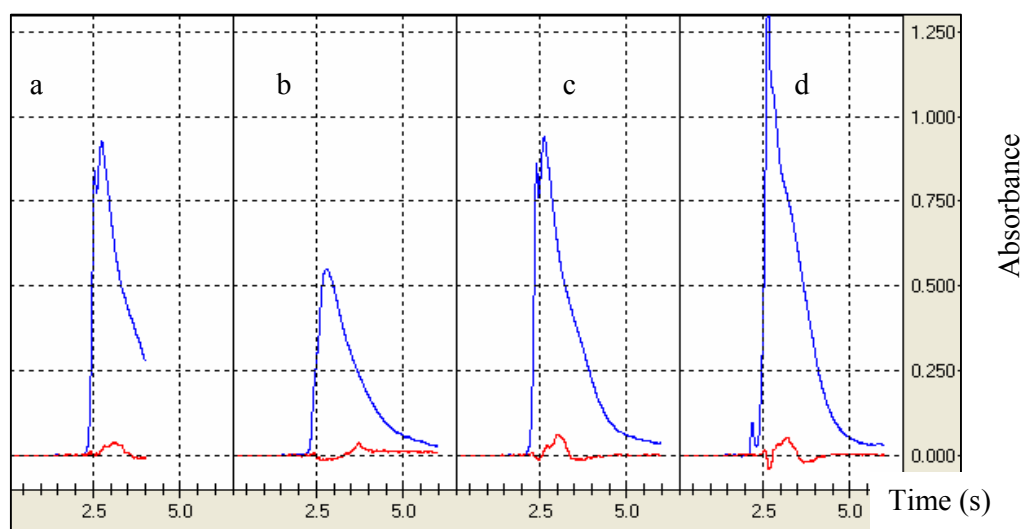


Fig.5.38 Signal for Al determination with Shimadzu tube, a. Pyrolysis at 1000°C ; b, diluted sample ($T_{\text{py}} = 1000^\circ\text{C}$); c. ($T_{\text{py}} = 700^\circ\text{C}$); d. Pd modifier ($T_{\text{at}} = 2300^\circ\text{C}$).

Figure c shows the absorption signal using less pyrolysis temperature to test the percent loss of the analyte as compared with the higher pyrolysis temperature. 700°C is used in this measurement but no correct measurement as mentioned before. Finally if we increase the atomization temperature from 2000°C to 2300°C with direct atomization as shown in figure 5.38; d.

As discussed before with all analyzed elements, it is not possible to analyze elements in standard non diluted urine sample (seronorm™) directly with out complicated pre-treatment steps and dilution because it contains very high interfering components.

5.4.2.2.4 Quantitative analysis of copper by non coated T-shaped graphite furnace

Standard addition method for quantitative determination of copper in standard non diluted urine sample using T-shaped furnace with continuous flow high temperature gas chromatography is tested. The measurement of absorption signals of copper at 324.8 nm and hollow cathode lamp with lamp current of 6mA and slit width of 0.5 nm were done. Temperature program for this determination is shown in table 5.12

Table.5.12 Temperature program for determination of copper $\lambda = 324.8$ nm in urine using T-shaped graphite furnace and continuous flow mode

Step	T °C	Time (s)	Mode	Inner argon (ml/min)	Purge argon (ml/min)
Drying	120	10	Ramp	500	30
Drying	120	20	Hold	500	30
Pyrolysis	1100	20	Ramp	500	30
Pyrolysis	1100	20	Hold	500	30
Atomization	2300	10	Hold	10	30
Cleaning	2500	3	Hold	1.0	30

Figure 5.39 shows the signals for urine sample and the spiked samples for the determination of Cu in urine sample. The appearance of Cu signals in all cases is after the appearance of the matrix means that the analyte and matrix signals are separated from each other by small time interval due to the use of T-shaped furnace with high temperature gas chromatography approach. Due to this separation, the amount of Cu in the sample is can be determined completely free from any interference.

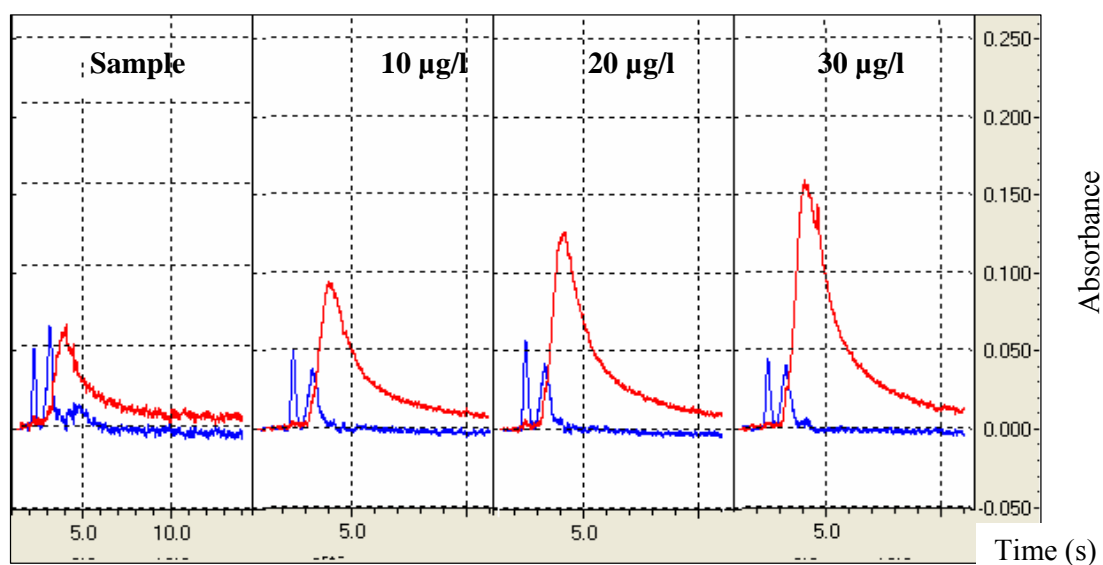


Fig.5.39 Signals for Cu determination in standard non diluted urine sample non pyrocoated T-shaped graphite furnace and continuous flow mode.

The sensitivity of the determination is about the same sensitivity of Cu in case of standard solution. Figure 5.40 represents the linear relationship during the copper determination. The data shows straight line with correlation coefficient of 0.996 and relative standard deviation between 3-6.5% .

The amount of Cu in non diluted urine sample has been found with value of 17.0 µg/l, which is in good agreement with the certified value given by value of (16.5±3 µg/l).

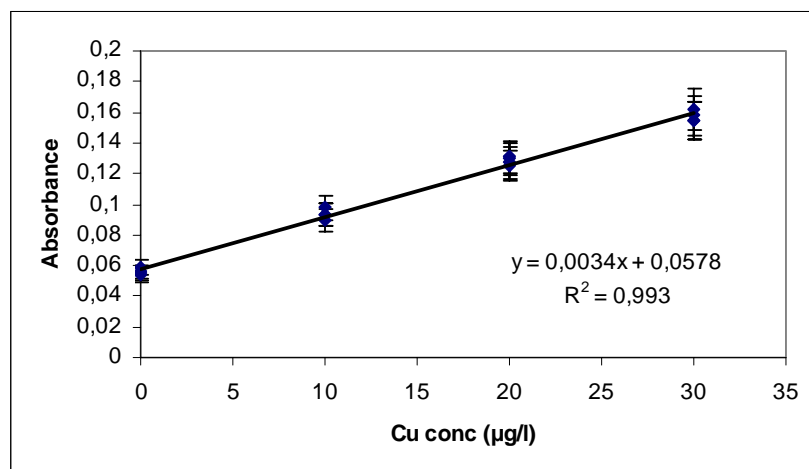


Fig.5.40 Standard addition method for determination of Cu in urine using non pyrocoated T-shaped graphite furnace and continuous flow mode

As a result of a series of determinations of trace elements in non diluted urine sample using T-shaped furnace with short time or conventional temperature program, analysis could be done with separated signals or free from background interference which is impossible to be done using all conventional and developed AAS-systems.

5.5 ANALYSIS WITH PYROCOATED T-SHAPED GRAPHITE FURNACE

The analysis of samples with atomic absorption spectrometer using pyrocoated graphite tube usually shows relatively higher sensitivity as compared with the same analysis using the non pyrocoated one as mentioned before. This is because of many reasons such as the possibility of side reaction in case of the non coated tube is higher because it contains more active sites then forming stable compounds which cause in reducing sensitivity especially when analysing middle and low volatile elements, another reason is the diffusion of the analyte through the furnace walls which is also known to be more in case of the non pyrocoated tubes.

5.5.1 ANALYSIS OF TRACE ELEMENTS IN URINE

5.5.1.1 ANALYSIS OF HIGH VOLATILE ELEMENTS

5.5.1.1.1 Analysis of cadmium

The determination of cadmium was carried out at the resonance line of cadmium with $\lambda = 228.8$ nm and hollow cathode lamp with a recommended current of 4.0 mA. The temperature program used is described in table 5.13 using continuous argon flow mode during

the atomization stage instead of stop flow mode purge gas in this determination was 30.0 ml/min.

Table 5.13 Short time temperature program for quantitative analysis of Cd $\lambda = 228.8$ in urine sample using pyrocoated T-shaped furnace

Step	Temperature (°C)	Heating mode	Time (s)	Inner argon (ml/min)	Purge argon (ml/min)
Drying	120	Ramp	15	500	30
Drying	120	Hold	20	500	30
Atomization	3000	Ramp	9	10	30
cleaning	3000	Hold	4	500	30

As can be seen from the figure 5.40, that cadmium shows absorption signals of 0.3A, which is relatively higher as compared with the same sample signals in case of non coated tubes. The separation of the analyte signal from the background signals is also possible with the pyrocoated T-shaped graphite furnace and high temperature gas chromatography approach and short time temperature program.

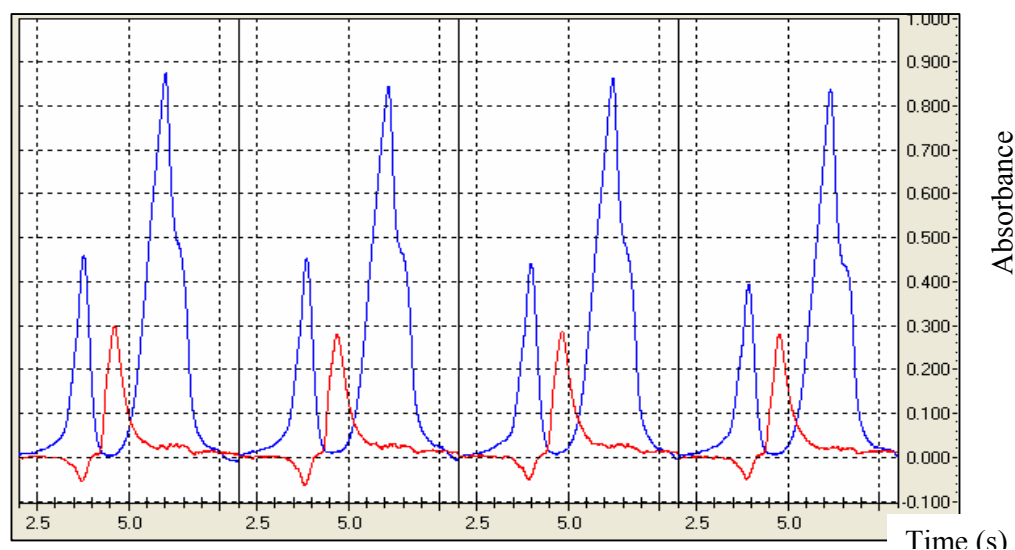


Fig.5.40 Signal for cd determination in standard urine sample (5.5 $\mu\text{g/l}$) using short time temperature program with high temperature chromatography.

Since the direct analysis of the standard urine sample with out dilution shows high absorption signals, and it is not recommended to analyse samples with higher absorption signal than 0.5 A, standard addition method is not created for this sample.

The signals for cadmium in standard non diluted urine sample (seronorm) using the non coated tube showed absorption values of about 0.190 A (figure 5.19), while with the coated T-shaped furnace in the above figure shows absorption value of 0.290A which is more than 1.5 times higher than the signals with the non coated furnace. This means that the sensitivity in cadmium determination in non diluted urine sample is two times higher for the analysis with the coated T-shaped furnace than non coated one.

5.5.1.2 ANALYSIS OF MIDDLE VOLATILE ELEMENTS

5.5.1.2.1 Analysis of copper with pyrocoated T-shaped furnace

The analysis of copper in the diluted urine sample using the non coated T-shaped graphite furnace, the sample shows absorbance signals between 0.05 – 0.075 depending on the furnace position, furnace situation, argon flow, and the furnace adjustments, while the same sample as shown if figure 5.42 below indicates higher absorption values (0.4A) using the pyrocoated T-shaped graphite furnace, which is about more than eight times higher than the signals with the non coated furnace.

The two analyses were done at the same absorption copper line, hollow cathode lamp and lamp current. Note that very low background signal although it is highly interfering matrix (urine) which indicates that the use of T-shaped graphite furnace allow the determination of Cu in non diluted urine completely free from interferences. Fore sure the analysis of Cu in non diluted urine using original Shimadzu tube will show the same behaviour of Cr since both have same atomization properties. The analysis was carried out using normal temperature program with pyrolysis step at temperature of 1000°C for 40 seconds (20 s ramp and 20 s holding time) and palladium as recommended chemical modifier.

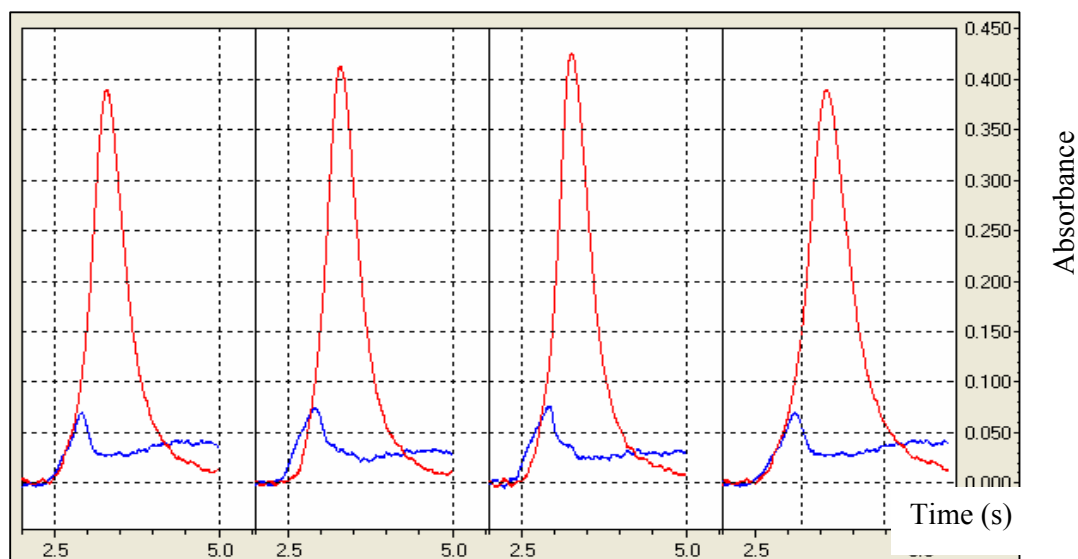


Fig.5.42 Signals for analysis of Cu in standard urine sample (Seronorm 16 µg/l) using coated T-shaped furnace and high temperature chromatography.

5.5.1.2.2 Short time and conventional temperature program in analysis of manganese with pyrocoated T-shaped furnace

In order to compare the two different temperature programs, analysis of manganese is done using pyrocoated T-shaped furnace with conventional temperature program (including pyrolysis step) and with short time temperature program (temperature gradient). In both case separation of matrix and analyte is possible. Short time temperature program with high temperature chromatography approach shows better separation, sensitivity and shorter analysis time as will discussed in the following sections.

Analysis of Mn in urine sample using conventional temperature program

The analysis using pyrocoated graphite furnace is known to be more sensitive and less memory effect because of less active sites in pyrocoated graphite than the non-pyrocoated one, hence less reaction tendency of pyrocoated graphite with urine sample components. Also the penetration of atomized sample into the graphite wall is less in case of pyrocoated tube. Signals for analysis of manganese in standard non diluted non acidified urine sample are

5. RESULTS AND DISCUSSION.

shown in figure 5.43; the signals are more symmetrical and uniform than that with the non-pyrocoated furnace. The temperature program used is shown in table 5.14.

Table.5.14 Temperature program for determination of manganese in urine using pyrocoated T-shaped graphite furnace and continuous flow mode

Step	T °C	Time (s)	Mode	Inner argon (ml/min)	Purge argon (ml/min)
Drying	120	10	Ramp	500	30
Drying	120	20	Hold	500	30
Pyrolysis	1200	20	Ramp	500	30
Pyrolysis	1200	20	Hold	500	30
Atomization	2400	5	Hold	10	30
Cleaning	2600	3	Hold	1000	30

As can be seen from table the temperature program used for the analysis consists of four steps, drying, pyrolysis, atomization and cleaning. The total time of each analysis is approximately the same with that used in case of the non pyrocoated tube. The purge gas was the same in both two cases with value of 30 ml/min during the whole measurements.

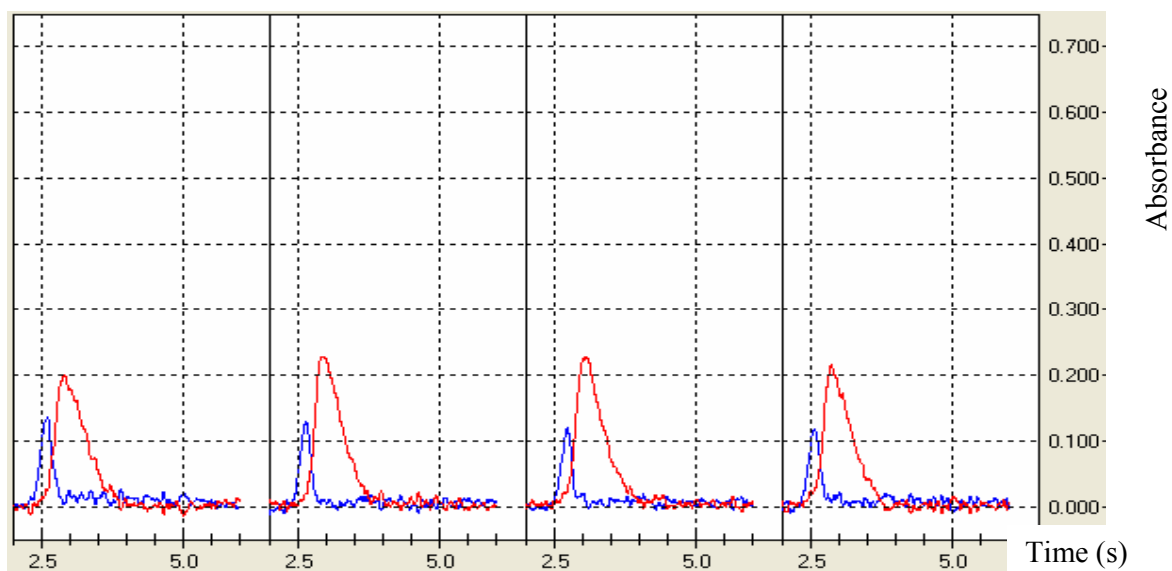


Fig.5.43 Signals for Mn in non diluted non acidified urine sample (Serorm 11.0 ppb)
($T_{Py} = 1200^{\circ}\text{C}$, $T_{At} = 2400^{\circ}\text{C}$)

By comparing the signals of manganese in urine using the non pyrocoated T-shaped graphite furnace shown in figure 5.33 with that signals using the pyrocoated tube shown in figure 5.43, one can observe that the difference in sensitivity between non-pyrocoated tube with absorbance value in terms of peak height ($A = 0.074$) and pyrocoated tube is found to be ($A = 0.220$). The sensitivity in case of pyrocoated furnace is three times higher than that with the non pyrocoated furnace. The signals are repeatable RSD of value 3.5% ($n = 5$).

The background absorbance in the first case was near to zero, which means that the effect of the matrix on the absorption of manganese is completely reduced, while in case of pyrocoated furnace the background signal was the half value of the absorbance value, this was because of higher sensitivity in case of the pyrocoated tube. The difference in appearance time of manganese and matrix component indicates the possibility of separation of the signals of analyte and matrix using the T-shaped graphite furnace.

The characteristic mass of manganese in standard non diluted urine sample with continuous flow measurements using the pyrocoated furnace is found to be 2.2 pg, while it was 6.5 pg in case of the non pyrocoated graphite furnace.

Figure 5.44 shows the analysis of standard non diluted urine sample at different pyrolysis temperatures (800 and 1200°C) with the higher background signal in case of the lower pyrolysis temperature (800°C), which is three times higher than the signal in the case of the second pyrolysis temperature (1200°C). In both cases the separation of the background and the analyte signals were possible and the absorbance values expected to be more correct than that if the two signals are super imposable on each other (all conventional AAS-systems).

The shape of the peak is sharper in the second case (1200°C) is because of the difference between the pyrolysis and the atomization temperature in the second case (1200°C) is less than the difference between them in the first case (1600°C), so that the atomization temperature in the second case could be achieved easier because of the smaller difference in the temperature between the pyrolysis and atomization temperatures and higher heating rate in the second case than that in the first case.

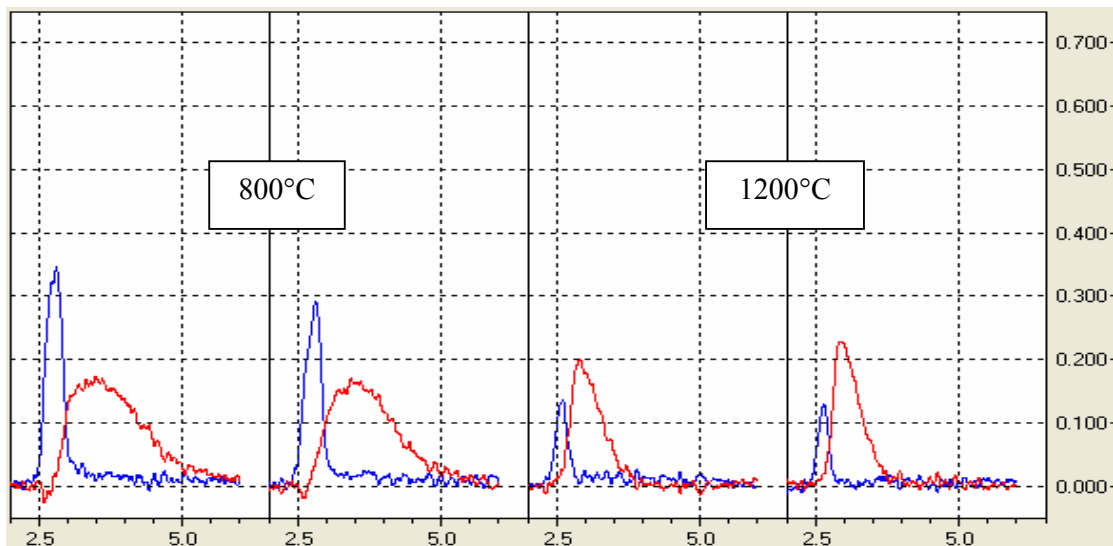


Fig.5.44 Mn signals in standard urine sample Seronorm (10 μ l of 11.0 μ g/l) using T-shaped furnace and continuous flow mode at different pyrolysis temperatures ($T_{Py} = 800^{\circ}\text{C}$, 1200°C).

Analysis of Mn in urine sample using short time temperature program

Standard urine sample with lower amount of manganese is used in order to create quantitative analysis of Mn using T-shaped graphite furnace with high temperature gas chromatography approach (temperature gradient) and short time temperature program. The short time temperature program is another advantage of analysis using the T-shaped graphite furnace. The short time temperature program consists of drying step and atomization step with slow heating rate (temperature gradient) and it may contain cleaning step depending on the type of the sample. The temperature program used is presented in table 5.15 below.

Table 5.15 Short time temperature program used for quantitative analysis of manganese in urine sample (Biorad Mn < 3.5 μ g/l)

Step	T $^{\circ}\text{C}$	Time (s)	Mode	Inner argon (ml/min)	Purge Argon (ml/min)
Drying	120	10	Ramp	300	30
Drying	120	20	Hold	300	30
Atomization	3000	10	Ramp	10	30

The amount of manganese in urine sample (Biorad) with certified value less than $3.50 \mu\text{g/l}$. Comparing to the conventional temperature programs, the short temperature program consists of three steps with total analysis time of 40 seconds instead of 5-8 steps with total analysis time of about 150 seconds. Short time temperature program means less analysis time and more samples could be analysed and longer life time of the graphite furnace.

The direct determination of the sample without pre-treatment or dilution and modifier addition in the pyrolysis step reduces the contamination risk of the sample which may be caused by these pre-treatment steps. A non acidified sample has less corrosive effect on the inner walls of the graphite furnace than the acidified one because of the reaction of nitric acid with the hot graphite walls of the furnace. Figure 5.45 shows the signals of analyses of manganese in urine sample with the short time temperature program; the atomization step was carried out with slow heating rate (temperature gradient) instead of atomization with maximum heating rate.

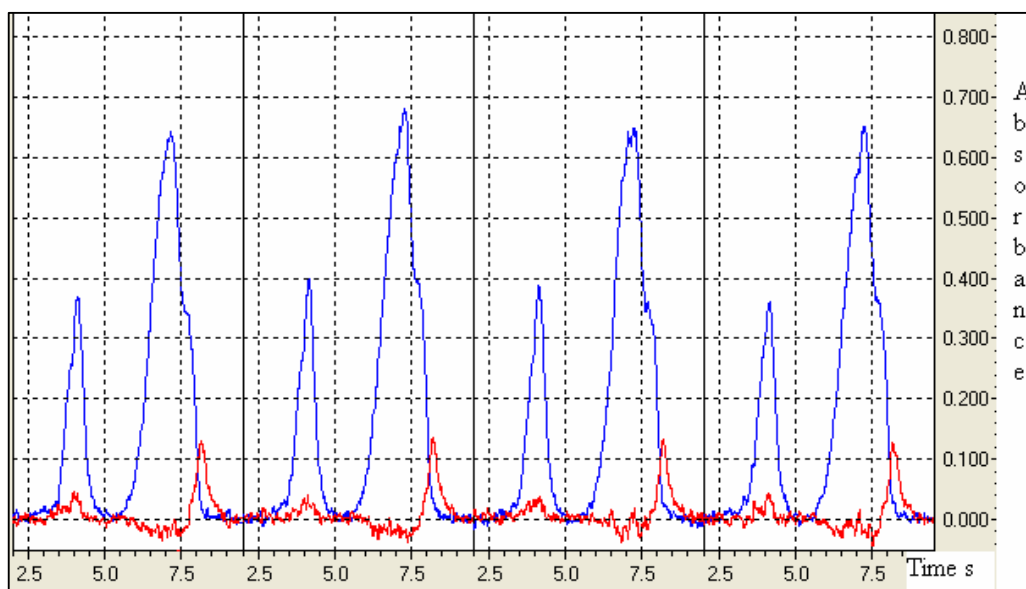


Fig.5.45 Signals for Mn in urine ($<3.5 \mu\text{g/l}$) using T-shaped graphite furnace with short time temperature program and high temperature chromatography.

As can be seen from figure 5.45, high background signal compared with the analyte signal (about seven times lower than the background signal), such case is not possible to be

corrected with the deuterium lamp background correction if the two signals appear at the same time. Because the appearance time of the analyte and background signals is not the same when using the T-shaped graphite furnace with short time temperature program and additional purge argon, and the signals are separated from each other, the analysis of non diluted urine sample is possible with very good reproducibility and precision.

Figure 5.46 is the magnification of the signals of manganese in urine sample, the separation and the reproducibility is clearer and the analyte absorbance value in term of beak height is five times higher than the background absorbance value which can be easily corrected with this system.

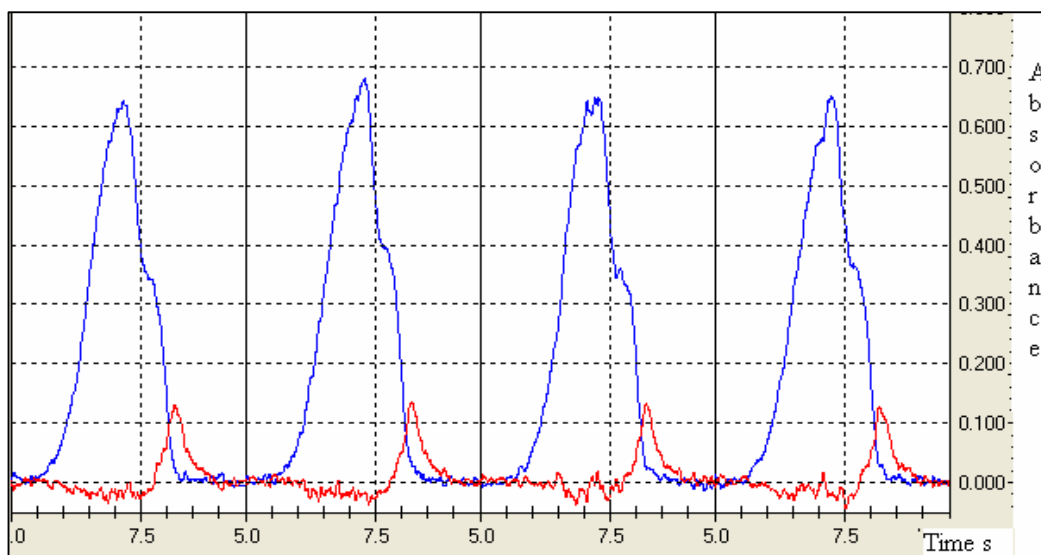


Fig.5.46 Magnification of signals in fig.5.45

Figure 5.47 shows the signals of determination manganese in non diluted urine sample, 1st, 2nd and 3rd spiked urine sample for quantification of manganese in this sample. The separation of the analyte and the background signals of all spiked sample allow the direct determination of manganese in this sample. Linear relationship between urine and three spiked samples with correlation coefficient of 0.996 as shown in figure 5.48

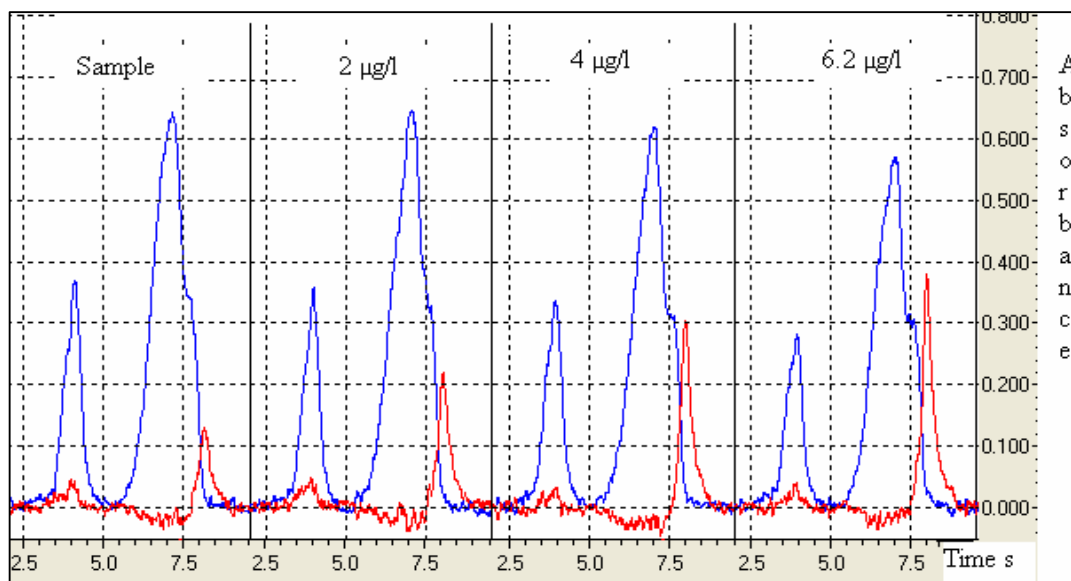


Fig.5.47 Signals for standard addition method for Mn determination in non diluted urine sample (Biorad <math><3.5 \mu\text{g/l}</math>) using pyrocoated T- shaped furnace and short temperature program.

The statistical analysis shows low standard deviation values for all measurements, which in turn indicates that the analysis was with low relative standard deviations values are within the range of 2-6.5 % for $n = 5$ measurements, which are excellent values especially when the measurements carried out in terms of peak height values.

The extrapolation of the straight line will cross the concentration axes at the value of the urine sample. The amount of manganese in this urine sample is certified by value less than $3.5 \mu\text{g/l}$, and found to be with value of $3.2 \mu\text{g/l}$ Mn using T-shaped furnace and short program with continuous flow measurement. The same sample is analysed after pre-treatment (5-times dilution and pyrolysis with chemical modifier) using THGA equipped with platform (SIMAA6000 from Perkin-Elmer), the amount of Mn is found to be of value $3.00 \mu\text{g/l}$.

The characteristic mass for manganese with short time temperature program was found to be 0.3 pg and of 0.65 pg using the conventional temperature program.

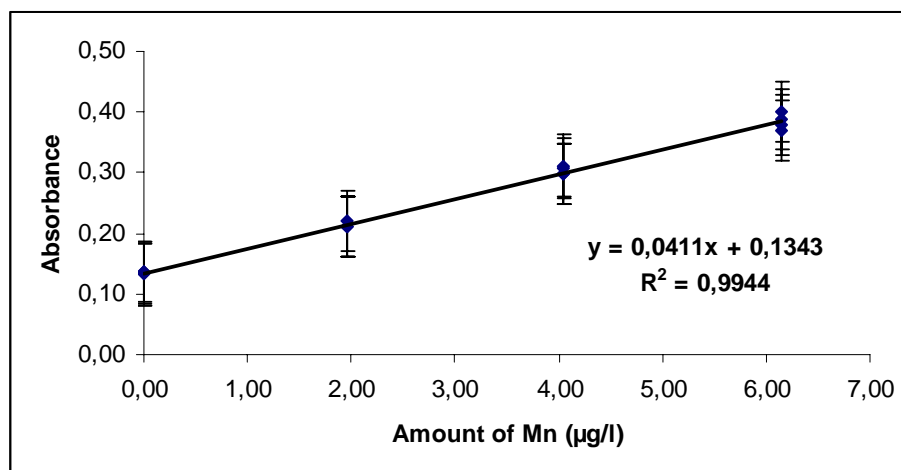


Fig.5.48 Standard addition method for Mn determination in standard non diluted urine sample (Biorad <3.5 µg/l) using pyrocoated T-furnace and short temperature program

One can say again that with using the short time temperature program with high temperature chromatography approach, the analysis of urine is standard urine samples is possible with higher sensitivity and less background interferences.

Figure5.49 illustrates the difference in sensitivity between the analyses of Manganese in standard non diluted urine sample (seronorm) using the short time temperature program with out pyrolysis step (figure 5.49A) where the absorbance value was 0.580 and the normal temperature program with pyrolysis step and chemical modifier (figure 5.49B) where the absorbance value is 0.220.

Further more the peaks attained using short temperature program is very sharp and symmetric with total time of 0.8 second, while the peak in case of normal temperature program is relatively broad with total time of 1.5 seconds, the sharpness of peaks with continuous flow mode T-shaped furnace leads to complete separation of analyte and matrix signals such that analysis of non diluted urine sample becomes possible with shorter analysis time and less contamination risk. The sensitivity when using the short time temperature program is about 2.5 times higher than with the conventional temperature program.

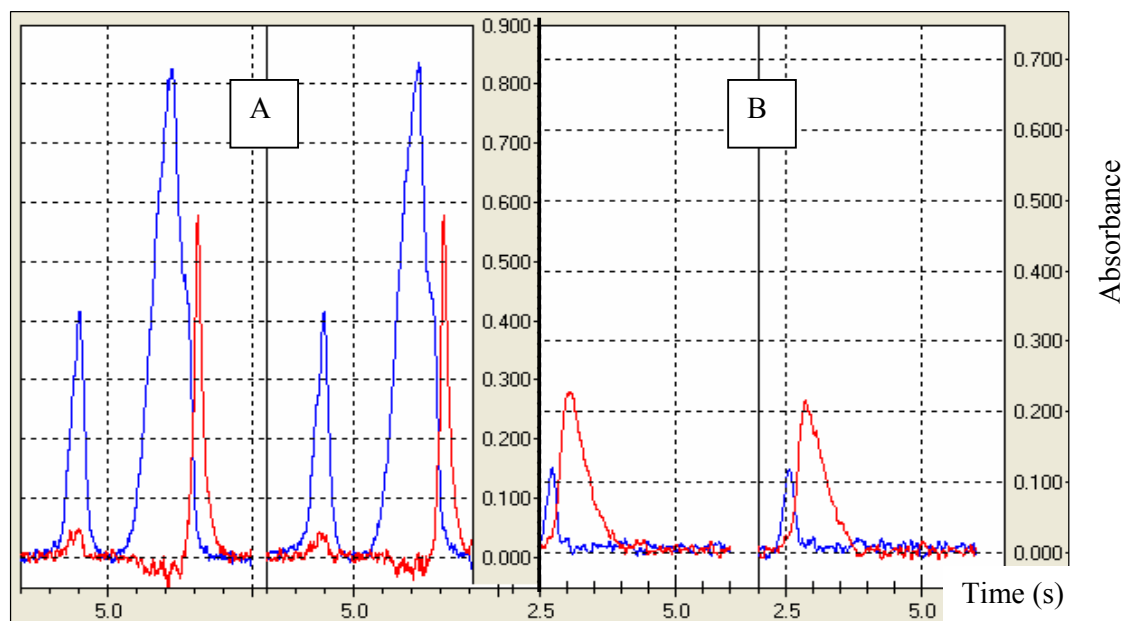


Fig.5.49 (A) Analysis with short time temperature program. (B) analysis with pyrolysis step 1200° C.

Since manganese is highly volatile element compared with elements in the same middle volatile element group and manganese signals could be separated from the urine background signal with higher retention times (urine matrix evaporized first then manganese), one can expect that analysis of elements with less volatility than manganese should also be separated from the background signals with higher separation and resolution factor values.

5.5.1.2.3 Analysis of Aluminium in urine

Analysis of aluminium in standard non diluted urine sample using the pyrocoated T-shaped graphite furnace shows higher sensitivity compared with non-coated furnace as mentioned before in case of analyzing middle and low volatile elements. Aluminium in urine shows absorbance values of about 0.05 using the non-coated tube (figure 5.35), and the same sample shows absorbance value of about 0.28 using the pyrocoated T-shaped furnace and the same urine sample. The sensitivity difference is about five times higher than that with non coated tube. Figure 5.50 illustrates the absorption signals of aluminium in urine using the pyrocoated furnace. The background absorbance is very small as compared with background signals measured by original Shimadzu tube, this is because of T-shaped function since the sample

atomized in the neck and transferred to the measuring zone, while in case of original tube the sample (analyte and matrix) atomized and measured in the same position and time. The analyte (aluminium) signal as expected before is completely separated from the background signal (urine matrix) as can be seen from the figure below when using T-shaped graphite furnace and temperature chromatography approach. Referring to analysis of aluminium using original Shimadzu furnace where the same sample was impossible to be analyzed. The signals are baseline separated and no need to calculate separation factor since it is clear on the figure.

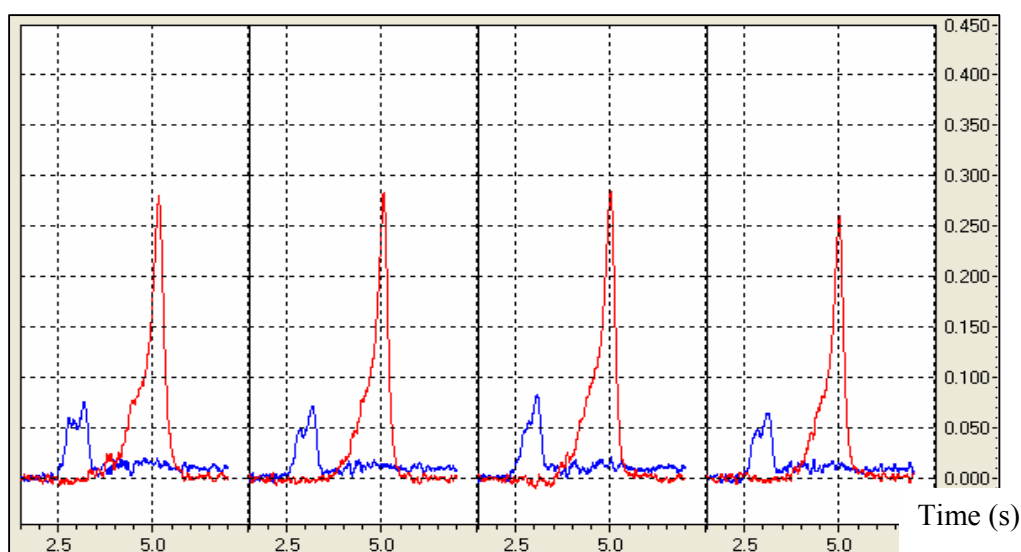


Fig.5.50 Signals of Al in standard non diluted urine sample (Serorm 105 μ g/l) using T-shaped furnace and short time temperature program.

5.5.2 ANALYSIS OF TRACE ELEMENTS IN BODY FLUIDS

In order to test the performance and applicability of the pyrocoated T-shaped graphite furnace with high temperature chromatography and short time temperature program, other samples with strongly interfering matrices such as bovine liver and bovine muscle were tested.

Standard reference sample of bovine liver (BCR-CRM 185R) was used. A certain weight of the solid sample was digested in purified redistilled nitric acid over night, and then measured. Figure 5.51 shows the absorption signals for Cd in standard bovine liver sample using the T-

shaped furnace and short time temperature program composed of only two steps, drying step followed by atomization with slow heating rate for 12 seconds i.e. the total temperature program time is only 42 seconds. The signals of the background and analyte are relatively separated as compared with that obtained normally by conventional systems and the relatively low background signal can be corrected with the deuterium lamp corrector.

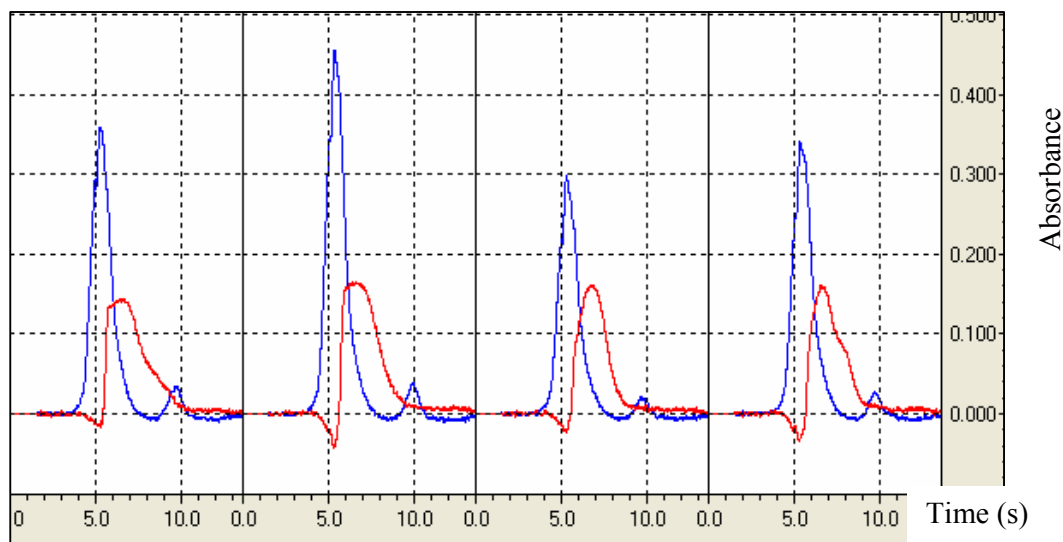


Fig.5.51 signals for Cd in bovine liver using T-shaped furnace and short time temperature program

To study the effect of change the heating rates of the sample by run the measurements of the bovine liver sample with different short temperature programs. Figure 5.52 shows the change of the signal forms with changing the temperature program. First two signals using 14 seconds to show the repeatability of the signals, the third signal with 12 seconds and the last signal with using only 7seconds. As can be seen from the same figure, when using 14 seconds time interval the furnace heated slowly to reach 3000°C within this time interval (the heating rate is $215^{\circ}/\text{s}$) the analyte signal is about 2-times broader than that using 7 seconds ($425^{\circ}/\text{s}$). In case of highly heating rate the analyte and background signals are sharp and better separated.

When using middle heating rate of 12 seconds ($250^{\circ}/\text{s}$), the signals are middle sharp and not completely separated. In such kinds the short temperature program can be used, but it still

needs to be optimized in order to get the best condition for the separation of the analyte and matrix.

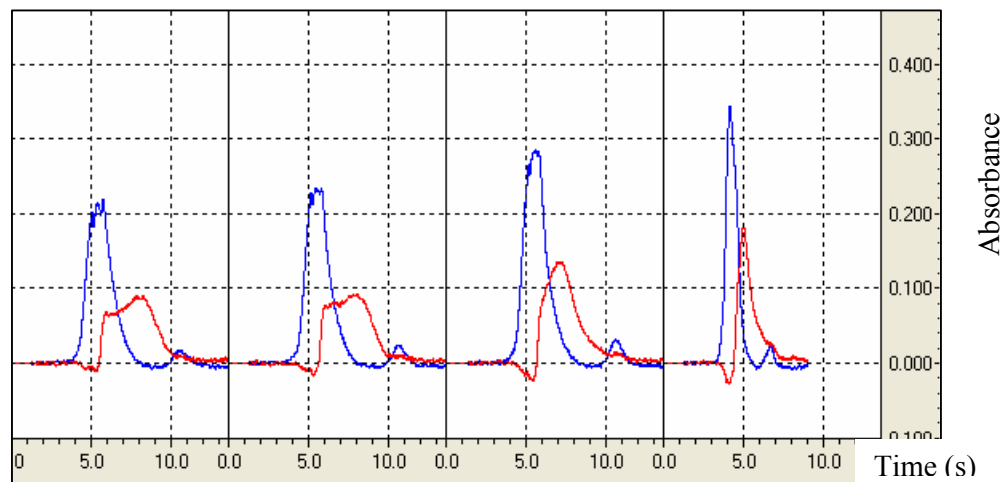


Fig.5.52 signals for Cd in bovine liver with different heating rates 215°/s, 215°/s, 250°/s, and 420°/s

From both figures above, one can note that the bovine liver matrix atomized faster than Cd atoms which in turn classified as high volatile element hence one can expect that all metals of middle and low volatile group elements can be determined in bovine liver completely free from interferences using the T-shaped graphite furnace and short time temperature program with high temperature gas chromatography approach. The same situation could be applied in case of middle and low volatile elements in urine (refer to fig 5.50 for Al analysis).

Manganese is the highest volatile element in the middle volatile element group, the measurement of absorption signal of Mn in bovine liver shows a complete separation of the analyte and background, even the sample contains large amount of Mn but the background signal is almost equal to zero at the appearance time of Mn, this means that it is possible to analyse Mn in bovine liver free from interferences. The absorption signals are shown in figure 5.53. The separation factor in this case more than 1.8.

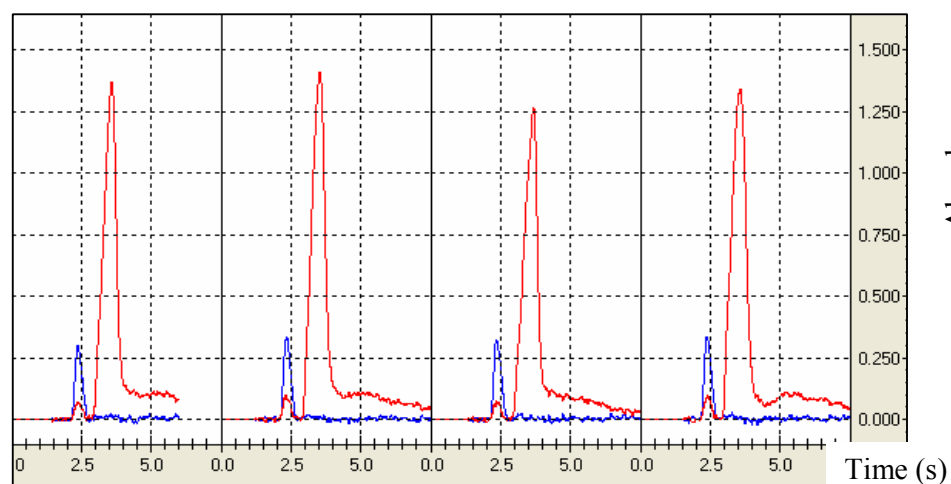


Fig.5.53 Signals for Mn in bovine liver using T-shaped furnace and short time temperature program

Another kind of matrix is also tested for analysis of middle volatile elements. Chromium is taken as example of this group. The absorption signals of Cr in standard reference material of bovine muscle (BCR-CRM 184) are shown in figure 5.54.

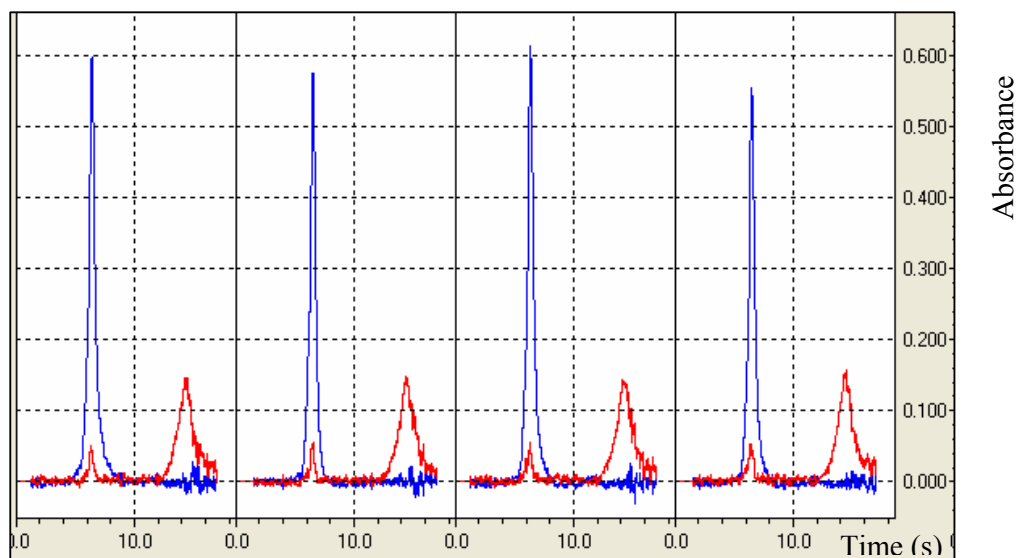


Fig.5.54 Absorption signals for Cr in bovine muscle using T-shaped furnace using short temperature program and high temperature chromatography.

The effectiveness of the T-shaped graphite furnace can be clearly seen also in this figure because of the big difference in retention time of the matrix and analyte since the matrix appears after 4 seconds, while the analyte, which is also middle volatile appears after 12 seconds. In this case the separation factor could be calculated and found to be equal 3. The values of separation factors indicate the complete separation of the analyte and matrix is possible using the T-shaped graphite furnace with short time temperature program and high temperature gas chromatography approach as can be seen from the above chromatograms. Resolution factor which is more important in chromatography than resolution factor and its value gives information about which signals are separated. The value is found to be of value 3.2 in case of Cr in bovine muscle and 1.7 in case of Mn in bovine liver. Both values are greater than the recommended value for good separation which is 1.5.

5.6 SUMMARY OF THE RESULTS

Table 5.15 shows the summary of characteristic masses (M_{ch}) values for high volatile elements obtained by using T-shaped graphite furnace (non-coated and pyrocoated). As can be seen from the table, the values obtained by the non-pyrocoated T-shaped furnace are nearly equal to that values with different furnace designs illustrated in the table, more over the determination using T-shaped furnace and non diluted urine samples, while other systems used many pre-treatment steps, dilution and chemical modification. In case of Cd with pyrocoated T-shaped furnace the value obtained is comparable with the best value obtained by Grinshtein using TSAVP and diluted urine sample i.e. our system still have the advantages.

Table 5.16 Summary of characteristic masses (M_{ch}) values obtained for Cd and Bi and comparable values from literature

Element	sample	furnace	M_{ch} pg	M_{ch} (literature)*
Cd	standard	Non coated	1.9
Cd	urine	Non coated	1.3
Cd	urine	Pyrocoated	0.6	0.3 ¹ , 1.3 ² [46], 2 ³ , 1.2 [83] ⁴ , 0.4 [52] ⁵
Ag	standard	Non coated	1.9	1.8 [46] ¹ , 4.5 [83] ²
Bi	standard	Non coated	50
Bi	urine	Non coated	30
Bi	urine	Pyrocoated	29.2 [85] ⁶ , 49 [87] ²

1. TSA proposed by Frech

2. THGA

3. THGA. Normal cone

4. THGA with end capped

5. TSAVP proposed by Grinshtein

6. THGA from Hitachi

*. All values obtained using pyrocoated graphite furnaces

The situation is the same in case of silver and bismuth since our values with non-pyrocoated T-shaped furnace and short temperature program values are comparable with the other systems using pyrocoated once. The sensitivity with pyrocoated furnaces is known to be 3-10

times better than that with non pyrocoated depending on the type of the element to be analyzed.

Table 5.17 illustrates the M_{ch} values obtained for the Cr and Mn and the comparable values obtained from the literature survey.

Element	sample	furnace	M_{ch} pg	M_{ch} (literature)
Cr	standard	Non coated
Cr	urine	Non coated	24
Cr	urine	Pyrocoated	8 [46] ¹ , 7 [46] ²
Mn	standard	Non coated	10	1.8 [46] ¹ , 4.5 [46] ²
Mn	urine	Non coated	6.8
Mn	urine	pyrocoated	0.3*
Mn	urine	Pyrocoated	0.65	6.3 [46] ¹ , 4.6 [79] ² , 4.5 [80] ²

* This value obtained using the short time temperature program

As can be seen from the table, middle volatile elements can be determined using the T-shaped graphite furnace with good sensitivity as compared with that using conventional systems and two-step atomizer systems proposed by Frech and Grinshtein. From the value calculated for Cr using the non-pyrocoated furnace (24 pg) one can estimate the characteristic mass M_{ch} for Cr if pyrocoated tube is used, since it is known that the sensitivity is about 6-8 times better than the sensitivity using non pyrocoated tube, hence the value is comparable with that in literature or even better.

For Mn the situation is much better by comparing the characteristic mass M_{ch} which is 0.3-0.65 using pyrocoated furnace with literature data. Further more the sensitivity in case of Mn is better using T-shaped graphite furnace and short temperature program ($M_{ch} = 0.3$ pg) than that when conventional temperature program is used ($M_{ch} = 0.65$ pg).

Table 5.18 shows the characteristic mass M_{ch} , values for Cu and Al. both are relatively low volatile as compared with Cr and Mn the measured values are also good as compared with what is known in literatures.

Table 5.18 Characteristic mass, M_{ch} values obtained for Cu and Al and the comparable values obtained from the literature data.

Element	Sample	Furnace	M_{ch} pg	M_{ch} (literature)
Cu	standard	Non coated	10
Cu	urine	Non coated	12
Cu	urine	Pyrocoated	1.8*	11.7 [80], 17.7 [81] ²
Al	standard	Non coated
Al	urine	Non coated	19
Al	urine	pyrocoated	16*	14 [46] ¹ , 31 [46] ²

* Value obtained using pyrocoated and short time temperature program

Note that the M_{ch} , calculated for Cu with the pyrocoated is about five times better than the compared values in the table, and that for Al is in good agreement.

Table 5.19 illustrates the values found for amounts of trace elements under investigation in standard non diluted urine sample using T-shaped graphite furnace with high temperature chromatography approach and continuous flow mode.

Table 5.19 Values for trace elements analysis in standard non diluted urine sample and the certified values

Element	Amount found ($\mu\text{g/l}$)	Certified ($\mu\text{g/l}$)
Cd (seronorm)	5.7	5.2
Cr (seronorm)	16.0	16.0
Bi (seronorm)	19.3	20.9
Al (seronorm)	105.6	105
Cu (seronorm)	17.0	16.1
Mn (seronorm)	12.5	11.1
Mn (Biorad)	3.2	< 3.5

The amounts found are compared with the certified amount given by each producer. Excellent agreement between the found and certified values indicates that the T-shaped furnace can analyse traces in presence of highly interfering matrices which was not possible before when using all conventional and developed AAS-systems.

No quantitative determination in case of bovine liver and bovine muscle, but the separation of signals of analyte and background indicates that the quantitative determination of these analytes is possible without interference effect.

In all measurements the sample volume used was of 10 μ l of the liquid samples and digested solid samples. The sensitivity and reproducibility of the measurements are comparable with that obtained with the conventional AAS systems. Since most of the values obtained using conventional AAS systems were with injection of 20-40 μ l sample volume, hence better sensitivity expected with the T-shaped furnace when using larger sample volumes.

5.7 CONCLUSION

The installation of the T-shaped furnace in the AAS spectrometer (AAS 6800) was done with slight modifications in the original Shimadzu furnace housing and the graphite electrode. The installation was with very simple design as compared with the other two-step atomizers and graphite filter systems. The measurements were done using high temperature gas chromatography approach with continuous inner argon flow mode (10 ml/min) and additional argon gas purging (30 ml/min) through the furnace neck where the sample is injected. The T-shaped graphite furnace could be used for quantitative determination of trace elements in standard solutions and standard non diluted urine samples with excellent agreement of calculated and certified values. Urine sample can be measure directly without dilution and pre-treatment which is impossible to be done with all conventional and developed AAS-systems. Short temperature program can be applied for quantitative measurements of many trace elements with good reproducibility and sensitivity. Conventional temperature program can also be used if it is needed (in case of bismuth).

In case of short time temperature program the analyte and matrix signals are completely separated from each other which mean that the analyses performed are completely free from interferences since the signals are temporarily and spatially resolved, compared with the conventional systems. The background signals of non diluted urine using T-shaped furnace and conventional temperature program is very small compared with the same signal using the original graphite furnaces because the sample in this case dried, pyrolysed, atomized and measured at the same position and at the same time, while that is differ in case of the T-shaped furnace since the sample dried, pyrolysed, atomized in the neck of the furnace, then measured in the measuring zone. If the background signal is 3 times higher than the analyte the background absorption cannot be corrected using the deuterium lamp background correction which is the case during the analyses of all trace elements in non diluted urine using conventional AAS systems. The background signals are less than 2 times of the analyte signals in the worst cases using the T-shaped furnace and conventional temperature program.

Since short time temperature program contains no pyrolysis steps, the analyses could be done with less time and without using any additional materials such as matrix modifiers or dilution. The analyses could be done with less contamination risk, which is also known phenomenon when using the highly sensitive methods of analysis such as AAS.

The sensitivity of the measurements was excellent compared with the stop flow mode since the argon flow used was 30 ml/min or less during the all measurements. Additionally no salt precipitates was found at the tube ends after running of several measurements which is common phenomenon with many conventional AAS systems using the long heated graphite furnaces.

The characteristic masses of the elements under investigation are comparable with that obtained with the conventional and developed AAS-systems which indicate that the sensitivity of the method is comparable with the commercially available AAS systems.

High temperature chromatography is also applicable when using short time temperature program and continuous argon flow mode. The analyte and background signals are symmetrical and with sharp peaks as compared with that obtained by the developed systems such as L,vov plat-form and Two-step atomizers developed by Frech (1982-2001) and by Schlemmer (2006) where the analyte and background signals were broad, unsymmetrical and super imposed on each other. The sharpness of and symmetry of analyte peaks and background signals using T-shaped furnace allow the use of peak height mode in calculating of figures of merits, sensitivity and leads to a good to excellent separation of these peaks with high to acceptable separation factor values. The high temperature chromatography could be used in quantitative measurements of trace elements in non diluted urine sample and the same procedure is tested for other matrices such as bovine liver and bovine muscle. In both cases complete separation of analyte and matrix signals is observed for middle and low volatile elements and acceptable separation is observed for the high volatile elements group (Cd).

Short time temperature program reduces the analysis time and cost by increasing the lifetime of the tube and saving time of the operator and the instrument itself including the lamps operation time. The continuous flow measurements leads to the extension of the linear working ranges for the quantitative determination of trace elements using AAS.

With this new furnace design, it is possible to analyse large sample volume up to 100 μ l and solid samples without blocking the light path since the liquid sample injected in the neck of the T-shaped furnace and not in the light path as compared with the conventional AAS systems.

Finally T-shaped graphite furnace is very simple design with very effective results compared with all developed AAS-systems within the last three decades since original furnace housing is used with slight modification only in the graphite electrodes (no need for new furnace housing design) there for it can be commercially available with very low production costs.

SUGGESTIONS FOR FUTURE WORK

From my point of view, it is a completely new area of research. It is possible to analyse more elements present in different kinds of matrices, to improve the separation of these elements from their matrices using the short temperature program or even the conventional temperature program to analyse the elements which were not possible to be analysed using the conventional systems and all developed systems. Ballast body can be inserted in the neck of the furnace to test the improvement of the separation process of the signals. Direct introduction of Solid samples using the known methods for solid samples can be also applied.

REFERENCES

1. D. Skoog, F. Holler, and A. Timothy. "Principles of instrumental analysis". 5th edition (1998) by Harcourt Brace & company.
2. Welz Bernard, "Atomic absorption spectrometry". 2nd edition (1986), by spiraling.
3. Yoshihiro Hirano, Kyoko Imai, Kazuo Yasuda., *Accred Qual Assur.* Vol. 10 (2005) 190.
4. Francis Rouessac and Annick Rouessac. "Chemical analysis, modern instrumentation methods and techniques". 4th edition (2004) , John Wiley & Sons.
5. N. Massmann., *Spectrochimica Acta Part B* 23 (1968) 215.
6. K.W. Jackson. "Electrothermal atomization for analytical atomic spectrometry" 1st edition (1999) by JohnWiley & sons.
7. E. Lundberg and W.frech., *J. Anal.Chem.* Vol. 53 (1981) 1437.
8. B. Welz, G. schlemmer and J. R. Mudakavi. *J. Anal. At. Spectrom.* Vol. 3 (1988) 695
9. R. kawowska, E. Bulska and E. Hulanicki., *Talanta*, 27 (1980) 397.
10. D. Behne, P. Bräter W. Wolters., *Z. Anal.Chem.* Vol.277 (1975) 335.
11. C. W. Fuller., *Analyst.* Vol. 99 (1974) 739.
12. S. R. Koirtyohann, E. D. Glass and F. E. Lichte., *J. Appl. Spectrosc.* Vol. 35 (1981) 22.
13. R. C. Hutton, J. M. Ottaway, M. S. Epstein and T. C. Rains., *Analyst.* Vol. 102 (1977) 658.
14. B. L'vov and L.A. Pelievia., *Zh. Anal Khim.* Vol. 34 (1978)1572.
15. W. Frech, J. A. Pearson and A. Cedergren, *Prog. Analy.Atom.Spectrosc.* Vol.3 (1980) 279.
16. A. B. Volynskii., *J. Anal. Chem.* Vol.58 (2003) 905.
17. G. Schlemmer. "A Laboratory Guide to Graphite Furnace Analytical Atomic Spectroscopy", *springer-Verlag New York, Inc; 1st edition (1999).*
18. Ernest Beinrohr and Miroslav Rapta., *J. Anal . At. Spectrom,* Vol..6 (1991) 33.

19. Xiao-quan, Luan Shen and Zhe-mingt., *J. Anal. Atom. Spectrom*, Vol. 3 (1988) 99.
20. D. Christian Hassell, Vahid Majidit and James A. Holcombe., *J. Anal. At. Spectrom*. Vol.6 (1991) 105.
21. G. F. R. Gilchrist, C. L. Chakrabarti" and J. P. Byrnet., *J. Anal. At. Spectrom* Vol.4 (1989) 533.
22. A.J. Curtius, G. Schlemmer and B. Welz., *J. Anal. At. Spectrom*, Vol. 2 (1987) 115.
23. B. Docekal, H. Duekalova and E. Novotny., *J. Anal. At. Spectrom*, Vol.6 (1991) 661.
24. H.Niskavarag, U Havirtasalo and L. J. Lajunen., *Spectrochimica Acta*. Vol. 40 (1985) 1219.
25. S. Akman, B. Welz, and Nilgun Tokman., *Spectrochimica Acta Part B* 60 (2005) 1349
26. P. Grinberg and R. Campos., *Spectrochimica Acta Part B* 56 (2001) 1831.
27. E. Kopyś, E. Bulska., and R. Wennrich., *Spectrochimica Acta Part B* 58 (2003) 1515.
28. J. A. C. Broekaert., *Spectrochimica Acta*, 36B (1981), 931.
29. K. W. Jakson and G. Chen., Fundamental review. *Anal. Chem*, 68 (1996) 231R.
30. I.L. Grinshtein, Yu. A. Vilpan, V.A. Kopeikin, L.A.Vasilieva, M.A. Meshalkin, Two-step electrothermal atomizer with a vaporizer purge. in: H.-M. Kuss, U.Telgheder_Eds. *Modern Aspects of Analytical Chemistry Verlag Mainz, Aachen*, (1997) 88.
31. P. Ngobeni, C. Cana'rio, D. A. Katskov and Y. Thomassen. *J. Anal. At. Spectrom.*, Vol.18 (2003) 762.
32. D.A. Katskov, R.I. McCrindle, R. Schwarzer, P.J.J.G. Marais. *Spectrochimica Acta Part B* 50 (1995) 1543.
33. K.-R. Sperling., *Spectrochimica Acta part B* 39 (1984) 371.
34. A. V. Voloshin, A. Kh. Gil'mutdinov, Yu. A. Zakharov, and A. A. Sevast'yanov, *J. Anal. Chem*. Vol.59 (2004) 234.

35. W. Frech and B. V. L'vov., *spectrochimica Acta* part B 48 (1993) 1371.
36. N. Hadju and W. Frech., *spectrochimica Acta* part B 49 (1994) 445.
37. W. Frech, D. C. Baxter and E. Lundberg, *J. Anal. At. Spectrom* 43B (1988) 21.
38. D. C. Baxter and W. Frech., *Spectrochimica Acta* 50B (1995) 655.
39. Ilia L. Grinshteyn, Vladimir A. Kopeikin, Lubov A. Vasilieva, S.N. Golubev, Heinz M. Kuss. *Spectrochimica Acta* Part B 52 (1997) 1421.
40. E. Lundberg, W. Frech, D. C. Baxter and A. Cedergren., *Spectrochimica Acta* part B 43 (1988) 451.
41. D.D. Seimer., *J. Anal. chem.* Vol 55 (1983) 692.
42. D.D. Seimer and W. Frech., *Spectrochimica Acta* 39B (1984) 261.
43. E. Lundberg, W. Frech and J. Harnely., *J. Anal. At. spectrosc. Vol.3* (1988) 1115.
44. W. Frech and Jonsson., *spectrochimica Acta*, 37B (1982) 1021.
45. W. Frech, A. Cedergern, E. Lundberg and D. D. Seimer., *spectrochimica Acta* 38B (1983) 1435.
46. W. Frech, N. Hadju, D. Henriksson, B. Radziuk, G. Rodel, and R. Tamm. *Spectrochimica Acta* Part B 55(2000) 461.
47. C.M.M. Smith, J.M. Harnly., *J. Anal. At. Spectrom.* Vol.11 (1996) 1055.
48. K. Yu. Nagulin, A. Kh. Gil'mutdinov, and L. A. Grishin., *J. Anal. Chem.* Vol. 58 (2003) 389.
49. K. Yu. Nagulin and A. Kh. Gil'mutdinov., *J. Anal. Chem.* Vol. 59 (2004) 1042.
50. K.-Ch. Friese, M.D. Huang, G. Schlemmer, V. Krivan., *Spectrochimica Acta* Part B 61 (2006) 1054.
51. I. L. Grinshtein, Y.A. Vil'pan, L.A. Vasilieva, V.A. Kopeikin., *Spectrochimica Acta* Part B54 (1999) 745.

52. I. L. Grinshtein, Yuri A. Vilpan, Alexei V. Saraev, Lubov A. Vasilieva.,
Spectrochimica Acta Part B 56(2001) 261.
- 53 L. Lian., *Spectrochim. Acta Part B* 41 (1986) 1131.
54. J.P. Snell, S. Sandberg, W. Frech., *J. Anal. At. Spectrom.* Vol. 12 (1997) 491.
55. P. V. Oliveira . E. Oliveira., *Fresenius J Anal Chem.* 371 (2001) 909.
56. B. Radzuik, N.P. Romanova, Y. Thomassen., *J. Anal. Comun.* Vol. 36 (1999) 13.
57. Yu. A. Vil'pan, I. L. Grinshtein, A. A. Akatov, and S. Gucer., *J. Anal. Chem.* Vol. 60
(2005) 38.
58. Kiyohisa Ohta and Syang Yang Su., *J.Anal.Chem* Vol. 59 (1987) 540.
59. Xiandeng Hou and Muhsin, Ezer., *J. analytical science* Vol.17 (2001) 175.
60. Arthur Salido, Caryn L. Sanford, Bradley T. Jones., *Spectrochimica Acta Part B*
54 (1999) 1167.
61. Erika Krakovska, Dagmar Remeteiova., *Spectrochimica Acta Part B* 58 (2003) 1507.
62. R. D. Reid and E. H. Piepmeier., *J.Analytical.Chem.* Vol. 48 (1976) 338.
63. Rosa Moreno Camero, Jos´e Alvaradou, *Spectrochimica Acta Part B* 55 (2000) 875.
64. Mark Williams and E. H. Piepmeier., *J. Anal. Chem.* Vol. 44 (1972) 1342.
65. Yang Wei-min, Ni Zhe-ming., *Spectrochimica Acta Part B* 52 (1997) 241.
66. Shoji Imai, Azusa Satoh and Y. Akira., *Analytical science.*Vol.20 (2004) 1755.
67. Reinaldo C. Campos and Adilson J. Curtius, *J. Anal.Atom.Spectrom.*Vol.5 (1990) 669.
68. Kiyohisa Ohta, Wataru Aoki, and Takayuki Mizuno., *Mikrochim. Acta [Wien]* 1990, I,
81.
69. Xiandeng Hou and B. T. Jones., *Spectrochimica Acta Part B* 57 (2002) 659.
70. D. Siemer, J. F. Lech and R. Woodriff., *Spectrochimica Acta Part B* 28 (1973) 469.

71. Anna Anselmi, Paolo Tittarelli, and Dmitri A. Katskov., *Spectrochimica Acta Part B* 57 (2002) 403.
72. D. Katskov, R. McCrindle, R. Schwarzer, P.J. Marais., *Spectrochimica Acta Part B* 50 (1995) 1543.
73. D. A. Katskovt and A. M. Shtepan., *J. Anal.At. Spectrom.* Vol. 9 (1994) 321.
74. Dmitri A. Katskov., *Spectrochimica Acta Part B* 62 (2007) 89.
75. D.A. Katskov, R. Schwarzer. P.J.J.G. Marais and R.I. McGrindle, *J. Anal. At. Spectrom Vol. 9 (1994) 431.*
76. D.A. Katskov, R. Schwarzer. P.J.J.G. Marais and B. Ngobeni., *Spectrochimica Acta Part B* 53 (1998) 671.
77. D.A. Katskov., P.J.J.G. Marais and P. Tittarelli., *Spectrochimica Acta Part B* 51 (1996) 1169.
78. P.V. oliveira, E. Oliviera, Fresenius., *J. Anal. Chem.* Vol. 371 (2001) 909.
80. Yevgen Berkhoier. Ph. D dissertation Uni-Duisburg (2005).
81. K.L.A. Lelis, C.G. Magalhaes, C.A. Rocha, and J.B.B.Silva. *Analytical and Bioanalytical Chemistry.* Vol.12 (2002) 1556.
82. T. myöhänen, V. Mantylahti, K. Koivunen, R. Matilainen. *Spectro chimica Acta* 57B (2002) 1681.
83. G. Schlemmer, *J. At. Spectrosc.* Vol.17 (1996) 15.
84. R. E. Sturgeon., Fresenius., *J. Anal. Chem.* Vol. 355 (1996) 425.
85. Cristina Goncalves, Berta Rolla Nunes, Maria Bertilia and Oss Giacomelli. *J.Anal. At. Spectrom.* Vol. 18 (2003) 787.
86. László Bencs, Ottó Szakács, Norbert Szoboszlai, Zsolt Ajtony and Gábor Bozsai., *J. Anal. At. Spectrom,* 18 (2003) 105.
87. T. W. Lin, S. D. Huang, *Anal.Chem.* Vol. 73 (2001) 4319.